INCORPORATION OF THE PATERNÒ–BÜCHI REACTION INTO MASS SPECTROMETRY-BASED SYSTEMS FOR LIPID STRUCTURAL CHARACTERIZATION
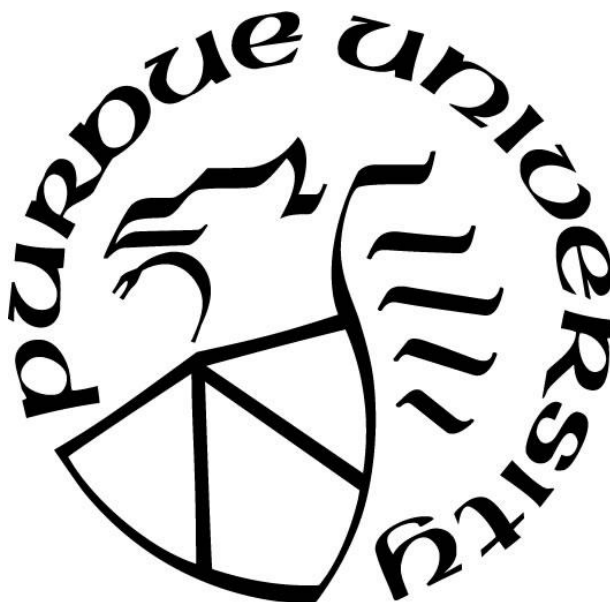
by

Elissia Franklin

A Thesis

Submitted to the Faculty of Purdue University

In Partial Fulfillment of the Requirements for the degree of

Doctor of Philosophy

Department of Chemistry

West Lafayette, Indiana

December 2019

THE PURDUE UNIVERSITY GRADUATE SCHOOL
STATEMENT OF COMMITTEE APPROVAL

Dr. Yu Xia, Co-Chair

Department of Chemistry

Dr. Scott A. McLuckey, Co-Chair

Department of Chemistry

Dr. Julia Laskin

Department of Chemistry

Dr. Angeline Lyon

Department of Chemistry

Approved by:

Dr. Christine A. Hrycyna

This is a continuation of my mother's legacy and a dedication to the future of my family.

ACKNOWLEDGMENTS

To the McLuckey group, John Lawler, Hsi-Chun Chao, Chris Harrilal, Abdirahman Abdillahi, David Foreman, Josh Johnson, Kenny Lee, Anthony Pitts-McCoy, Jay Bhanot, Nan Wang, Feifei Zhao, Caitlin Randolph, Mack Shih, Sarju Adhikari, De'Shovon Shenault, and Ian Carrick, it is amazing being in a space with some of the most intelligent people in the world and learning science with you all. It has been such a wonderful and humbling experience growing with each other. I wish greatness to the future of the group. To Anthony and Chris …. both of you are the problem! De'Shovon thank you for keeping me fed and continuing to pray over me through my challenges.

Chris Pulliam and Stella "Stellar" Betancourt your mentorship has been unsurpassed. You all poured so much knowledge into me in every area and it contributed to me making it this far. Moises, Saadia, Monita, Mavreen, Yan, Brianna thank you for riding with me since day one of the program. Through all our ups and down the friendships remain true and helped relieve a lot of the pressures of graduate school. Kiera you really helped keep me on track and motivated during my final stretch while getting this thesis submitted. You supported me when I didn't have the strength to do anything and kept me focused when I tried to control things out of my control. Thank you for keeping me level-headed.

Nicaila and the Mogul family. Thank you for supporting me as a continue to build as a professional and podcaster. It has been exciting learning how to find my audience and grow something from the ground up. The lessons that I learned from being a podcast mogul extends beyond online space and have impacted my overall life vision.

My ship, 33˚ F.A.H.R.E.N.H.E.I.T., is collectively pure greatness and beauty all wrapped up in one. Every day I grow more grateful to be a part of such a phenomenal group of extraordinary women. We have made great strides in our selected fields and I am so honored to have sisters like you who keep me inspired to believe bigger. I hope that this thesis makes you all proud. GG4L. Dr. LaGolden, Ariana T. Esq., Teryn, Janel S., Maya, and Essence thank you for being joyful, crazy, hurt and happy with me through this entire process.

Dr. Brittany Huff you're the greatest big sister a girl could have. You normalized my feelings and thoughts whenever I felt that I was being irrational in my academic pursuits. Thank you for the early mornings and late-night conversations that reminded me that I am always supported. Our conversations motivated me to keep going without regret. To Michael Omole, I appreciate you for being here for me as a voice of reason and supporting even my wildest

endeavors. Shantia, Chanel, and Nailah we've been through much over the years and the beautiful thing is that whenever it matters, we're always on time. To my oldest and coldest friend Jasmine Nathan, you literally been riding with me though all the years of me being super occupied with school and you still don't ever leave me out of the invitation list. Our friendship is immortal. Ahmad you entered my life with love and acceptance for my focus on pursing higher education. For four years, you showed me grace to really give graduate school the needed attention to finish successfully. Thank you.

To my brothers, Mike, Frank, Jayden and my brother-cousin Jerome, I love you all so deeply and feel your love as I pursue all endeavors. Christina you provide clarity and consistency in my life. I am so glad you are my cousin. I am grateful for the love from all my many aunties and uncles. Tanita thank you for being my rock through the good and the bad. Lisa you have brighten many of my days when I needed it the most and have always let me know that you got my back. Val I appreciate you for always coming though with your loving spirit and keeping me on my toes. Aunt Chandra thank you for all the support over the years. Tiffany you spent so much time and energy helping me get into graduate school and continue supporting me throughout my graduate school process. You have been a source of enlightenment and great overall life advice. Thank you to my god mother Krystal for all that you have done for me over the years and keeping me cute.

Of course, I must show love to my grandparents. Delores, Wilbert, Feb, James, Fern, Robert, and Emma thank you for giving all that you got. To NaNa and Wilbert thank you for being my second home and acting as a bed-and-breakfast whenever I need a "get away." You all do not miss a beat or event and continue to show me how loved I am. NaNa you have been the ultimate cheerleader and place of peace. Kizzy thank you for being such a supportive mother to me. You loved on me when I didn't think there was any strength left in me. You been loving me since day one and I know that you will never change.

To my parents Erica, James, Jordan and Valencia, you are literally the reason I am who I am, so this thesis is just as much yours as it is mine. You collectively created a place for me to "marinate" in potential success until I was ready move into pursing real-world obstacles. Jordan thank you for entering my life and always having me back. Valencia, I appreciate you always being there when I need you and having a place for me show up with all my extra-ness. My dad, James Franklin, you've been A1 since day one. The dad that never missed a beat. Thank you for always

reminding me to grind and to never forget who I am. You have encouraged me to always keep pushing even when I do not want. You have worked hard and supported with what you had to let me know that you got me. I got you for life. To Dr. Erica Jordan, you lead me with such resilience, elegance, sophistication, integrity and independence that if I follow your example, I am bound to always do greater. You always encouraged me to pursue my passion and even when I switched passions you welcomed my temporary craze. You never made me feel bad about wanting to give up and made me know that if I am quitting on something that is not serving me it is not failure it is self-preservation. You never allowed me to have excuses about why things cannot get done but reminded me that all things are by choice. You sacrificed so much to get me where I am and made a safe space for me to speak about my professional goals reminding me not to be so hard on myself. Thank you, ma, for pouring your all into me and loving me unconditionally.

Finally, I must acknowledge the culture which molded and kept me inspired to continue through rough times. From my favorite podcasts, The Friend Zone, Food Heaven Made Easy, Side Hustle Pro, and The Read to my favorite musical artists (ask for the PhD Apple Music playlist) thank you for your art and creativity which made the day-to-day more pleasurable and flavorful. As a product of Chicago's southside, I am eager to continue beating the odds and challenging the system. I love us for real. I also want to acknowledge you reading this because you landed here on this random lipid thesis reading acknowledgements so if I did not acknowledge you by name, I just want you to know that I appreciate you.

.

TABLE OF CONTENTS

LIST OF TABLES

ABSTRACT

Lipids are important cellular biomolecules that perform essential functional and biological roles. For instance, lipids in the cell are the compartmentalizer for the cytoplasm and an energy storage unit. The knowledge surrounding lipids is abundant, yet there is still so much to uncover. There are many categories of lipids and within each category the structural composition is extremely diverse. In turn, the dramatic structural complexity of lipids demands analytical methods capable of providing in-depth structural characterization of individual molecular structures. However, lipid structural elucidation has remained challenging, namely due to the presence of isomeric and isobaric species with a complex mixture. In particular, isomeric/isobaric lipid structures arise from variations in class, headgroup, fatty acyl chain, *sn*-position, and/or carbon-carbon double bond (C=C) position(s). Recently, recent research suggests C=C composition impacts lipid physical properties, metabolic fate, and intermolecular interactions. Thus, analytical strategies capable of localizing sites of unsaturation are of interest in the lipidomics community.

Mass spectrometry (MS) is a leading tool for lipid analysis. Electrospray ionization (ESI), a soft ionization method, is the most commonly used method for lipid ionization as a means of taking the ions from liquid-phase to gas-phase without extensive decomposition of the species. Utilizing ESI-MS, lipids can be identified at a sum compositional level via accurate mass measurements. . With tandem mass spectrometers, lipid ions can be further probed, utilizing tandem-MS (MS/MS) to generate structurally informative product ion spectra that facilitate the assignment of lipid molecular structure. More so, gas-phase ion/ion reactions represent a unique MS-based technique that has improved the analysis of lipids structures. Gas-phase ion/ion reactions allow for lipid species to be charge inverted from one polarity to the opposite polarity. This reaction enables lipids to be ionized in a polarity that is optimal for class identification and further investigated in the opposite polarity where more structural information is obtained. All the information provided is captured without the requirement of multiple solution conditions which is necessary when analyzing in both polarities. In the case of charge inverted lipids from positive ion mode to negative ion mode, fatty acyl composition can be obtained; however, C=C information is lacking.

MS can also be paired with other analytically technologies to assist with lipid analysis. One of those technologies is liquid chromatography (LC), which allows for the separation of lipids based on different characteristic depending on the column type being used. Reverse-phase LC (RPLC) allows for the separation of lipid molecular species based on structural composition. RPLC-MS/MS benefits from the ability to separate lipids and determine their fatty acyl chain composition but it is difficult to specify C=C location with the use of a synthetic standard that is identical to each molecular species being analyzed.

Commonality between the gas-phase ion/ion reactions for charge inversion of lipids and RPLC-MS/MS approaches is the inability to provide C=C coverage. In-solution and unique ion activation techniques have been developed for seeking such information. The Paternò–Büchi reaction is a UV-initiated [2 + 2]-cycloaddition of an excited carbonyl containing compound onto an olefin group. This reaction can be initiated onto the alkene group within an unsaturated lipid aliphatic chain to form an oxetane ring modification. There are two product ions that can be formed upon each unsaturation site due to a lack of regioselectivity the reagent can attach at either side of the C=C. The modified lipids can be taken into gas-phase and collisionally activated via low-energy collision induced dissociation, generating product ions indictive of C=C position(s). The work herein shows the incorporation of the PB reaction into the gas-phases ion/ion reaction and RPLC-MS/MS apparatuses for C=C localization. The methods have been applied to the lipid extracts of bovine liver and human plasma for confident molecule species determination.

CHAPTER 1.   INTRODUCTION

1.1   Overview

Biomolecules such as proteins, nucleic acids, and metabolites are all working together to sustain the operation of biological systems. One category of metabolites that have many functions throughout all cells are lipids. Lipids are defined as "hydrophobic or amphipathic small molecules that originate entirely or in part by carbanion-based condensations of thioesters and/or by carbocation-based condensations of isoprene units".[1] The main component of the eukaryotic cell membrane is glycerophospholipids (GPs), which act as a compartmentalizer for each organelle within the cell.[2,3] Lipids are responsible for transporting ions and other compounds through the membrane. Permeability is dependent on the types of lipids present. Each of the leaflets of a cell membrane differ in the distribution of classes lipids within it where cholesterol concentrated heavily in both layers.[4] Lipid rafts contain membrane proteins that play roles in signal transduction.[5] Within lipid rafts, there is an elevated concentration of glycosphingolipids and cholesterol. Lipids play a role in signal transduction as they are a chemical messenger and protein regulator.[4] Lipids are also a source of energy for cells. Cells will store chemical energy as lipids when there is an excess and supply energy in times of need. This is far from an inclusive list of functions and much is still being discovered about the influence of lipids on biological processes. With lipids having such an array of functions within a cell, it is expected that when cellular processes are not operating properly, lipid composition will be affected. Biomarkers measure whether biological processes are running smoothly using a biomolecule as an indicator. Stroke, diabetes, obesity, and other disorders are lipid related that can be monitored via lipid analysis.[4,6] In order to push forward the efforts of molecular medicine, nutrition, and many fields, there is a need for enhanced lipid analysis tool that can improve identification of lipid molecular species. This has been proven to be challenging as lipids vary structurally which is related to function and being able to distinguish the species is essential.

1.2   Lipid Structural Diversity

Based on the definition of lipids presented above, the molecule has been divided into 8 categories based on physical properties. The categories of lipids are fatty acyls (FA), glycerolipids

(GLs), glycerophospholipids (GPs), sphingolipids (SPs), sterol lipids (STs), prenol lipids (PRs), polyketides (PKs), and saccharolipids (SLs).[1] SLs are a class that consists of species that have fatty acids linked to a sugar backbone. The SP class is complex and consists of sphingoid base backbone. STs and PRs share a similar biosynthesis pathway however they differ in their overall structure and function. In PKs, there are alternating methylene and carbonyl groups. GPs are present in all organisms as they compartmentalize the cell cytoplasm, protein housing unit.[7] They also act as precursors to other lipids. GPs are divided into classes based the polar headgroup attached on the glycerol backbone at the *sn*-3 position in eukaryotic systems and the *sn*-1 position in archaebacteria.[8]

The major GP classes are glycerophosphocholine (PC), glycerophosphoethanolamine (PE), glycerophosphoserine (PS), glycerophosphoglycerol (PG), glycerophosphoglycerophosphate (PGP), glycerophosphoinositol (PI), glycerophosphate (PA), glyceropyrophosphate (PPA), glycerophosphoglycerophosphoglycerol (CL), and CDP-glycerol (CDP-DG),[1] which is not a comprehensive list. There may be radyl side chains at one or both *sn*-positions on the glycerol backbone. If only one side chain exists, the species is considered a lysophospholipids. Two fatty acids may also be esterified onto the glycerol backbone creating a diacyl species. The radyl chains may be bond to the glycerol forming an ether or vinyl ethyl moieties classifying the species as plasmanyl-phospholipids or plasmalogens, respectively.

GLs are a class of lipids that very similar in structural possibilities to that of GPs, but do not contain a polar headgroup. The classes of GLs are monoacylglycerol (MG), diacylglycerol (DG), and triacylglycerol (TG). It is very difficult to determine the position of the side chain upon the glycerol backbone. This challenge is especially true for DGs and TGs where it is possible to have 4 and 6 regioisomers (respective) if each acyl chain is different.[9] There is still the possibility of having the fatty acyl species linked via an ether and vinyl ether bond making the class even more structurally diverse.[10] The fundamental category of lipids is the FA as it is a major building block to more complex lipids. Although FAs are the simplest lipid structure, they possess a highly diverse composition.

Fatty acids have a terminal carboxylic acid with a series of methylene groups.[11] The species can be both saturated or unsaturated, where they are only composed of a straight chain of carbon-carbon single bonds or they can contain a straight chain with carbon-carbon double bonds (C=C). There may be one or more C=C present on the fatty acyl chain which can have a cis or trans

conformation. The species can also differ in the position of the C=C. Fatty acids also may contain a methyl branch, halogen, hydrocyclic ring, oxygen, or nitrogen.[12] This work focuses of this work is on lipids with the FA class fatty acid specifically, straight chain fatty acids and determining the structures of lipids.

1.3   Lipidomics Tools

Lipidomics is a field that is dedicated to understanding everything encompassing lipids. It is an important goal in lipidomic studies to understand the structures, functions, intermolecular interaction, and synthesis of each lipid within a given biological or living system.[8] The total lipidome in a single cell can consist of over 1000 molecular species each with specific structures that gives rise to information about the function.[4,13] There are multiple methods that are used for structural characterization of lipids. Mass spectrometry (MS) will be discussed in greater detail later because it is the method used in this thesis and it is a key player in the game of lipid analysis.

Thin-layer chromatography (TLC) is a fast separation technique and this method can be applied to the analysis of a complex sample without an extraction prior to application.[14] Depending on the mobile phase variations in separations take place. Oxidation of lipids using TLC is a challenge due to exposure to atmospheric oxygen. Nuclear magnetic resonance (NMR) spectroscopic methods have the power to analyze lipids under *in vivo* conditions. NMR can distinguish C=C isomers, cis/trans conformational isomers, and regioisomers. ^{1}H/^{13}C NMR can analyze basically every lipid, but in the cases where there is a mixture, spectra are complex.[15,16] ^{31}P NMR can only be used on phosphorus containing lipids and allows for all species to be quantified based on headgroup in a single spectrum.[16] This method could also be done to determine fatty acyl chain compositions as long as there is a significant difference between species. Gas chromatography (GC) allows for separation of volatile compounds. GC is capable of characterization of derivatized fatty acyls however complex lipids are not GC compatible.[17] Liquid chromatography (LC) is useful for separation of intact lipid molecules without any derivatization. Depending on the stationary phase the lipids are separated based on different properties. Herein we focus on reverse-phase LC (RPLC) separation.

In RPLC, molecular species are separated based on varying fatty acyl chain compositions. Ion-mobility (IM) separates ions under an electric field based on their mobility through an inert gas. Difference in the structures and shapes of ions allow for the separation of isomers that would

not typically be distinguishable using other techniques.[18] A limitation to both RPLC and IM is the lack of synthetic standards to be able to determine what species is present in a mixture.[18,19] Mass spectrometry imaging (MSI) is the only means of localizing variations in lipid structures *in situ*.[20] MSI uses the information taken from a MS spectrum to formulate an image that depicts the distribution of lipid throughout a sample such as tissue.

1.4   Mass Spectrometry

MS stands at the forefront of lipidomic techniques benefitting from its sensitivity, selectivity, and allows for high throughput analysis. Mass spectrometry requires three components: generating ions, mass analyzing, and detecting.[21] There is a plethora of methods for each of the components. The focus is to give an idea of the methods used in the thesis for generating ions and mass analyzing. Electrospray ionization was used for ionization in all experiments. The mass analyzers used included quadrupoles and time of flight components. A key component that each mass analyzer shares is that they separate ions based on the *m/z* in vacuum of about 10^{-5} to 10^{-8} torr.[21] These pressures allow for the increase of the mean free path of the ions such that they there is a reduction in the amount of collision with inert gases before reaching the detector.

1.4.1   Generation of ions

The formation of ions is an essential part of doing mass spectrometric analysis. There are many ionization methods on the market however, in modern lipidomic studies soft ionization methods are the most useful. Hard ionization methods are those that form ions using harsh conditions which result in not only the formation of the ionized molecular species of interest, but it is typically accompanied by fragmentation peaks in excess. Soft ionization methods are those that can create ions from intact molecules without extensive fragmentation. Some of those methods include matrix-assisted laser desorption/ionization (MALDI)[22] and different types of electrospray ionization.[23] In MALDI, crystallized molecules are used as a matrix for the compound of interest. The desorption is initiated by the laser activation of the matrix which takes with it may molecules including neutral and protonated species. The matrix ionizes the analyte through proton transfer and the protonated molecule is then introduced to the MS system. MALDI is a useful technique for MSI.

1.4.2 Electrospray Ionization(/Interface)

Electrospray ionization (ESI) has had such an influential impact on mass spectrometry analysis since being paired with MS in 1984.[24] John Fenn who originally used the methods for analyzing biomolecules won a Nobel Prize in chemistry in 2002.[25] The applications of ESI began to flourish in the 1980 and Fenn showed that it could be used to analyze biomolecules such as proteins, peptides, oligosaccharides and a wide range of other compounds.[26,27] Prior to ESI, only small volatile compounds were analyzed via MS because larger molecules could not be ionized. ESI was quickly picked up as a means of analyzing lipid species as early as 1991. Weintraub and Pinckard used the method for characterization of platelet-activating factor (the first GPs known to have messenger functions)[28] and Duffin and Henion were using it for the analysis of GLs.[29]

As one of the softest ionization methods, ESI which allows for the formation of ions under atmospheric conditions. In the presence of a high electric field, an emitter at the interface of the mass spectrometer sprays charged droplets at µL/min flowrates (or nL/min flowrates for nanoESI).[24,30] The droplets are formed due to the electric field force exceeding that of the surface tension of the emitter applied onto the solution. The force forms a cone shape and at a certain threshold of force a jet of liquid ejects from the cone starting the droplet formation process.[24] The ions are transferred from liquid-phase to gas-phase via droplet desolvation. Each droplet has a charge-to-volume ratio and upon reaching the Rayleigh limit (the maximum amount of charge the droplet can have) Coulomb repulsion leads to the droplet instability and droplets getting smaller until the ion is completely desolvated. The dry ions are then able to be transfer to the mass analyzer for analysis. ESI helps pair LC and MS to ionize molecules being eluted a separation column.

1.5 Mass analyzers

1.5.1 Time of Flight

Time of flight mass analyzer are the simplest and fastest of all commercially available mass analyzers. An acceleration voltage is applied to pulse the ions into a high vacuum region of a known length without an electric field.[32,33] Because all the ions are pulsed in with the same amount of kinetic energy the ions that are lighter will arrive at the detector sooner than the heavier ones. This equation is used to explain this phenomenon.

$$KE = zV = \frac{mv^2}{2}$$

$$\frac{m}{z} = \frac{2V}{v^2}$$

Where KE is kinetic energy, V is acceleration voltage, z is the charge of the ion, m is the mass of the ion and v is the velocity of the ion. Mass-to-charge and velocity are inversely related thus the greater the m/z the ion the slower it will be and the longer it will take to reach the detector.[33] Longer flight times can be used to improve resolution. Ion mirrors can be used to create longer flight time and to decrease KE distributions that naturally occur during the pulsing in of the ions.

1.5.2 Linear Quadrupoles and Ion traps

Quadrupole mass spectrometers are useful its mass-analyzing and ion trapping capabilities.[21] Quadrupoles benefit from being lightweight, easy to pair with other mass analyzers, ease of automation, and speed. The mass range for quadrupole can be 1-4000 m/z. The limitations to quadrupoles are that there is poor resolution and can require a lot of tuning. A linear quadrupole consists of four hyperbolically or cylindrically shaped electrodes arranged in a square configuration.[34] The electrodes which are opposite from each other are paired and set at the direct current (DC) fields and radio-frequency (RF) potentials.[35] The combination of RF and DC fields are used from mass-to-charge separation. As ions enter the quadrupole the force exerted on it is of the opposite polarity for attracting the ions and the ions are kept in an unstable position due to the voltages applied to the rods constant alternating allow the ions to move through the quadrupole due to stable motion in the direction parallel to the electrodes without hitting the rods. Advanced mathematical equations help calculate the stability of the ions when using specific frequencies, the quadrupole dimensions and voltages being applied.[12] Ions with the required ion stability will exit from the quadruple at the opposite end, while those that are not stable will not reach the quadrupole exit, which can be used for the isolation of a specific m/z. An RF only quadrupole have strong focusing properties allowing for them to be used as collision cells.[21] These cells are typically kept at higher pressures to ensure that more collisions occur to improve fragmentation efficiencies. Trapping ions in a quadrupole is made possible by placing a trapping potential at the axial ends of the electrodes to keep the ions from exiting the ion trap. The right frequencies and voltages allow

for the stable orbits of ions within the quadrupole and exit the trap by applying an electric field that makes the ions unstable such that they eject from the quadrupole.

1.5.3 Analyzers in tandem

Mass analyzers can be put in series to improve performance and allow for the activation of the ions of interest to get more structurally informative information. The instruments used in this work are a triple quadrupole mass spectrometer (QqQ), triple TOF (QqTOF), and quadrupole TOF (QTOF). In all instruments, multiple MS stages are done subsequently to achieve selective and specific ion characterization. These tandem mass spectrometers are useful for ion dissociation to determine molecular structures.

1.6 Tandem MS Techniques

1.6.1 Ion trap CID

Ion traps can isolate and activating precursor ions, then store the fragment ions within the same run. With enough ions, MS6 experiments have been achieved.[37] Ion trap CID is achieved by applying a waveform at the secular frequency in resonance with the ion of interest. The waveform is applied for enough time so that the kinetic energy turns to internal energy via collisions with the buffer gas in the trap.[38,39] The result of the increase in internal energy is fragmentation of the ion of interest.

1.6.2 Beam-type CID

In beam-type CID, mass selected ions that are in the first quadrupole are accelerated into a high-pressure RF only quadrupole. As the ions pass through the collision cells, the kinetic energy is transferred into internal energy via collisions with a neutral gas molecule.[21,40] The fragment ions enter the third mass analyzer (a quadrupole or TOF) for mass analysis. Beam-type CID is the method used for the common scanning modes. A precursor ion scan (PIS) mode is used to determine molecules that produce a fragment of a certain m/z. In PIS mode, the first quadrupole is scanning and after the ions from Q1 exit q2 Q3 allows only the transmission of ions of a certain m/z to pass to the detector.[12,21] The overall spectrum will only show the ions that produced that

m/z. The neutral loss scan (NLS) mode enables the scanning of both Q1 and Q3 such that after an ion is mass selected in Q1 is passes through the collision cell and if it forms a product that makes a fragment of a specific difference then the precursor is recorded on the mass spectrum.[41] The mass spectrum contains all the ions that correspond to a certain neutral loss.

1.6.3   Ion/ion reactions

Gas-phase ion/ion reactions using a mass spectrometer serves as a platform for the manipulation of generated ions for enhanced mass measurement and structural characterization capabilities.[42] The reactions involve the injection and trapping of ions into an ion trap mass analyzer followed by the introduction of ions of the opposite polarity into the same trap. The ions are stored and undergo different reaction depending upon the two sets of ions introduction. The reactions that can occur are proton transfer, electron transfer, metal transfer, covalent bond formation, and charge inversion.[42,43] One method of charge inversion reactions involves switching the polarity of the analyte by introducing a reagent that has more charges than the analyte. There is a long-lived electrostatic complex between the analyte and the reagent, which charge inverts the analyte. The product ions after charge inversion may lead to a deeper understanding of the analyte. Further activation steps can be initiated after charge-inversion for more molecular information.

1.7   Using Mass Spectrometry for Lipid Analysis

Mass spectrometry as a lipid analysis technique dates to the invention of the mass spectrometer by J.J. Thompson who generated gas-phase hydrocarbon ions from decaying lipids using a magnetic sector instrument.[12,44] With the invent of new and improved MS technologies the lipidomics community is moving closer to global lipidome characterization. Most of lipid analysis today is done thanks to the Wolfgang Paul who invented the quadrupole mass analyzer and ion trap.[45] Mass spectrometry allows for sensitive mass analysis and structural characterization of lipids. Like other biological molecules, the molecular weight does not provide enough information about the identity of the lipid thus here is a discussion on how MS can be used for the structural characterization of lipids. ESI allows for both bottom up and top down lipidomic approaches.

1.7.1 Shotgun Lipidomics

ESI is an especially useful method for lipid analysis because it allows for ions to move from being in solution to gas-phase such that the lipids are still intact, and the molecular species can be confidently determined.[29] Shotgun lipidomics is the direct infusion of a crude sample into the mass spectrometer without separation prior analysis.[46] This method easy, fast, and sensitive. Shotgun lipidomics especially benefits from high resolution mass analyzers for intrasource separation of isobaric species. Exact mass measures enable the lipid class and sum composition to be determined.

1.7.2 LC-MS

LC is especially useful because it allows for the separation of intact lipids. LC results are incredibly accurate, reproducible and sensitive. In order to achieve the ability to identify the global separation, LC allows for the separation of lipids based on class and species. Hydrophilic interaction chromatography (HILIC)[47,48] and normal-phase (NP) separation[49] is a method for interclass separation where HILIC is helpful for separation of polar lipid classes and NP enables non-polar lipid separation. Reverse phase (RP)[50,51] and Ag^+ separation[52,53] is used for the separation of molecular species. RPLC can be used for the separation of isomers that only differ in the location of the C=C with the fatty acyl chain. There have been many studies that create 2D[54,55] and even 3D[56] systems where a combination of separation modes is used. RP paired with NP or HILIC are especially common because of their orthogonal modalities. Some challenges of LC approaches are that they require long run times, separation of species cannot always happen in a high throughput manner due to the complexity of lipid extraction samples, and the method alone does not provide informative structural characterization without the use of synthesis standard which are lacking in the lipidomic community.

1.7.3 MS/MS

As mentioned previously, mass analyzers can be placed in tandem to extend the capabilities a MS to allow selective ion characterization. This is especially beneficial for the analysis of complex samples such as human plasma where it is composed on many species of lipids at different *m/z*. Lipid analysis is typically facilitated on a triple quadrupole mass analyzer to allow for the

isolating and probing specific species of interest. Utilization of NLS and PIS enable the profiling of lipids based on their structure. In the case of GPs, positive ion mode fragmentation leads to loss of the headgroups. The differences in the headgroup moieties leads to product ions that are indicative of specific GP class.

Protonated PCs are profiled by performing a PIS for *m/z* 184 leading to a spectrum contain each species that correlate with the loss.[57] The NLS of 141 Da allows for the determination of protonated PEs in a complex mixture.[58] TGs do not have a headgroup on the glycerol backbone so there is not a scanning mechanism to profile all the species within the class.[10] Instead, NLS are used for profiling TGs that contain a specific fatty acyl chain. Each lipid species has a predicted MS/MS spectrum making it possible to characterize lipids in samples. Fragmentation in both positive and negative ion modes allow for the determination of lipid species fatty acyl chain composition to be determined.

1.7.4   Phosphatidylcholine analysis

The glycerol backbone within a PC species is esterified with two fatty acids at the *sn*-1 and *sn*-2 positions. At the *sn*-3 position of the glycerol is a phosphocholine. The PCs naturally occur as zwitterionic species where the positive charge at the quaternary ammonium group is neutralized by the negative charge at the phosphate group. In the ESI process, PCs are readily ionized independent of the pH of the solution. The number of carbons and C=Cs on the fatty acyl chains vary creating different sum composition and masses. The fragmentation of PCs differs in positive and negative ion mode. The PC is ionized in positive ion mode with a proton or alkali metal such as Na^+, Li^+, or K^+ forming $[M + Na]^+$ $[M + Li]^+$, and $[M + K]^+$.[57,59] In negative mode, PC appears as a demethylate species $[M -15]^-$ or is adducted by various ions like Cl^-, CH_3CO_2, etc. Activation of the protonated molecule $[PC + H]^+$ results in an abundant ion at *m/z* 184 corresponding in the phosphocholine ion. Usually FA chain information is inaccessible in positive ion mode due to the low abundance of the FA chain loss as ketene ($[M + H \ RCH =C=O]^+$), although the fragments are still possible and have been used to structural characterization.

Alkaline metals can be used for ionization of PCs ($[M + X]^+$ where X = Na, Li, or K) and fragmentation differs from that of the protonated species. The formation of the metal adduct is dependent on the availability of the alkali ion is the solution thus in most cases there is the presence of a sodiated species in mass spectra due the natural occurs of sodium in solvents. Common

fragmentation among the alkaline metal adducted PCs leads to varies losses of the headgroup. The fragmentation ions produced are a result of a trimethylamine loss, phosphocholine loss, and alkaline cholinephosphate loss ([M + X - 59]$^+$, [M + X - 183]$^+$, and [M + X - (X + 182)]$^+$, respectively. Activation of [M + X]$^+$ also lead to low abundant fragments related to the fatty acyl chains. The chains can be loss as a free fatty acid before and after the loss of the trimethylamine [M + X - RCOOH]$^+$ and [M + X - (RCOOH + 59)]$^+$, respectively, and as an alkaline metal adduct species [M + X - RCOOX]$^+$.[3,57] The fragmentation for fatty acyl chain information is most abundant for the lithiated species but is still relatively low and abundance. A method for obtaining more emphasized fatty acyl chain characterization is by negative ion mode analysis.

Negative ion mode analysis of PCs is typically done via forming adducts to an anionic base that helps ionize the otherwise neutral lipid (in basic conditions) into a negatively charge ion.[57] The anionic complex readily forms the demethylated PC ion [M - 15]$^-$ which sustains its negative charge via the phosphate anion. Both fragmentation of the anionic complex and the demethylate species result in the abundant presence of fatty acyl carboxylate ions for the loss of both chains. The relative abundance of the fatty acyl chain losses may be useful for determining the *sn*-1 and *sn*-2 position in some cases, but the use of intensities for *sn*-position determination is an over simplification in most case. In a negative ion mode CID spectrum, there will also be the presence of the loss of the fatty acyls as free fatty acid and as ketenes, but these fragments are substantially lower in abundance relative to the carboxylate ion. The free fatty acid loss and the ketene loss have found to be a better means for determining *sn*-1 and *sn*-2 position.[60]

1.7.5 Phosphatidylethanolamine analysis

PE structures share a similar assembly as PC species with the only difference being that instead of a choline at the *sn*-3 position of the glycerol backbone there is an ethanolamine group bond to the phosphate.[61] The incorporation of the ethanolamine group leads to different fragmentation ions than what is found for PC in positive ion mode. PEs readily ionization as a protonated species [M + H]$^+$ in positive ion mode. However, the ionization of PEs is less efficient to that of PCs because the fixed quaternary ammonium group provides a permanent charge site.[62–64] CID of the protonated PE species yield an abundant peak for the NL of 141 Da and there may be small fragment ions associated with acylium ions from the loss of each fatty acyl chain. For the

most part MS/MS of PEs in positive ion mode gives information about the polar head group and NLS for the loss of 141 Da can be used for the determination of PEs in a complex mixture of lipids.

PEs adducted with alkaline metals are formed depending on the presents of the metal in the sample solution and fragmentation of these species are similar to that of PCs. The most abundant fragments are related to the neutral loss of the phosphoethanolamine and the phosphoethanolamine with the alkaline metal as $[M + X - 141]^+$ and $[M + X - (140 + X)]^+$, respectively.[57,65] Equivalent to the $[M + X - 59]^+$ for PCs is the $[M + X - 43]^+$ corresponding to the loss of aziridine. There are also fragments corresponding to the loss of the fatty acyl chains as carboxylic acid before the loss of the aziridine $[M + H - RCOOH]^+$, and after $[M + H - (RCOOH + 43)]^+$. The fatty acyl chain is also loss as an alkaline metal adduct $[M + X - (43 + RCOOX)]^+$ $[M + X - RCOOX]^+$. In basic solution conditions, PEs will deprotonate making negative ion mode analysis easy and creating PE ions efficiently even in the presence of PC.[61] The challenge in negative ion mode for PEs the presence of other GPs species that ionize well leading to overlapping isobaric species. The negative ion mode CID spectrum for PEs share the sample pattern as PCs with an additional product ion at *m/z* 196 representing the glycerophosphoethanolamine anion.

1.7.6   Triacylglycerol analysis

TGs species consist of a glycerol molecule with three carboxylic acid chains esterified onto each of the alcohols. Each fatty acyl chain can have varying chain lengths and degrees of unsaturation leading to overall mass differences. However, due to the complexity of the TG composition fatty acyl chain isomers may exist. For example, TG (52:2) could consist of one or a mixture of the following TG (16:0_18:1_18:1), TG (16:0_18:0_18:2), TG (16:0_16:1_20:1), TG (14:1_22:1_16:0), and/or many other compositional isomer. Each of the species contain 52 carbons and two C=C within the aliphatic chains but each fatty acid may vary. The fatty acyls chains present within a subclass of TGs can be determined using CID. Ionization of TGs using ESI is achieved by formation of an ammonium ($[M + NH_4]^+$) or alkali metal adducts (i.e. $[M + Na]^+$/$[M + Li]^+$).[10] Fragmentation patterns like GPs depend on the adducting ion used for ionization. The $[M + NH_4]^+$ ions are commonly probed because of the ease of adding ammonium formate or acetate in LC solvent systems for pH regulation. Activation of the ammonium adducted species leads to a spectrum containing the $[M + H]^+$ and product ions that correspond to the neutral loss of ammonia and each fatty acyl chain as a carboxylic acid $[M + NH_4 - NH_3 - RCOOH]^+$. As many as 12 fatty

acid losses has been seen for a single CID spectrum which makes identifying molecular species a challenge.[66]

Subsequent fragmentation of $[M + NH_4 - NH_3 - RCOOH]^+$ allows for the determination of the two fatty acyl chains remaining on the ions.[67] MS^3 generates an acylium and an acylium ion plus 74 Da for each remaining ion. Thus, the initial MS/MS experiment identifies one of the aliphatic chains and the MS^3 identifies the other two allowing for the identification the molecular species. Although fatty acyl chain composition exists, this method alone does not give the esterification site of the chains along the glycerol backbone.

The CID spectra of $[M + Li]^+$ and $[M + Na]^+$ is more complex than that of a $[M + NH_4]^+$ spectrum. Although the ammonium adducted TG forms the simplest spectrum, it is the most labile of the species.[68] Similar to the $[M + NH_4]^+$ ion, the alkali metal adducted TG lose the fatty acid as a neutral carboxylic acid $[M + X - RCOOH]^+$ (where X = Na or Li). The chain can also be loss as a sodiated or lithiated species $[M + X - RCOOX]^+$ In all cases, there is a preferential cleavage of the *sn-1/3* position over the *sn-2* position. When analyzing biological samples, it is not to be assumed that because a fragment has a larger relative abundance that it is as a result of a *sn-1/3* positional cleavage due to the possibility of multiple isomeric species sharing a fatty acyl chain composition. TGs are not typically analyzed in negative ion mode, however, negative mode analysis is possible through the covalent modification of the C=C of TG species by a thiol containing anionic tag.[69]

1.8   The Paternò–Büchi reaction of mass spectrometry-based lipid analysis

1.8.1   Mechanism

Oxetane rings can be formed using the Paternò–Büchi (PB) reaction.[70] The reaction entails a [2 + 2]-cycloaddition between an excited carbonyl compound and an alkene group. It is photo-initiated via UV-irradiation where the n → π* is accessed allowing for the electron transfer with an alkene to provide two sets of radicals.[71,72] Depending on the compounds that are being reacted, the molecule can form regioisomers. In some case, regioselectivity is present leading to the formation of a single product or a dominant product when one product forms more stable intermediates. Once the oxetane ring is formed the reaction is not reversible using the same wavelength that was used to form the ring.

1.8.2   Shotgun analysis with PB

The use of [2+2]-cycloaddition products for mass spectrometric lipid analysis is not novel to the PB reaction utilization. Ferrer-Correia et al. reported in 1976 that using vinyl methyl ether quasi-molecular ion as a reagent ion is suitable for reacting with olefin species for the determination of double bond position in high pressure mass spectrometry.[73] In these experiments, a four membered ring is formed between two olefin groups and fragments of the ring infer the double bond position. Lipid analysis using the PB reaction takes advantage of regioisomers formation during the synthesis of the oxetane ring. Originally the application of the Paternò–Büchi reaction for the structural analysis of lipids was reported by Ma et al. in 2014.[74] Acetone was used as a solvent and the carbonyl reagent such that upon UV-irradiation the excited molecule forms an oxetane ring with the lipid unsaturation site. In the case of polyunsaturated lipid species, each molecule within a sample may form an oxetane ring at any of the C=C positions thus creating a mixture species modified at different unsaturation sites. The modified lipids are then ionized via electrospray ionization (ESI) and activated via collision induced dissociation (CID). The activated species fragments to diagnostic ions which are 26 Da apart. These ions are indicative of the lipid fragmenting at the oxetane ring that was formed via the PB reaction. The method confidently determine the C=C location with fatty acids and glycerophospholipids.[74] The method was later determined to be useful the quantitation of unsaturated lipid species.[75] The efficiency of the reaction is low thus a method to improve was by changing the reaction apparatus. A simple means of initiating the reaction is by placing the reactor at the interface of the instrument and allow the reaction to occur during the ionization process. Another means of conducting the reaction is the use a flow microreactor that flows the lipid solution through a UV transparent capillary and transfers the solution to an ESI sources for MS analysis. The use of a flow microreactor enables the increased reaction efficiency by allowing the control of exposure time, flow rate, and an even exposure of the UV.[76] The reaction yield using the microreactor was 40-50% compared to the a 10% reaction from doing an offline batch reaction in a quarts tube. The expansion of the PB reaction onto all unsaturated fatty acyl chain containing lipids would be beneficially for structural characterization. The unsaturation sites within cholesteryl ester have be probed such that MS[3] spectra give rise to diagnostic ions corresponding to the C=C locations.[77]. Pairing trapped ion mobility spectrometry (TIMS) with the PB reaction for conjugated fatty acids analysis shows enables the determination of C=C within the chain. The PB reaction of CFAs showed to have high

regioselectivity and forms unique diagnostic ions and geometric isomers are separated by TIMS.[78] Benzophenone and acetylpyridine are two reagents that have shown to be beneficial for lipid analysis. Benzophenone as a molecular weight of 182 Da allowing for the PB product to be easily distinguish from the intact lipid species after reaction. After activation of the PB product, diagnostic ions spaced 150 Da apart helps finding the number of C=C within a species.[79] After the PB reaction, the product can be applied to a RPLC column for molecular species separation and was flowed by MS/MS experiments. Acetylpyridine enables the charging of unsaturated lipids for enhancement of positive ion mode signal and the assignment of C=C positions.[80] The reagent was successful at ionizing and characterizing fatty acids, fatty acid esters, cholesteryl esters, triglycerides, and unsaturated hydrocarbons. Acetophenone is another applicable reagent for the PB reaction. After modification, UVPD is applied to PC and the reagent acts as a chromophore that increased dissociation selectivity.[81]

Online LC experiments have also been accomplished. LC was used for the separation and characterization of bis(monooleoylglycero) phosphate and dioleoyl-phosphatidylglycerol [82]. A HILIC column was used for the separation of GPs class and a post column PB reaction microreactor enabled C=C locations to be determined for analysis human plasma for breast cancer and type II diabetes patients. It was found that C=C location ratios are more robust than looking at sum composition and fatty acyl chain level.[48]

1.8.3   The PB reaction on tissue samples

The PB reaction was coupled with a surface-coated probe (SCP) for microscale in-situ analysis and determination of C=C location isomers.[83] A biocompatible solid-phase microextraction (SPME) probe was used for microscale sampling and extraction. Benzophenone was used as a PB reagent for the determination of the C=C. A stainless-steel wire was used for the *in-situ* sampling of lipids in tissues followed by in-capillary extraction of lipid and application of the PB reaction onto the capillary. [84,85] This method enables the rapid analysis of GPs C=C isomers in rat brain. Localization of lipids species within a tissue sample is useful for understanding the importance of specific species within a biological system. Mass spectrometry imaging is the only tool that allows for the visualization of the distribution of C=C isomers within a sample. Benzaldehyde was used as a MALDI matrix and PB reaction reagent for the imaging of C=C

isomers distributions.[86] Using this method, GPs and glycolipid species were characterized and their distribution within brain tissues were imaged.

1.9   Thesis Objective

One of the challenges faced by mass spectrometric approaches for lipid structural elucidation is determining the C=C location of individual molecular species. Low-energy CID form structurally informative information regarding unsaturation site thus establishing methodologies to approach this challenge is necessary. The main objective of this thesis is to demonstration a C=C probing technique that can be made compatible with multiple MS-based systems for lipid characterization. The PB reaction is used for the modification of lipid species to C=C localization. Chapter 2 evaluates the use of the PB reaction combined with charge inversion via ion/ion reactions for in-depth molecular species identification. Chapter 3 describe the incorporation of the headgroup modification with the analysis of the PB and ion/ion reactions for improved ionization of GPs with structural characterization. In chapter 4, a method for the analysis of TG species is developed that involves the online PB reaction and LC-MS/MS experiments. Chapter 5 gives an overall conclusion and ideas for future directions of MS-based lipid analysis.

1.10   References

1. Fahy, E. *et al.* Update of the LIPID MAPS comprehensive classification system for lipids. *Journal of Lipid Research* **50**, S9–S14 (2009).

2. Quehenberger, O. The Human Plasma Lipidome. *The New England Journal of Medicine* 12 (2011).

3. Pulfer, M. & Murphy, R. C. Electrospray mass spectrometry of phospholipids. *Mass Spectrometry Reviews* **22**, 332–364 (2003).

4. van Meer, G. Cellular lipidomics. *EMBO J* **24**, 3159–3165 (2005).

5. Pike, L. J. Lipid rafts: bringing order to chaos. *J. Lipid Res.* **44**, 655–667 (2003).

6. Ståhlman, M. *et al.* Clinical dyslipidaemia is associated with changes in the lipid composition and inflammatory properties of apolipoprotein-B-containing lipoproteins from women with type 2 diabetes. *Diabetologia* **55**, 1156–1166 (2012).

7. Bou Khalil, M. *et al.* Lipidomics era: Accomplishments and challenges. *Mass Spectrometry Reviews* **29**, 877–929 (2010).

8. Zhao, Y.-Y., Vaziri, N. D. & Lin, R.-C. Lipidomics. in *Advances in Clinical Chemistry* vol. 68 153–175 (Elsevier, 2015).

9. Xu, Y. & Brenna, J. T. Atmospheric Pressure Covalent Adduct Chemical Ionization Tandem Mass Spectrometry for Double Bond Localization in Monoene- and Diene-Containing Triacylglycerols. *Analytical Chemistry* **79**, 2525–2536 (2007).

10. Murphy, R. C. Chapter 4. Glyceryl Esters. in *Tandem Mass Spectrometry of Lipids: Molecular Analysis of Complex Lipids* 105–129 (Royal Society of Chemistry, 2014). doi:10.1039/9781782626350-00105.

11. Murphy, R. C. *Tandem Mass Spectrometry of Lipids: Molecular Analysis of Complex Lipids*. (The Royal Society of Chemistry, 2015). doi:10.1039/9781782626350.

12. Functional Lipidomics. 350.

13. Brügger, B. Lipidomics: Analysis of the Lipid Composition of Cells and Subcellular Organelles by Electrospray Ionization Mass Spectrometry. *Annu. Rev. Biochem.* **83**, 79–98 (2014).

14. Fuchs, B., Süß, R., Teuber, K., Eibisch, M. & Schiller, J. Lipid analysis by thin-layer chromatography—A review of the current state. *Journal of Chromatography A* **1218**, 2754–2774 (2011).

15. Li, J., Vosegaard, T. & Guo, Z. Applications of nuclear magnetic resonance in lipid analyses: An emerging powerful tool for lipidomics studies. *Progress in Lipid Research* **68**, 37–56 (2017).

16. Spyros, A. & Dais, P. Application of ^{31}P NMR Spectroscopy in Food Analysis. 1. Quantitative Determination of the Mono- and Diglyceride Composition of Olive Oils. *J. Agric. Food Chem.* **48**, 802–805 (2000).

17. Mareš, P. High temperature capillary gas liquid chromatography of triacylglycerols and other intact lipids. *Progress in Lipid Research* **27**, 107–133 (1988).

18. Hinz, C., Liggi, S. & Griffin, J. L. The potential of Ion Mobility Mass Spectrometry for high-throughput and high-resolution lipidomics. *Current Opinion in Chemical Biology* **42**, 42–50 (2018).

19. Yamada, T. *et al.* Development of a lipid profiling system using reverse-phase liquid chromatography coupled to high-resolution mass spectrometry with rapid polarity switching and an automated lipid identification software. *Journal of Chromatography A* **1292**, 211–218 (2013).

20. Paine, M. R. L. *et al.* Mass Spectrometry Imaging with Isomeric Resolution Enabled by Ozone-Induced Dissociation. *Angewandte Chemie International Edition* **57**, 10530–10534 (2018).

21. Gross, J. H. *Mass Spectrometry: A Textbook*. (Springer-Verlag Berlin Heidelberg, 2004).

22. Karas, M., Bachmann, D., Bahr, U. & Hillenkamp, F. Matrix-assisted ultraviolet laser desorption of non-volatile compounds. *International Journal of Mass Spectrometry and Ion Processes* **78**, 53–68 (1987).

23. Fenn, J. B., Mann, M., Meng, C. K., Wong, S. F. & Whitehouse, C. M. Electrospray ionization-principles and practice. *Mass Spectrom. Rev.* **9**, 37–70 (1990).

24. Yamashita, M. & Fenn, J. B. Electrospray ion source. Another variation on the free-jet theme. *The Journal of Physical Chemistry* **88**, 4451–4459 (1984).

25. Gross, R. W. & Han, X. Lipidomics at the Interface of Structure and Function in Systems Biology. *Chemistry & Biology* **18**, 284–291 (2011).

26. Fenn, J., Mann, M., Meng, C., Wong, S. & Whitehouse, C. Electrospray ionization for mass spectrometry of large biomolecules. *Science* **246**, 64–71 (1989).

27. Covey, T. R., Bonner, R. F., Shushan, B. I., Henion, J. & Boyd, R. K. The determination of protein, oligonucleotide and peptide molecular weights by ion-spray mass spectrometry. *Rapid Commun. Mass Spectrom.* **2**, 249–256 (1988).

28. Weintraub, S. T., Pinckard, R. N., Hail, M. & Gaskell, S. J. Electrospray ionization for analysis of platelet-activating factor. *Rapid Commun. Mass Spectrom.* **5**, 309–311 (1991).

29. Duffin, K. L., Henion, J. D. & Shieh, J. J. Electrospray and tandem mass spectrometric characterization of acylglycerol mixtures that are dissolved in nonpolar solvents. *Anal. Chem.* **63**, 1781–1788 (1991).

30. Rustam, Y. H. & Reid, G. E. Analytical Challenges and Recent Advances in Mass Spectrometry Based Lipidomics. *Analytical Chemistry* **90**, 374–397 (2018).

31. Lee, H.-R., Kochhar, S. & Shim, S.-M. Comparison of Electrospray Ionization and Atmospheric Chemical Ionization Coupled with the Liquid Chromatography-Tandem Mass Spectrometry for the Analysis of Cholesteryl Esters. *International Journal of Analytical Chemistry* **2015**, 1–6 (2015).

32. Wolff, M. M. & Stephens, W. E. A Pulsed Mass Spectrometer with Time Dispersion. *Review of Scientific Instruments* **24**, 616–617 (1953).

33. Cotter, R. J. The New Time-of-Flight Mass Spectrometry. *Anal. Chem.* **71**, 445A-451A (1999).

34. March, R. E. An Introduction to Quadrupole Ion Trap Mass Spectrometry. *JOURNAL OF MASS SPECTROMETRY* **32**, 19 (1997).

35. Knight, R. The General Form of the Quadrupole Ion Trap Potential. *International Journal of Mass Spectrometry and Ion Physics,* **51**, 127–131 (1983).

36. Dawson, P. *Quadrupole mass spectrometry and its applications*. (Elsevier: Amsterdam, 1976).

37. Axelsson, J., Palmblad, M. & Ha, K. Electron capture dissociation of substance P using a commercially available Fourier transform ion cyclotron resonance mass spectrometer. *Rapid Commun. Mass Spectrom.* 4 (1999).

38. McLuckey, S. A. & Goeringer, D. E. SPECIAL FEATURE:TUTORIAL Slow Heating Methods in Tandem Mass Spectrometry. *Journal of Mass Spectrometry* **32**, 461–474 (1997).

39. Goeringer, D. E. & McLuckey, S. A. Evolution of ion internal energy during collisional excitation in the Paul ion trap: A stochastic approach. *The Journal of Chemical Physics* **104**, 2214–2221 (1996).

40. Xia, Y., Liang, X. & McLuckey, S. A. Ion Trap versus Low-Energy Beam-Type Collision-Induced Dissociation of Protonated Ubiquitin Ions. *Anal. Chem.* **78**, 1218–1227 (2006).

41. de Hoffmann, E. Tandem mass spectrometry: A primer. 10.

42. Prentice, B. M. & McLuckey, S. A. Gas-phase ion/ion reactions of peptides and proteins: acid/base, redox, and covalent chemistries. *Chem. Commun.* **49**, 947–965 (2013).

43. McLuckey, S. A. & Huang, T.-Y. Ion/Ion Reactions: New Chemistry for Analytical MS. *Anal. Chem.* **81**, 8669–8676 (2009).

44. Thomson, J. J. Rays of positive electricity. *The London, Edinburgh, and Dublin Philosophical Magazine and Journal of Science* **21**, 225–249 (1911).

45. Paul, W. & Steinwedel, H. A New Spectrometer without a Magnetic Field. *Zeitschrift fuer Naturforschung (West Germany) Divided into Z. Nautrforsch., A, and Z. Naturforsch., B: Anorg. Chem., Org. Chem., Biochem., Biophys* **: a8**, (1953).

46. Han, X. & Gross, R. W. Shotgun lipidomics: Electrospray ionization mass spectrometric analysis and quantitation of cellular lipidomes directly from crude extracts of biological samples. *Mass Spectrometry Reviews* **24**, 367–412 (2005).

47. Vosse, C., Wienken, C., Cadenas, C. & Hayen, H. Separation and identification of phospholipids by hydrophilic interaction liquid chromatography coupled to tandem high resolution mass spectrometry with focus on isomeric phosphatidylglycerol and bis(monoacylglycero)phosphate. *Journal of Chromatography A* **1565**, 105–113 (2018).

48. Zhang, W. *et al.* Online photochemical derivatization enables comprehensive mass spectrometric analysis of unsaturated phospholipid isomers. *Nature Communications* **10**, (2019).

49. McLaren, D. G. *et al.* An ultraperformance liquid chromatography method for the normal-phase separation of lipids. *Analytical Biochemistry* **414**, 266–272 (2011).

50. Ovčačíková, M., Lísa, M., Cífková, E. & Holčapek, M. Retention behavior of lipids in reversed-phase ultrahigh-performance liquid chromatography–electrospray ionization mass spectrometry. *Journal of Chromatography A* **1450**, 76–85 (2016).

51. Momchilova, S., Tsuji, K., Itabashi, Y., Nikolova-Damyanova, B. & Kuksis, A. Resolution of triacylglycerol positional isomers by reversed-phase high-performance liquid chromatography. *Journal of Separation Science* **27**, 1033–1036 (2004).

52. Holčapek, M. & Lísa, M. Silver-Ion Liquid Chromatography–Mass Spectrometry. in *Handbook of Advanced Chromatography /mass Spectrometry Techniques* 115–140 (Elsevier, 2017). doi:10.1016/B978-0-12-811732-3.00004-2.

53. Holčapek, M., VelÃnskÃ¡, H., LÃsa, M. & Česla, P. Orthogonality of silver-ion and non-aqueous reversed-phase HPLC/MS in the analysis of complex natural mixtures of triacylglycerols. *Journal of Separation Science* **32**, 3672–3680 (2009).

54. Lísa, M., Cífková, E. & Holčapek, M. Lipidomic profiling of biological tissues using off-line two-dimensional high-performance liquid chromatography–mass spectrometry. *Journal of Chromatography A* **1218**, 5146–5156 (2011).

55. Wang, S. *et al.* A novel stop-flow two-dimensional liquid chromatography–mass spectrometry method for lipid analysis. *Journal of Chromatography A* **1321**, 65–72 (2013).

56. Wang, S., Shi, X. & Xu, G. Online Three Dimensional Liquid Chromatography/Mass Spectrometry Method for the Separation of Complex Samples. *Anal. Chem.* **89**, 1433–1438 (2017).

57. Chapter 5. Glycerophospholipids. in *New Developments in Mass Spectrometry* 130–193 (Royal Society of Chemistry, 2014). doi:10.1039/9781782626350-00130.

58. Isaac, G. Electrospray Ionization Tandem Mass Spectrometry (ESI-MS/MS)-Based Shotgun Lipidomics. in *Metabolic Profiling* (ed. Metz, T. O.) vol. 708 259–275 (Humana Press, 2011).

59. Han, X. *Lipidomics: Comprehensive mass spectrometry of lipids*. (John Wiley & Sons, 2016).

60. Hsu, F.-F. & Turk, J. Charge-remote and charge-driven fragmentation processes in diacyl glycerophosphoethanolamine upon low-energy collisional activation: A mechanistic proposal. *J Am Soc Mass Spectrom* **11**, 892–899 (2000).

61. Colsch, B., Fenaille, F., Warnet, A., Junot, C. & Tabet, J.-C. Mechanisms governing the fragmentation of glycerophospholipids containing choline and ethanolamine polar head groups. *European Journal of Mass Spectrometry* **23**, 427–444 (2017).

62. Wasslen, K. V., Canez, C. R., Lee, H., Manthorpe, J. M. & Smith, J. C. Trimethylation Enhancement Using Diazomethane (TrEnDi) II: Rapid In-Solution Concomitant Quaternization of Glycerophospholipid Amino Groups and Methylation of Phosphate Groups via Reaction with Diazomethane Significantly Enhances Sensitivity in Mass Spectrometry Analyses via a Fixed, Permanent Positive Charge. *Analytical Chemistry* **86**, 9523–9532 (2014).

63. Canez, C. R. *et al.* Trimethylation Enhancement Using ^{13}C-Diazomethane (^{13}C-TrEnDi): Increased Sensitivity and Selectivity of Phosphatidylethanolamine, Phosphatidylcholine, and Phosphatidylserine Lipids Derived from Complex Biological Samples. *Analytical Chemistry* **88**, 6996–7004 (2016).

64. Betancourt, S. K. *et al.* Trimethylation Enhancement Using ^{13}C-Diazomethane: Gas-Phase Charge Inversion of Modified Phospholipid Cations for Enhanced Structural Characterization. *Analytical Chemistry* **89**, 9452–9458 (2017).

65. Hsu, F.-F. & Turk, J. Electrospray ionization with low-energy collisionally activated dissociation tandem mass spectrometry of glycerophospholipids: Mechanisms of fragmentation and structural characterization. *Journal of Chromatography B* **877**, 2673–2695 (2009).

66. Murphy, R. C. Challenges in mass spectrometry-based lipidomics of neutral lipids. *TrAC Trends in Analytical Chemistry* **107**, 91–98 (2018).

67. Hsu, F.-F. & Turk, J. Structural characterization of triacylglycerols as lithiated adducts by electrospray ionization mass spectrometry using low-energy collisionally activated dissociation on a triple stage quadrupole instrument. *Journal of the American Society for Mass Spectrometry* **10**, 587–599 (1999).

68. Herrera, L. C., Potvin, M. A. & Melanson, J. E. Quantitative analysis of positional isomers of triacylglycerols via electrospray ionization tandem mass spectrometry of sodiated adducts. *Rapid Communications in Mass Spectrometry* **24**, 2745–2752 (2010).

69. Adhikari, S., Zhang, W., Xie, X., Chen, Q. & Xia, Y. Shotgun Analysis of Diacylglycerols Enabled by Thiol–ene Click Chemistry. *Analytical Chemistry* **90**, 5239–5246 (2018).

70. D'Auria, M. & Racioppi, R. Oxetane Synthesis through the Paternò-Büchi Reaction. *Molecules* **18**, 11384–11428 (2013).

71. D'Auria, M. The Paternò–Büchi reaction – a comprehensive review. *Photochem. Photobiol. Sci.* 10.1039.C9PP00148D (2019) doi:10.1039/C9PP00148D.

72. Brogaard, R. Y. *et al.* The Paternò–Büchi reaction: importance of triplet states in the excited-state reaction pathway. *Phys. Chem. Chem. Phys.* **14**, 8572 (2012).

73. Ferrer-Correia, A. J. V., Jennings, K. R. & Sharma, D. K. S. The use of ion-molecule reactions in the mass spectrometric location of double bonds. *Org. Mass Spectrom.* **11**, 867–872 (1976).

74. Ma, X. & Xia, Y. Pinpointing Double Bonds in Lipids by Paternò-Büchi Reactions and Mass Spectrometry. *Angewandte Chemie International Edition* **53**, 2592–2596 (2014).

75. Ma, X. *et al.* Identification and quantitation of lipid C=C location isomers: A shotgun lipidomics approach enabled by photochemical reaction. *Proceedings of the National Academy of Sciences* **113**, 2573–2578 (2016).

76. Stinson, C. A. & Xia, Y. A method of coupling the Paternò–Büchi reaction with direct infusion ESI-MS/MS for locating the C☐C bond in glycerophospholipids. *The Analyst* **141**, 3696–3704 (2016).

77. Ren, J., Franklin, E. T. & Xia, Y. Uncovering Structural Diversity of Unsaturated Fatty Acyls in Cholesteryl Esters via Photochemical Reaction and Tandem Mass Spectrometry. *Journal of The American Society for Mass Spectrometry* **28**, 1432–1441 (2017).

78. Xie, X. & Xia, Y. Analysis of Conjugated Fatty Acid Isomers by the Paternò-Büchi Reaction and Trapped Ion Mobility Mass Spectrometry. *Anal. Chem.* **91**, 7173–7180 (2019).

79. Xu, T., Pi, Z., Song, F., Liu, S. & Liu, Z. Benzophenone used as the photochemical reagent for pinpointing C=C locations in unsaturated lipids through shotgun and liquid chromatography-mass spectrometry approaches. *Analytica Chimica Acta* **1028**, 32–44 (2018).

80. Esch, P. & Heiles, S. Charging and Charge Switching of Unsaturated Lipids and Apolar Compounds Using Paternò-Büchi Reactions. *Journal of The American Society for Mass Spectrometry* (2018) doi:10.1007/s13361-018-2023-x.

81. Wäldchen, F., Becher, S., Esch, P., Kompauer, M. & Heiles, S. Selective phosphatidylcholine double bond fragmentation and localisation using Paternò–Büchi reactions and ultraviolet photodissociation. *Analyst* **142**, 4744–4755 (2017).

82. Jeck, V., Korf, A., Vosse, C. & Hayen, H. Localization of double-bond positions in lipids by tandem mass spectrometry succeeding high-performance liquid chromatography with post-column derivatization. *Rapid Commun Mass Spectrom* **33**, 86–94 (2019).

83. Deng, J. *et al.* Coupling Paternò-Büchi Reaction with Surface-Coated Probe Nanoelectrospray Ionization Mass Spectrometry for In Vivo and Microscale Profiling of Lipid C=C Location Isomers in Complex Biological Tissues. *Anal. Chem.* **91**, 4592–4599 (2019).

84. Su, Y. *et al.* Mapping lipid C=C location isomers in organ tissues by coupling photochemical derivatization and rapid extractive mass spectrometry. *International Journal of Mass Spectrometry* **445**, 116206 (2019).

85. Zou, R. *et al.* Point-of-Care Tissue Analysis Using Miniature Mass Spectrometer. *Anal. Chem.* **91**, 1157–1163 (2019).

86. Bednařík, A., Bölsker, S., Soltwisch, J. & Dreisewerd, K. An On-Tissue Paternò-Büchi Reaction for Localization of Carbon-Carbon Double Bonds in Phospholipids and Glycolipids

by Matrix-Assisted Laser-Desorption-Ionization Mass-Spectrometry Imaging. *Angewandte Chemie International Edition* **57**, 12092–12096 (2018).

.

CHAPTER 2. IN-DEPTH STRUCTURAL CHARACTERIZATION OF PHOSPHOLIPIDS BY PAIRING SOLUTION PHOTOCHEMICAL REACTION WITH CHARGE INVERSION ION/ION CHEMISTRY

2.1 Abstract

Shotgun lipid analysis based on electrospray ionization-tandem mass spectrometry (ESI-MS/MS) is increasingly used in lipidomic studies. One challenge for the shotgun approach is the discrimination of lipid isomers and isobars. Gas-phase charge inversion via ion/ion reactions has been used as an effective method to identify multiple isomeric/isobaric components in a single MS peak by exploiting the distinctive functionality of different lipid classes. In doing so, fatty acyl chain information can be obtained without recourse to condensed-phase separations or derivatization. This method alone, however, cannot provide carbon-carbon double bond (C=C) location information from fatty acyl chains. Herein, we provide an enhanced method pairing photochemical derivatization of C=C via the Paternò–Büchi reaction with charge inversion ion/ion tandem mass spectrometry. This method was able to provide gas-phase separation of phosphatidylcholines and phosphatidylethanolamines, the fatty acyl compositions, and the C=C location within each fatty acyl chain. We have successfully applied this method to bovine liver lipid extracts and identified 40 molecular species of glycerophospholipids with detailed structural information including head group, fatty acyl composition, and C=C location.

2.2 Introduction

Amongst all the classes of lipids in mammalian cells, glycerophospholipids (GPs) are the most abundant, constituting approximately 60 mol% of lipid mass within the cell membrane.[1-2] GPs are the key component in cell membrane structure3; they function as signaling molecules[1,2] and secondary messengers in cell metabolism.[1-3] GP profiles have been used as phenotypical signals[3-5] for imaging of diseased tissues[6] and systems biology studies.[7-9] GPs are assembled from

three building blocks, a glycerol backbone, two fatty acyl or alkyl chains linked at the *sn1* and *sn2* positions of the glycerol, and a phosphate-containing head group.[10-13] The identity of the head group defines the GP subclass; for example, phosphatidylethanolamine (PE) and phosphatidylcholine (PC) head groups consist of ethanolamine and choline esterified to the phosphate, respectively.

Lipid analysis via mass spectrometry (MS) can be performed using two main approaches: liquid chromatography-mass spectrometry (LC/MS) and direct-infusion electrospray mass spectrometry. The use of LC/MS allows for complex lipid components in a sample to undergo chromatographic separation prior to being analyzed by the MS, thus providing increased sensitivity and selectivity.[14-17] Direct-infusion electrospray mass spectrometry, or shotgun lipid analysis, is a fast and sensitive method that analyzes the lipids directly from the crude extract without chromatographic separation.[18-24] Shotgun analysis benefits from the use of high-resolution MS instruments, which helps distinguish isobaric peaks and allows for more accurate identification due to better peak separation. However, high mass resolving power alone cannot provide isomeric separation. Separation in shotgun lipidomic approaches can also be done via in-solution modifications. Functional group selective modification, such as targeting the vinyl ether bond,4 on the GP head groups[25,26], or a one-step methylation of the phosphate,[27] has been demonstrated to improve identification and quantitation for isomeric/isobaric GPs and boosting the detection of low abundance GPs.

Gas-phase ion/ion reactions have been used to separate isomeric and isobaric species post-ionization thereby obviating the need for in-solution modification. Spraying PCs and PEs in the positive ion mode and subjecting the ions to gas-phase ion/ion interaction with a dicarboxylate reagent effectively charge inverts the cationic lipids and separates PC and PE isomers based on distinct reaction chemistry between their head groups and the reagent.[28,29] The negatively charged ions resulting from charge inversion ion/ion reactions provide abundant fatty acyl fragment ions upon collision-induced dissociation (CID), leading to confident identification of fatty acyl composition including the number of carbons and degree of unsaturation.[30-31] However, the carbon-carbon double bond (C=C) location cannot be determined from such a process.

Notable gas-phase activation methods of determining C=C location of lipids include charge-remote fragmentation induced by high energy CID,[32] ozone-induced dissociation (OzID),[33-35] 193 nm ultraviolet photodissociation (UVPD),[36] radical directed dissociation (RDD),[37,38] helium

metastable atom-activated dissociation (He-MAD),[39,40] and electron impact excitation of ions from organics (EIEIO).[41,42] All these methods either utilize high-energy collisions or require significant instrument alterations. The Xia group introduced using UV-initiated reactions without instrument modification for localization of C=Cs, including ozonolysis[43,44] and the in-solution Paternò–Büchi (PB).[45-48] The PB reaction has been employed with subsequent ESI-MS/MS via low energy CID on multiple classes of lipids.[49] In such a method, acetone serves both as the PB reagent and a co-solvent for ESI-MS of lipids. Upon 254 nm UV irradiation of the solution, acetone selectively adds onto a C=C, forming a four-membered oxetane ring structure. Low energy CID of the PB reaction products ruptures the oxetane ring yielding fragment ions that are specific to the C=C location. The PB-MS/MS method is versatile as it can be performed on various MS instruments that have CID and ESI capabilities. Confident structural identification of unsaturated GPs at C=C location level builds upon the capability of determining fatty acyl/alkyl composition. For situations where lipids experience competitive ion suppression, such as detecting lower abundance PC in negative ion mode, or when lipid isobaric and isomeric isomers co-exist, fatty acyl chain assignment from MS^2 CID in negative ion mode is often complicated by chemical interferences.[47] Combining the in-solution PB reaction and the gas-phase charge inversion reaction is promising for high level characterization of GP structures for shotgun lipidomics. In this study, synthetic standards of unsaturated PC and PE were used for method development. The performance of pairing the PB reaction with ion/ion charge inversion for complex mixture analysis was evaluated with a polar lipid extract of bovine liver, which led to confident identification of 40 PC and PE molecular species with detailed structural information including head group, fatty acyl composition, and C=C location.

2.3   Materials & Methods

2.3.1   Nomenclature.

We follow the lipid annotation recommended by LIPID MAPS.[50] In short, PC 16:0_18:2(Δ9,12) identifies the phosphocholine (PC) head group, two fatty acyl chains with the carbon number (the value before the colon, *i.e.* 16 and 18), the degree of unsaturation (the value after the colon, *i.e.* 0 and 2), and the location of C=C counting from the carboxylic carbon towards the fatty chain end (*i.e.* Δ9 and Δ12 in C18:2). The underscore (_) suggests that the *sn*-positions

of fatty acyl chains are not specified, while a forward slash (/), identifies the fatty acyls occupy the *sn*1 and *sn*2 location, respectively, as the order indicated in the annotation. Only when the conformation of a C=C is known, a letter E or Z is used to indicate the trans- or cis-conformation, respectively.

2.3.2   Materials.

1-palmitoyl-2-oleoyl-glycero-3-phosphocholine (PC 16:0/18:1(9Z)), *1-palmitoyl-2-oleoyl-sn-glycero-3-phosphoethanolamine* (PE 16:0/18:1(9Z)), and polar lipid extract of bovine liver (in chloroform) were purchased from Avanti Polar Lipid, Inc. (Alabaster, AL). 1,4-phenylenedipropionic acid (PDPA) and ammonium acetate were purchased from Sigma Aldrich (St. Louis, MO). Formic acid was purchased from Fisher Chemical. Organic solvents were LC-grade, and ultrapure water was obtained from a purification system at 0.03 µS cm.

2.3.3   The PB Reactions Setup.

A flow microreactor was constructed using UV transparent fused silica capillary as the flow cell (fluoropolymer-coated, 100 µm i.d. 363 µm o.d.; Polymicro Technologies/Molex; Phoenix, AZ). The fused silica capillary and a low-pressure mercury lamp with emission centered around 254 nm wavelength (BHK, Inc. Ontario, CA) were placed in parallel with a 1 cm distance, providing an effective UV exposure length of 4 cm. For safety considerations, the reactor was enclosed in an aluminum-lined cardboard box to prevent stray UV light. When conducting the PB reaction, the UV lamp was turned on and the lipid solution was pumped through the reactor via a syringe pump at a flowrate of 4-6 µL/min, enabling 4-5 second reaction times. All lipids were dissolved in 69/29/1/1 (v/v/v/v) of acetone/water/formic acid/isopropyl alcohol solution for the PB reaction. Ammonium acetate (10 mM) was added to the solvent system for conducting experiments when direct-injection negative ion mode was used. About 5-10 µL of the reaction solution was collected in a pre-pulled nanoESI tip and immediately subjected to subsequent MS analysis.

2.3.4   Mass Spectrometry

For prior analysis of the lipids in the bovine liver polar lipid extract, samples were analyzed using a QTRAP 4000 hybrid triple quadrupole/linear ion-trap mass spectrometer (Sciex, Toronto,

ON, Canada) equipped with a home-built nanoESI source. The lipid extract was diluted to 100 µM in a 69/29/1/1 (v/v/v/v) of acetone/water/formic acid/isopropyl alcohol solvent system. Mass spectrometer parameters were as follows: spray voltage 1450-1600 V; curtain gas, 3 psi; declustering potential, 80 V; collision gas, high. Precursor ion scan (PIS) and neutral loss (NL) scan (NLS) were employed to identify the head group of the GPs.

2.3.5   Gas-phase charge inversion ion/ion reactions.

Structural analyses were performed using a TripleTOF 5600 triple quadruple/time-of-flight mass spectrometer (Sciex, Concord, ON, Canada) that was previously modified to perform mutual storage of cation and anions.[51] The dual nanoESI emitter setup allowed sequential formation of the PB modified lipid cations and PDPA dianions ([PDPA - 2H]$^{2-}$), which were each mass selected in Q1 and transferred into the q2 linear ion trap for ion/ion reactions. The ions in q2 were mutually stored for 30 ms and the products of interest were isolated via a notched broadband waveform. CID was performed using a single frequency resonance excitation at *q-value* of 0.18. Third generation ion of interest was fragmented by placing it at a *q-value* of 0.14 and implementing a third resonance excitation event.

2.4   Results and Discussion

2.4.1   Conducting the PB reactions in an off-line microreactor.

A graphic representation of the off-line flow microreactor for conducting the PB reaction is shown in Figure 2.1a and the reaction scheme is shown in Figure 2.1b. We have previously shown that using a flow microreactor to initiate the PB reaction allows for high photon efficiency leading to higher yield and the ability to control side reactions.[46] This setup is especially beneficial for the dual-emitter apparatus for alternatively injecting cations and anions for ion/ion reactions. The PB reaction conditions for unsaturated PC and PE were optimized by monitoring the PB product percent yield (the relative ion intensity of the PB products normalized to that of the intact lipid before UV exposure), using PC 16:0/18:1(9Z) and PE 16:0/18:1(9Z) as model compounds, respectively. Figure 2.1c and 1d represent typical nanoESI-MS spectra of the unsaturated PC and PE after the PB reactions. The PB products are clearly detected at *m/z* 818.7 for protonated PC

44

16:0/18:1(9Z), of the form $[^{PB}PC + H]^+$ in Figure 2.1c and at *m/z* 776.7 for protonated PE 16:0/18:1(9Z), of the form $[^{PB}PE + H]^+$ in Figure 2.1d, with limited evidence for side reactions resulting from Norrish Type I cleavage of acetone.[46] These PB products have a characteristic 58 Da increase in mass relative to the intact lipids, consistent with one acetone addition to the C=C in lipids. By monitoring the reaction kinetics, we found the PB reaction of PC 16:0/18:1(9Z) plateaued at approximately 6 seconds with 35% yield (inset of Figure 2.1c). For PE 16:0/18:1(9Z), the PB reaction yield was maximized around 3 seconds at 30% (kinetic curve shown in the inset of Figure 2.1d), while longer reaction times slightly decreased the yield due to increased contributions from side reactions. Based on these observations, the reaction time used for later studies was generally between 4-5 seconds to ensure adequate PB product yield and minimize the extent of side reactions.
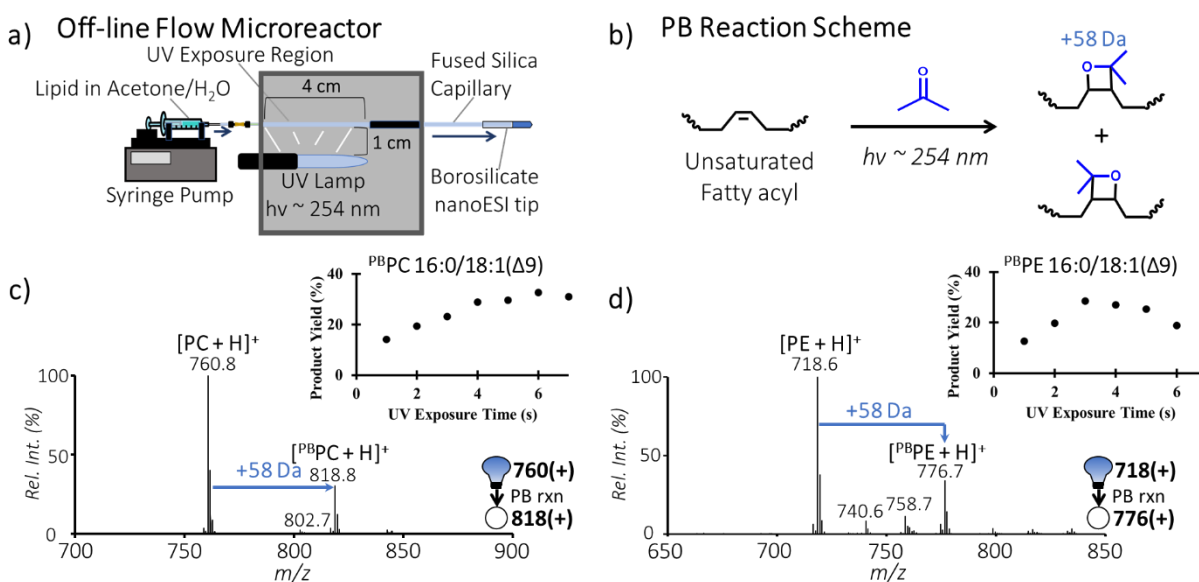
Figure 2.1. a) Schematic of an off-line flow microreactor for conducting the PB reaction; b) The PB reaction scheme, involving acetone addition to a C=C in a fatty acyl chain; the positive ion mode nanoESI-MS spectra of c) 5 µM PC 16:0/18:1(9Z) after 5 s UV exposure d) 5 µM PE 16:0/18:1(9Z) after 4 s UV exposure. Insets in c) and d) represent the PB reaction kinetic curve of PC and PE standard, respectively, with respect to UV exposure time. Positively charged ions are represented by (+).

2.4.2 Charge inversion of the PB reaction products.

Using the optimized PB conditions for unsaturated PC and PE, we further explored pairing the PB reaction with charge inversion ion/ion reactions and subsequent CID experiments for structural characterization to the C=C location level. The typical workflow for unsaturated PC analysis is illustrated in Figure 2.2 and Figure 2.3a-c, using the model compound PC 16:0/18:1(9Z) as an example. First, the PB product of PC 16:0/18:1(9Z) ([^{PB}PC + H]$^+$) was mass-isolated and subjected to ion/ion reaction with [PDPA - 2H]$^{2-}$. The ion/ion reaction products included dominant complex formation of the two reactant ions, [^{PB}PC + PDPA - H]$^-$ (*m/z* 1038), and a minor peak at *m/z* 802 resulting from demethylation of the ^{PB}PC anion as shown in Figure 2.2.
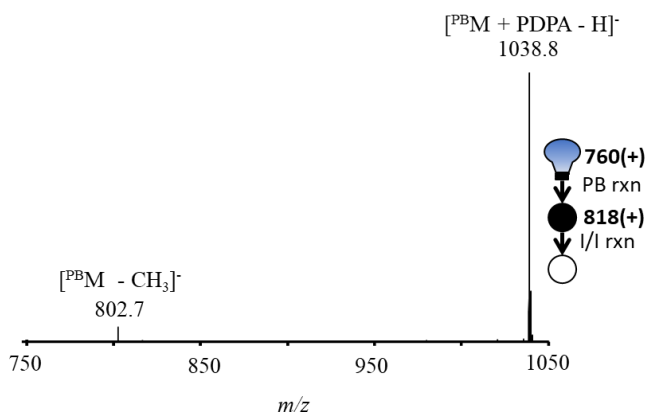
Figure 2.2. Negative ion mode mass spectrum of the ion/ion reaction between [PDPA-2H]$^{2-}$ and [^{PB}PC 16:0/18:1(9Z) + H]$^+$.

Collisional activation of the complex ion at *m/z* 1038 mainly led to the formation of [^{PB}PC - CH$_3$]$^-$ ion (*m/z* 802.7, Figure 2.3a), formed from NL of methylated PDPA (236 Da). In previous work, the operational efficiency of protonated PC species to demethylated species was calculated as about 50%, although absolute efficiency could not be calculated due to difference in detector response to positive and negative ions.[28] Further CID of this fragment produced abundant fatty acyl anions (Figure 2.3b), including [C16:0 - H]$^-$ (*m/z* 255.3) and the PB modified C18:1 ([^{PB}C18:1 - H]$^-$, *m/z* 339.2), and fragments (*m/z* 480.4 and *m/z* 536.3) due to ketene NL of ^{PB}C18:1 and C16:0, respectively. A small intact C18:1 anion peak at *m/z* 281.3 was also observed, likely formed from loss of acetone from [^{PB}C18:1 - H]$^-$ due to sequential fragmentation. The relatively higher abundances of ketene NL ions and carboxylate anions from the *sn2* chain relative to those formed

from *sn1* chain, corroborate that the *sn1* and *sn2* chains are C16:0 and C18:1, respectively, verifying the *sn*-positions for the synthetic molecules. In previous studies using charge inversion of PC, the fatty acyl chain determination was the final piece of information provided. In this study, CID of the PB product of the C18:1 ([^{PB}C18:1 - H]$^-$, *m/z* 339.2) produced C=C diagnostic ions at *m/z* 171.1 and 197.2 (Figure 2.3c), allowing confident determination of the site of unsaturation at Δ9.
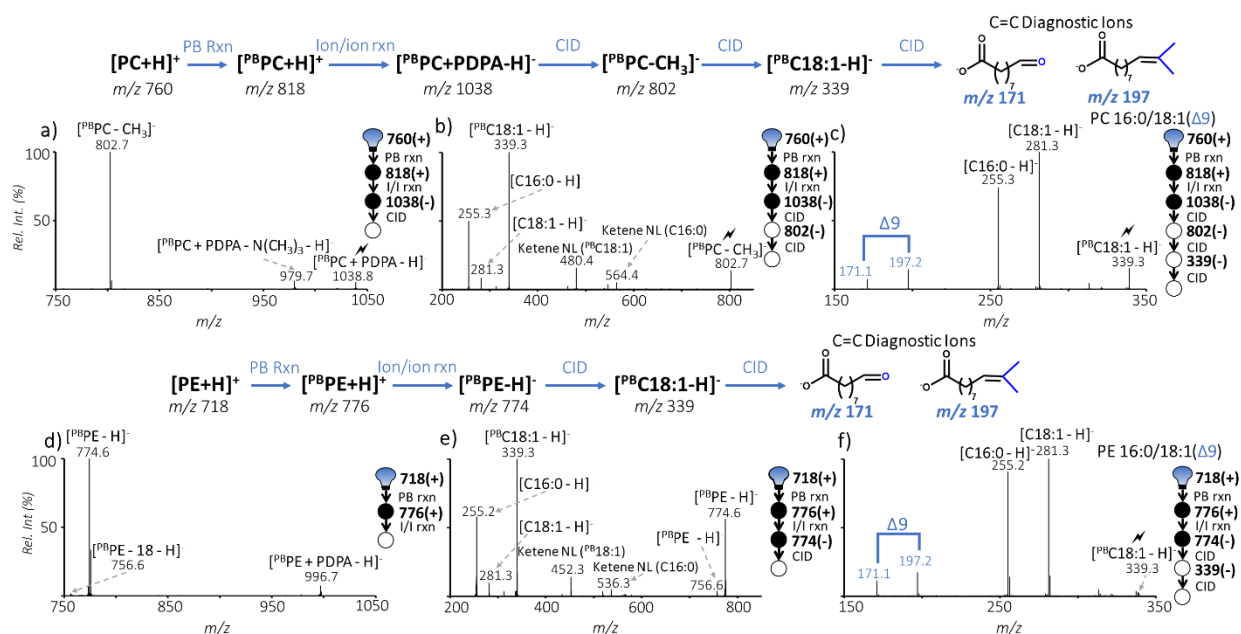
Figure 2.3. Sequence of events post-ion/ion reaction between GP standard cations and PDPA dianion; a) Ion trap CID of [^{PB}PC + PDPA - H]-; b) Ion trap CID of [^{PB}PC - CH$_3$]$^-$; c) Subsequent ion trap CID of [^{PB}C18:1 - H]- d) Result of ion/ion reaction between [PDPA-2H]$^{2-}$ and [^{PB}PE + H]$^+$; e) Ion trap CID of [^{PB}PE - H]$^-$; f) Subsequent ion trap CID of [^{PB}C18:1 - H]$^-$; Schematics in a-c and d-f are layouts of the process for determining the GP structure. CID of a target ion is depicted by a lightning bolt (↯). Cations and anions are represented by (+) or (-), respectively.

Figure 2.3d-f demonstrate the process of structural characterization for unsaturated PE, using PE 16:0/18:1(9Z) as an example. The workflow is slightly different from that of the PC, due to the difference in charge inversion ion/ion chemistry between a primary amine (in PE) and a quaternary amine (in PC). As shown in Figure 2.3d, the dominant charge inversion product of [^{PB}PE + H]$^+$ (*m/z* 776.6) is the corresponding deprotonated ion ([^{PB}PE - H]$^-$, *m/z* 774.6), accompanied only by a very small extent of complex formation (the peak at *m/z* 996.7). Collisional activation of [^{PB}PE - H]$^-$ (Figure 2.3e) resulted in the formation of abundant PB reaction modified

47

C18:1 ([^{PB}C18:1 - H]$^-$, *m/z* 339.3) and C16:0 ([C16:0 - H]$^-$, *m/z* 255.2) fatty acyl anions as well as the ketene NL of the *sn2* chain (*m/z* 452.3) and *sn1* chain (*m/z* 536.3). Subsequent CID of [^{PB}C18:1 - H]$^-$ produced characteristic C=C diagnostic ions that are 26 Da apart at *m/z* 171.1 and 197.2, confirming the C=C location at Δ9 in C18:1.

The above analysis using PC and PE synthetic standards demonstrates that the PB reaction and gas-phase charge inversion ion/ion reactions can be efficiently paired and applied for confident structural identification of GPs at the C=C location level. Charge inversion of PB products exhibits equivalent information to unmodified GPs with the addition of the C=C localization and was applied to a biological extraction sample.

2.4.3 Shotgun analysis of the polar lipid extract from bovine liver.

Polar lipid extract from bovine liver was employed as the benchmark test to evaluate the performance of coupling the PB reaction with ion/ion reaction for shotgun lipid analysis. By employing linked scans in positive ion mode, *i.e.* PE via 141 Da NLS and PC via *m/z* 184 PIS, these two lipid subclasses were identified (Figure 2.4); however, the fatty acyl composition, could not be obtained. The positive ion mode nanoESI mass spectrum of the lipid extract is shown in Figure 2.5a. Herein, we exemplify the power of the detailed structural analysis for unsaturated PC and PE by pairing the PB reaction and charge inversion ion/ion reactions. For clarity, those peaks that we demonstrate in later discussions are labelled in red in Figure 2.5a (*i.e. m/z* 744.6, *m/z* 768.6, *m/z* 788.7, and *m/z* 834.7).
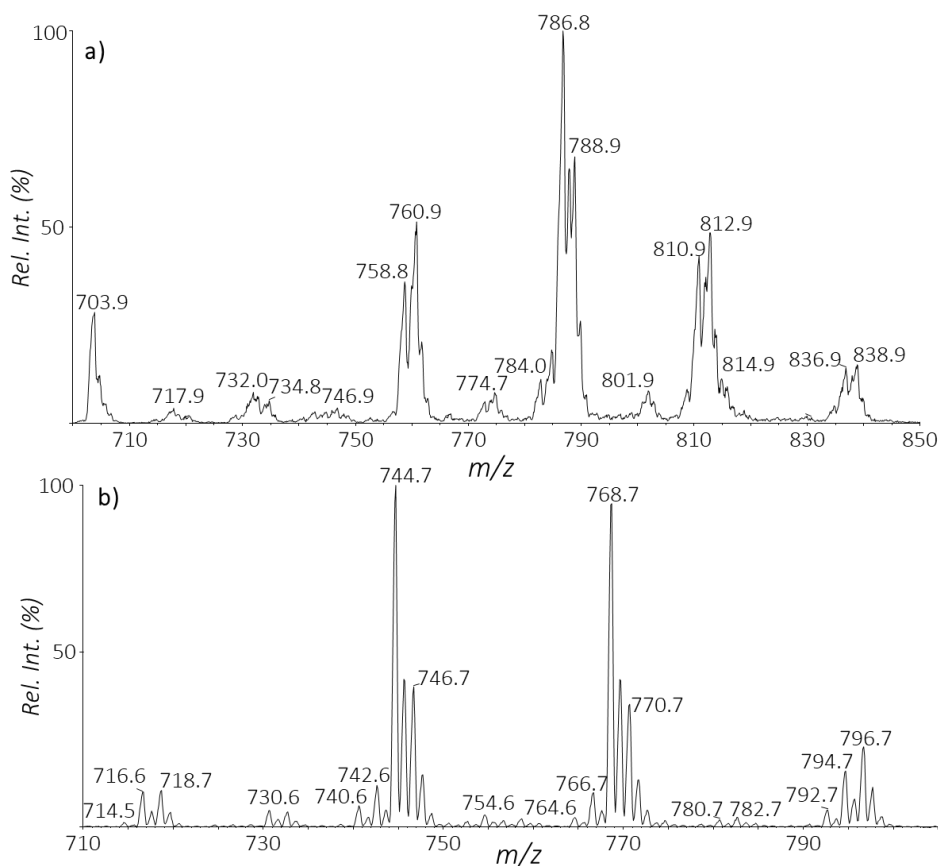
Figure 2.4. Positive ion mode nanoESI spectrum of polar lipid extract from bovine liver (100 μM) without PB reaction. a) Precursor ion scan of *m/z* 184; b) Neutral loss scan of 141 Da.

Individual PB reacted peaks were isolated from the UV irradiated, diluted lipid extract. The PB reaction product (*m/z* 846.8) of a relatively abundant lipid peak (*m/z* 788.7) was isolated using a unit mass isolation window and subjected to ion/ion reaction with the PDPA dianion. As shown in Figure 2.5b, the resulting spectrum was dominated by ions at *m/z* 1066.8 from complex formation ([^{PB}M + PDPA - H]$^-$), a very minor peak at *m/z* 844.7 due to double proton transfer, and a small fragment ion (*m/z* 830.7) due to NL of methylated PDPA. Based on the distinct ion/ion charge inversion chemistry of PC and PE, i.e. complex formation vs. double proton transfer, it is evident that the peak at *m/z* 788.7 in Figure 2.5a consists of PC 36:1 as a major component and PE 39:1 as a minor component. In order to identify the fatty acyl composition and C=C location in PC 36:1, the ion complex at *m/z* 1066.8 was subjected to sequential CID experiments as depicted in Figure 2.3a. The CID spectrum of *m/z* 830.7 (([^{PB}PC - CH$_3$]$^-$, Figure 2.5c) indicated that PC 36:1 consists primarily of C18:0 and C18:1. This is consistent with the fatty acyl composition inferred

from charge inversion and CID of the intact ions at *m/z* 788.The glycerol backbone location of C18:1 is likely at *sn2* given the high abundance of associated ketene NL, however, the method currently is limited in its ability to determine *sn*-position due to possible coexisting isomers.

The PB modified C18:1 ion population was detected at *m/z* 339.3; further CID of these ions produced two C=C diagnostic ion pairs at *m/z* 171.1/197.2 and *m/z* 199.1/225.2, providing definitive evidence for locations of C=Cs at Δ9 and Δ11 in C18:1, respectively. Combining all above information, PC 36:1 could be confidently identified as a mixture of PC 18:0_18:1(Δ9) and PC 18:0_18:1(Δ11). The PC 18:0_18:1(Δ9) specie is the major isomer based on the relative abundances of its C=C diagnostic ions relative to those of the Δ11 isomer (Figure 2.5d). Due to the low ion signal of PE 39:1, C=C location determination could not be obtained after ion/ion reaction. Figure 2.6 highlights that in a single spectrum, it is possible to differentiate GP class isomers, fatty acyl isomers, and C=C isomers.

Figure 2.5. a) Positive ion mode nanoESI MS spectrum of polar lipid extract from bovine liver (100 µM) without PB reaction, b) The PB reaction of ions at 788.7 in panel (a) followed by charge inversion ion/ion reaction, c) Subjecting product ions at *m/z* 1066.8 and 830.7 in panel (b) to CID allows confident identification of this lipid at fatty acyl level, d) CID spectrum of *m/z* 339.3 produced in panel (c). Detection of two pairs of C=C diagnostic ions at *m/z* 171.1/197.2 and *m/z* 199.1/225.2 from C18:1 chain identifies the lipid at *m/z* 788.7 in panel (a) as PC 18:0_18:1(Δ9) and PC18:0_18:1(Δ11).
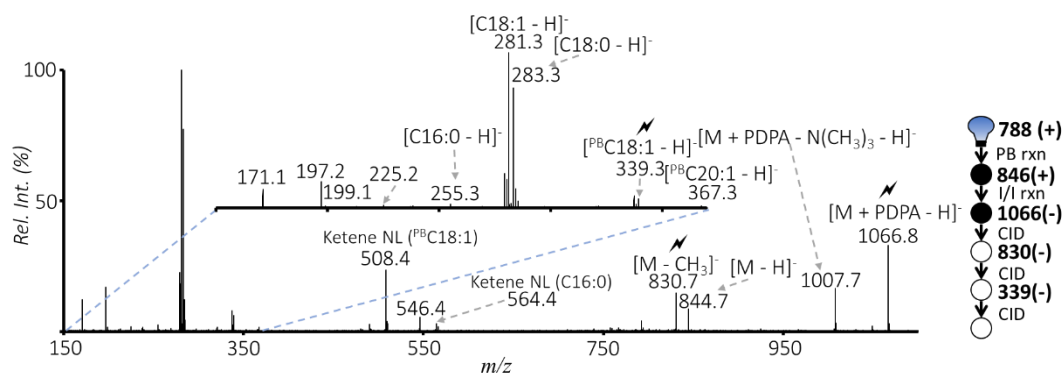
Figure 2.6. Full mass spectrum of the charge inversion of PB product at *m/z* 788 followed by sequential steps of CID to express phospholipid class isomers, fatty acyl chain isomers, and C=C location isomers (for C18:1).

Although charge inversion of the PB products was powerful in pinpointing detailed structural information of unsaturated PC and PE, the need of performing multi-step CID made it difficult to analyze lower abundance lipids. Furthermore, CID of the PB modified polyunsaturated fatty acid anions would not provide as abundant C=C diagnostic ions as performed in the positive ion mode. This limitation can be overcome by conducting ion/ion charge inversion and the PB reaction in two separate experiments. That is, first to charge invert the peak of interest to verify headgroup and fatty acyl identification, then use positive ion mode PB-MS/MS for determination of C=C location. Separately using PB-MS/MS and ion/ion reaction allows for increased sensitivity of C=C diagnostic information and a rapid structural analysis compared to combination of the methods.

Structural analysis of polyunsaturated GPs is demonstrated by probing the ions at *m/z* 834.7 ([M + H]$^+$) in Figure 2.5a, because of the structural complexity and minor relative abundance. Based on the PIS for *m/z* 184 combined with the LipidMaps structural database, the lipid peak was expected to contain PC 40:6. Following the conventional method for fatty acyl identification, the possible PC species (acetate adduct at *m/z* 892.8, [M + Ac]$^-$) was probed in the negative ion mode from nanoESI of lipid solution added with 10 mM of ammonium acetate. Figure 2.7a shows the MS^2 CID spectrum of [M + Ac]$^-$, the same nominal *m/z* as the acetate adduct ion of PC 40:6. The major fragment peaks include ions at *m/z* 255.3 and 281.3, corresponding to C16:0 and C18:0,

respectively, with a few smaller peaks corresponding to other fatty acyl chains. The combination of fatty acyl chains C16:0 and C18:0 would not provide the correct identification of PC 40:6 achieved from positive ion mode, largely due to poor ionization efficiency of the acetate adduct and ion suppression of PC in negative ion mode. Thus, it is evident that in negative ion mode the ions presented at *m/z* 892.8 contained isobaric GP species that were not the analyte of interest. Charge inversion ion/ion reaction of *m/z* 834.7 from positive ion mode produced abundant ions at *m/z* 1054.8 and 818.8, which are characteristic for the presence of PC 40:6. The appearance of ions at *m/z* 832.7 suggested the presence of PE 43:6 as a minor component. The CID spectrum of the demethylated PC 40:6 (*m/z* 818.8) is shown in Figure 2.7b. The negative ion mode spectrum contains abundant peaks of C18:0 and C22:6 at *m/z* 283.3 and 327.3, respectively. This set of data demonstrates the utility of charge inversion ion/ion chemistry in confidently providing fatty acyl chain information for less abundant PCs, which otherwise would be difficult to obtain using conventional shotgun lipid analysis methods.
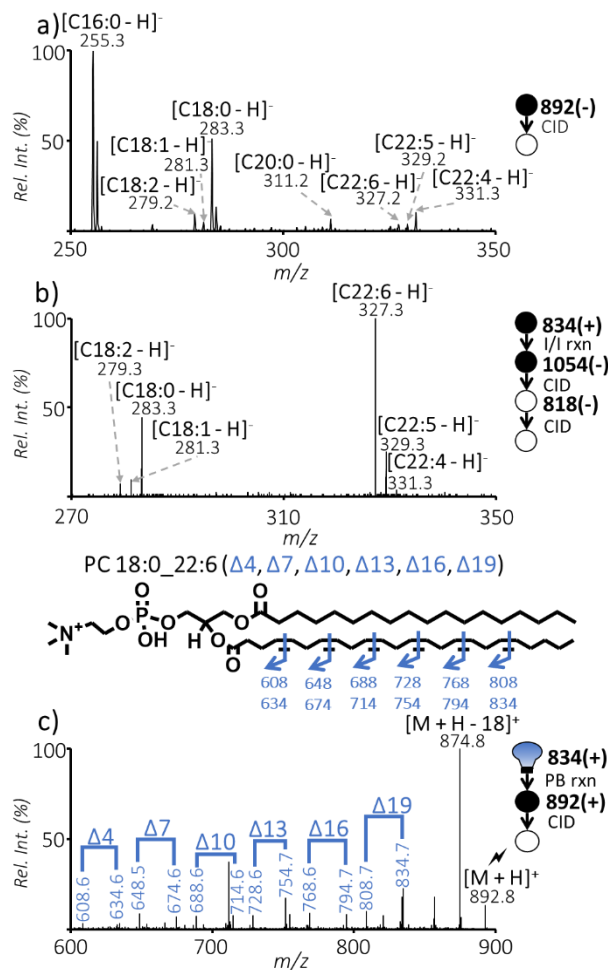
Figure 2.7. a) Direct negative ionization of bovine liver polar lipid extract. Isolation followed by beam-type CID of ions at *m/z* 892.8 (positive *m/z* 834.7 from Figure 2.5a complexed with acetate anion, [M+Ac]⁻, 100 µM with 10 mM ammonium acetate); b) Charge inversion and subsequent ion trap CID spectrum of the peak found at *m/z* 834.7 in the positive ion mode spectrum; c) Positive ion mode ion-trap CID of the PB product of *m/z* 834.7 peak, [^{PB}M + H]⁺, at *m/z* 892.8.

In order to assign the locations of unsaturation in C22:6, the PB-MS/MS experiment was performed separately in positive ion mode. Figure 2.7c shows ion-trap CID of *m/z* 892.8 ([^{PB}M + H]⁺), which contains six distinct pairs of diagnostic ions (*m/z* 608.6/634.6, *m/z* 648.5/674.6, *m/z* 688.6/714.6, *m/z* 728.6/754.7, *m/z* 768.6/794.7, and *m/z* 808.7/834.7) that align with C=Cs at positions Δ4, Δ7, Δ10, Δ13, Δ16, and Δ19. The diagnostic ions thus allowed for confident identification of PC 18:0_22:6(Δ4, Δ7, Δ10, Δ13, Δ16, Δ19), which contains polyunsaturated omega-3 fatty acyl.
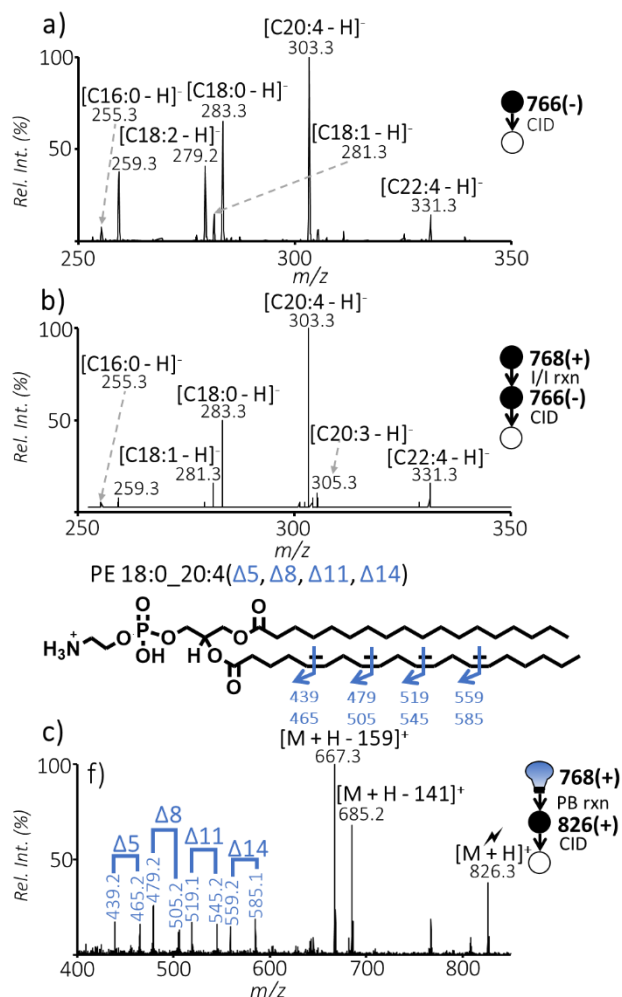
Figure 2.8. a) Direct ionization of bovine liver polar lipid extract in negative ion mode. Isolation and beam-type CID of ions at *m/z* 766.5 (positive *m/z* 768.6 from Figure 2.5a); b) Charge inversion and subsequent ion trap CID spectrum originating from positive ions present at *m/z* 768.6; c) Positive ion mode beam-type CID of the peak at *m/z* 826.3 (PB product of *m/z* 768.6).

Figure 2.8a shows MS^2 CID of ions at *m/z* 766.5, the same nominal mass as deprotonated PE 38:4 in negative ion mode. The fatty acyl chains that correspond to the PE species can be determined as mainly C20:4 and C18:0 classifying the peak as PE 18:0_20:4. Based on Figure 2.8a, however, there were still peaks present in high abundance that do not correspond to the lipid class being targeted. For example, a peak that corresponds to C18:2 at *m/z* 279.2 is prominent, but there is no parallel ion for C20:2 (*m/z* 307), the fatty acyl chain that would complement C18:2, suggesting that the C18:2 ion may arise from an isobaric species not related to PE, despite its high abundance. Figure 2.8b shows the charge inversion of the *m/z* 768.6 [M + H]$^+$ ion and subsequent

ion trap CID of 766.5 ($[M - H]^-$) to determine that the fatty acyl chains present for PE 38:4 to be C18:0 and C20:4 at *m/z* 283.3 and 303.3, respectively, identifying the major species as PE 18:0_20:4, while several other minor components, i.e., PE 18:1_20:3 and PE 16:0_22:4, coexist. Note that the prominent *m/z* 279.2 ion observed in Figure 2.8a is largely absent in Figure 2.8b, which further suggests that the charge inversion process provides a degree of discrimination against possible isobaric interferences presence in direct negative ion mode ionization. Positive ion mode CID of the *m/z* 768.6 PB product at *m/z* 826.3, shown in Figure 2.8c, displays four C=C diagnostic ion pairs (*m/z* 439.2/465.2, *m/z* 479.2/505.2, *m/z* 519.1/545.2, and *m/z* 559.2/585.1), corresponding to the $\Delta 5$, $\Delta 8$, $\Delta 11$, and $\Delta 14$ C=C locations on the 20:4 fatty acyl chain (an omega-6 fatty acyl). This set of data identified that PE 18:0_20:4 ($\Delta 5$, $\Delta 8$, $\Delta 11$, $\Delta 14$) was the major component for the peak *m/z* 786.6 from shotgun analysis in the positive ion mode.

When compared to using direct negative ionization for PC and PE analysis, charge inversion is shown to be efficient at determining fatty acyl chain information that is relevant to the peak of interest. The added ability to pair the fatty acyl chains determined to C=C location information allows novel information where ambiguity is minimized. Polyunsaturated PCs and PEs with greater than two double bonds, along with those with relative abundances less than 4% were analyzed using this method for confident double bond position siting.

Figure 2.9. a) Charge inversion of cations at *m/z* 744.6 followed by ion trap CID of ions at *m/z* 964.8; b) Sequential CID of ions at *m/z* 742.8; c) CID of ions at *m/z* 337.3 resulting from sequential CID of charge inverted PB products; d) Direct positive ion mode ionization of bovine liver polar lipid extract. Isolation followed by beam-type CID of the *m/z* 802.7 ions (positive *m/z* 744.6 from Figure 2.5a). The blue and red texts emphasize the diagnostic ions resulting from PE 18:0_18:2(Δ9, Δ12) and PE 18:1(Δ9)_18:1(Δ9), respectively.

It is desirable for a method to be able to distinguish PC and PE isomers with the added ability to determine the C=C location. Investigation of the *m/z* 744.6 ions in the bovine liver extract via charge inversion is provided in Figures 9 and 10 to illustrate such a capability. Charge inversion followed by CID of the *m/z* 964.8 ion showed a dominant peak at *m/z* 742.6, a deprotonated PE 36:2 as well as a lower abundance peak at *m/z* 728.6 (demethylated anions of PC 33:2), indicating the co-existence of isomeric PE and PC in the lipid sample (Figure 2.9a). Ion trap CID of the *m/z* 742.6 ion resulted in ions at *m/z* 279.3, 283.3, and 281.3 representing fatty acyls C18:2, C18:0 and C18:1, respectively, as shown in Figure 2.9b. Based on the relative ion intensities of these fatty acyl anions, the PE 36:2 species in the sample was determined to contain PE 18:0_18:2 as a major component with PE 18:1_18:1 as a minor component. The PB product (*m/z* 802.7) of the peak at *m/z* 744.6 was subjected to charge inversion followed by sequential steps of CID of the ions of *m/z* 1022.7 and *m/z* 800.6. Fatty acyl related products are detected at *m/z* 337.3, 283.3, 339.3, and 281.3 further confirming that PE 18:0_18:2 and PE 18:1_18:1 are present. The relative abundance of the

m/z 337.3 ion was sufficiently high to allow for a subsequent CID for C=C localization. Diagnostic peaks with 26 Da differences are present at *m/z* 171/197 and *m/z* 211/237 to determine the double bond locations to be at Δ9 and Δ12 identifying the major PE species content to PE 18:0_18:2(Δ9, Δ12) (Figure 2.9c). The minor PE 18:1_18:1 species was not abundant enough to identify in negative ion mode and was probed using beam-type CID of the PB product (*m/z* 802.7) in positive ion mode. In Figure 2.9d, the major product ions at *m/z* 495.2/521.3 and *m/z* 535.2/561.2 represent the species PE 18:0_18:2(Δ9, Δ12). There is also a pair of diagnostic ions at *m/z* 493.2/519.2 identifying the species PE 18:1(Δ9)_18:1(Δ9).
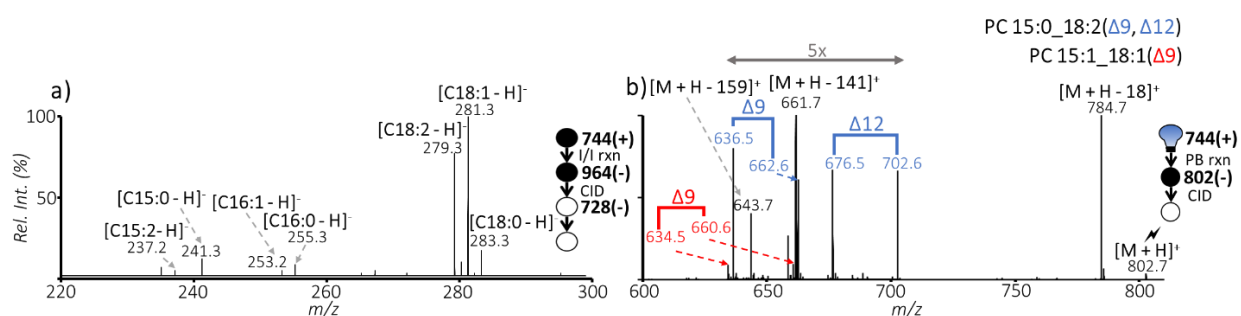
Figure 2.10. a) Sequential CID of ions at *m/z* 728.6 from Figure 2.9a. b) Positive ion trap CID of PB reaction product at *m/z* 802.7.

The isomeric PC 33:2 was analyzed by subjecting the demethylated anions to CID (Figure 2.10a). The detection of fatty acyl anions at *m/z* 281.3, 279.3, 283, 241.3, and 237.2 are C18:1, C18:2, C18:0, C15:0 and C15:2, respectively, meaning isomers PC 15:0_18:2, PC 15:1_18:1, and PC 15:2_18:0 are present. Positive PB product analysis (Figure 2.10b) was used to analyze the C=C location. Ion-trap CID in positive ion mode resulted in diagnostic ions that are 26 Da apart determining the major components to be PC 15:0_18:2(Δ9, Δ12) and PC 15:1_18:1(Δ9).

It is worth noting that the diagnostic ions for C15:1 with a Δ9 C=C location would be at *m/z* 676.5 and 702.6, meaning that they overlap with the diagnostic ions of Δ12 C=C in PC 15:0_18:2(Δ9, Δ12). This is a limitation of the direct positive ion mode approach that can be overcome via the charge inversion route, but only when the fatty acyl anion abundances are sufficiently high. The commonly present C18:2(Δ9, Δ12) motif inclined us to ascribe the *m/z* 676.5 and 702.6 ions as arising from the Δ12 position and do not report the presence of C15:1(Δ9). Further improvement of signal for low abundant monounsaturated fatty acyls will allow for the

confident determination of C=C. Nonetheless, by pairing ion/ion charge inversion with the PB reaction, 40 distinct unsaturated PC and PE structures were determined with fatty acyl composition and C=C locations from bovine polar lipid extract as shown in Table 1. This level of identification compares favorably to those reported from UVPD[36] and epoxidation.[52]

Table 2.1. Identified GPs in bovine liver polar lipid extract via pairing the PB reaction with gas-phase ion/ion charge inversion. Green and blue correspond to the diagnostic ions present for 18:1(Δ9) and 18:2(Δ9, Δ12), respectively.

[M+H]$^+$ (m/z)	Fatty Acyl Ions (m/z)	Fatty Acyl Composition	Double Bond Diagnostic Ions (m/z)	Identified Lipid
732	225; 281	PC 14:0_18:1	622/648	PC 14:0_18:1(Δ9)
732	225; 281	PC 14:0_18:1	622/648	PC 14:0_18:1(Δ11)
732	253; 255	PC 16:0_16:1	650/676	PC 16:0_16:1(Δ9)
744	239; 281	PC 15:1_18:1	634/660	PC 15:1_18:1(Δ9)
744	239; 281	PC 15:1_18:1	662/688	PC 15:1_18:1(Δ11)
744	241; 279	PC 15:0_18:2	636/662; 676/702	PC 15:0_18:2(Δ9, Δ12)
746	241; 281	PC 15:0_18:1	636/662	PC 15:0_18:1(Δ9)
746	241; 281	PC 15:0_18:1	664/690	PC 15:0_18:1(Δ11)
746	267; 255	PC 17:1_16:0	650/676	PC 17:1(Δ9)_16:0
746	239; 283	PC 15:1_18:0	678/704	PC 15:1(Δ9)_18:0
758	255; 279	PC 16:0_18:2	171/197; 211/237	PC 16:0_18:2(Δ9, Δ12)
760	255; 281	PC 16:0_18:1	171/197	PC 16:0_18:1(Δ9)
760	255; 281	PC 16:0_18:1	199/225	PC 16:0_18:1(Δ11)
772	269; 279	PC 17:0_18:2	664/690; 704/730	PC 17:0_18:2(Δ9, Δ12)
774	269; 281	PC 17:0_18:1	664/690	PC 17:0_18:1(Δ9)
774	281; 267	PC 18:0_17:1	678/704	PC 18:0_17:1(Δ9)
782	255; 303	PC 16:0_20:4	594/620; 634/660; 674/700; 714/740	PC 16:0_20:4(Δ5, Δ8, Δ11, Δ14)
784	255; 305	PC 16:0_20:3	636/662; 676/702; 716/742	PC 16:0_20:3(Δ8, Δ11, Δ14)
784	281; 279	PC 18:1_18:2	674/700; 676/702; 716/742	PC 18:1(Δ9)_18:2(Δ9, Δ12)
786	283; 279	PC 18:0_18:2	171/197; 211/237	PC 18:0_18:2(Δ9, Δ12)
786	281	PC 18:1_18:1	676/702	PC 18:1(Δ9)_18:1(Δ9)
788	283; 281	PC 18:0_18:1	171/197	PC 18:0_18:1(Δ9)
788	283; 281	PC 18:0_18:1	199/225	PC 18:0_18:1(Δ11)
808	281; 303	PC 18:1_20:4	620/646; 660/686; 700/726; 740/766	PC 18:1_20:4(Δ5, Δ8, Δ11, Δ14)
808	301; 283	PC 20:5_18:0	622/648; 662/688;702/728; 742/768; 782/808	PC 18:0_20:5(Δ5, Δ8, Δ11, Δ14, Δ17)
810	283; 303	PC 18:0_20:4	622/648; 662/688; 702/728; 742/768	PC 18:0_20:4(Δ5, Δ8, Δ11, Δ14)
812	283; 305	PC 18:0_20:3	157/183; 197/223; 237/263	PC 18:0_20:3(Δ8, Δ11, Δ14)
834	283; 327	PC 18:0_22:6	608/634;648/674;688/714; 728/754;768/794;808/834	PC 18:0_22:6(Δ4, Δ7, Δ10, Δ13, Δ16, Δ19)
836	283; 329	PC 18:0_22:5	650/676; 690/716; 730/756; 770/796; 810/836	PC 18:0_22:5(Δ7, Δ10, Δ13, Δ16, Δ19)
836	281; 331	PC 18:1_22:4	648/674; 688/714; 728/754; 768/794	PC 18:1_22:4(Δ7, Δ10, Δ13, Δ16)
838	283; 331	PC 18:0_22:4	650/676; 690/716; 730/756; 770/796	PC 18:0_22:4(Δ7, Δ10, Δ13, Δ16)

Table 2.2. Identified PEs in bovine liver polar lipid extract via pairing the PB reaction with gas-phase ion/ion charge inversion

[M+H]⁺ (m/z)	Fatty Acyl Ions (m/z)	Fatty Acyl Composition	Double Bond Diagnostic Ions (m/z)	Identified Lipid
718	255; 281	PE 16:0_18:1	467/493	PE 16:0_18:1(Δ9)
732	269; 281	PE 17:0_18:1	481/507	PE 17:0_18:1(Δ9)
740	279	PE 18:2_18:2	491/517; 531/557	PE 18:2(Δ9, Δ12)_18:2(Δ9, Δ12)
744	283; 279	PE 18:0_18:2	171/197; 211/237	PE 18:0_18:2(Δ9, Δ12)
744	281	PE 18:1_18:1	493/519	PE 18:1(Δ9)_18:1(Δ9)
746	283; 281	PE 18:0_18:1	495/521	PE 18:0_18:1(Δ9)
746	283; 281	PE 18:0_18:1	523/549	PE 18:0_18:1(Δ11)
766	301; 283	PE 20:5_18:0	439/465; 479/505; 519/545; 559/585; 599/625	PE 20:5(Δ5, Δ8, Δ11, Δ14, Δ17)_18:0
768	283; 303	PE 18:0_20:4	439/465; 479/505;519/545; 559/585	PE 18:0_20:4(Δ5, Δ8, Δ11, Δ14)

2.5   Conclusion

In this work, we have paired the Paternò–Büchi reaction with charge inversion by ion/ion reaction aiming to achieve high level structural information for unsaturated PEs and PCs using the shotgun approach. The method allows for confident identification of the double bond location in a specific fatty acyl chain containing one or two degrees of unsaturation. Double bond location isomers were distinguished along with the ability to characterize PE and PC isomers. A limitation to conducting charge inversion and PB-MS/MS in one experiment is that C=C diagnostic fragment ions of polyunsaturated fatty acyl chain is difficult to obtain in negative ion mode.[49] This limitation can be overcome by merging accurate fatty acyl chain information from charge inversion in negative ion mode with the information provided by positive ion mode PB-MS/MS for C=C location in two separate experiments.

For relatively abundant PCs and PEs or situations where chemical interference is minimal, charge inversion is not a necessity. However, for PCs and PEs at lower abundances, i.e. 2-10% of the most abundance species, charge inversion significantly reduces chemical interference, leading to both improved sensitivity and specificity for structural identification. As a simple comparison, without charge inversion we identified 24 GP species (18 PCs and 6 PEs) at C=C location level; while the combined methods allowed for identification of 40 GP species (31 PCs and 9 PEs). Dynamic range of such method is estimated to be 50-times. For GPs of lower than 2% relative abundance, a possible path to improve their identification will be application of this method on

GPs that have been modified to improve ionization efficiency, such as ^{13}C-Trimethylation Enhancement Using Diazomethane.

Although not demonstrated here, quantitation for lipid C=C location isomers can be achieved in positive ion mode using methods already established from PB-MS/MS, while relative quantitation for fatty acyl composition isomers can be obtained from charge inversion followed by CID. A home-modified Q-TOF instrument has been employed in this study for charge inversion ion/ion reactions and PB-MS/MS; in principle, commercial MS instruments capable of ETD, such as an LTQ-Orbitrap, should support charge inversion as long as the doubly charged reagent anions can be introduced into linear ion trap for ion/ion reactions. Overall, the present work shows that gas-phase charge inversion paired with the PB reaction is a useful method for structural elucidation of unsaturated phospholipids.

2.6   References

1. Han X, Gross RW. Shotgun Lipidomics: Electrospray Ionization Mass Spectrometric Analysis and Quantitation of Cellular Lipidomes Directly from Crude Extracts of Biological Samples. Mass Spectrom Rev. 2005;24(3):367–412.

2. Armstrong D, editor. Lipidomics [Internet]. Totowa, NJ: Humana Press; 2009 [cited 2017 Oct 8]. (Methods in Molecular Biology; vol. 579). Available from: http://link.springer.com/10.1007/978-1-60761-322-0

3. Han X, Gross RW. Shotgun Lipidomics: Multidimensional MS Analysis of Cellular Lipidomes. Expert Rev Proteomics. 2005;2(2):253–64.

4. Fhaner CJ, Liu S, Ji H, Simpson RJ, Reid GE. Comprehensive Lipidome Profiling of Isogenic Primary and Metastatic Colon Adenocarcinoma Cell Lines. Anal Chem. 2012;84(21):8917–26.

5. van Meer G, Voelker DR, Feigenson GW. Membrane lipids: Where They Are and How They Behave. Nat Rev Mol Cell Bio. 2008;9(2):112–24.

6. Eberlin LS, Dill AL, Golby AJ, Ligon KL, Wiseman JM, Cooks RG, Agar NYR. Discrimination of Human Astrocytoma Subtypes by Lipid Analysis Using Desorption Electrospray Ionization Imaging Mass Spectrometry. Angew Chem Int Ed. 2010;49(34):5953–6.

7. Gross RW, Han X. Lipidomics at the Interface of Structure and Function in Systems Biology. Chem Biol. 2011;18(3):284–91.

8. Ejsing CS, Sampaio JL, Surendranath V, Duchoslav E, Ekroos K, Klemm RW, Simons K, Shevchenko A. Global Analysis of the Yeast Lipidome by Quantitative Shotgun Mass Spectrometry. Proc Natl Acad Sci U S A. 2009;106(7):2136–41.

9. Loizides-Mangold U. On the Future of Mass Spectrometry-based Lipidomics. FEBS J. 2013;280(12):2817–29.

10. Fahy E, Subramaniam S, Murphy RC, Nishijima M, Raetz CRH, Shimizu T, Spener F, van Meer G, Wakelam MJO, Dennis EA. Update of the LIPID MAPS Comprehensive Classification System for Lipids. J Lipid Res. 2009;50(Supplement):S9–14.

11. Whiley L, Sen A, Heaton J, Proitsi P, García-Gómez D, Leung R, Smith N, Thambisetty M, Kloszewska I, Mecocci P, Soininen H, Tsolaki M, Vellas B, Lovestone S, Legido-Quigley C. Evidence of Altered Phosphatidylcholine Metabolism in Alzheimer's Disease. Neurobiol Aging. 2014;35(2):271–8.

12. Phoenix DA, Harris F, Mura M, Dennison SR. The Increasing Role of Phosphatidylethanolamine as a Lipid Receptor in the Action of Host Defense Peptides. Prog Lipid Res. 2015;59:26–37.

13. Guan Z-Z, Wang Y-N, Xiao K-Q, Hu P-S, Liu J-L. Activity of Phosphatidylethanolamine-N-Methyltransferase in Brain affected by Alzheimers disease. Neurochem Int. 1999;34(1):41–7.

14. Brouwers JF. Liquid Chromatographic–Mass Spectrometric Analysis of Phospholipids. Chromatography, Ionization and Quantification. BBA-Mol Cell Bio Lipids. 2011;1811(11):763–75.

15. Wang C, Kong H, Guan Y, Yang J, Gu J, Yang S, Xu G. Plasma Phospholipid Metabolic Profiling and Biomarkers of Type 2 Diabetes Mellitus Based on High-Performance Liquid Chromatography/Electrospray Mass Spectrometry and Multivariate Statistical Analysis. Anal Chem. 2005;77(13):4108–16.

16. Bird SS, Marur VR, Sniatynski MJ, Greenberg HK, Kristal BS. Lipidomics Profiling by High-Resolution LC−MS and High-Energy Collisional Dissociation Fragmentation: Focus on Characterization of Mitochondrial Cardiolipins and Monolysocardiolipins. Anal Chem. 2011;83(3):940–9.

17. Nygren H, Seppänen-Laakso T, Castillo S, Hyötyläinen T, Orešič M. Liquid Chromatography-Mass Spectrometry (LC-MS)-Based Lipidomics for Studies of Body Fluids and Tissues. In: Metz TO, editor. Metabolic Profiling [Internet]. Totowa, NJ: Humana Press; 2011 [cited 2017 Oct 17]. p. 247–57. Available from: http://link.springer.com/10.1007/978-1-61737-985-7_15

18. Brügger B, Erben G, Sandhoff R, Wieland FT, Lehmann WD. Quantitative Analysis of Biological Membrane Lipids at the Low Picomole Level by Nano-Electrospray Ionization Tandem Mass Spectrometry. Proc Natl Acad Sci U S A. 1997;94(6):2339.

19. Han X, Gross RW. Electrospray Ionization Mass Spectroscopic Analysis of Human Erythrocyte Plasma Membrane Phospholipids. Proc Natl Acad Sci U S A. 1994;91(22):10635–9.

20. Han X, Gross RW. Global Analyses of Cellular Lipidomes Directly from Crude Extracts of Biological Samples by ESI Mass Spectrometry: A Bridge to Lipidomics. J Lipid Res. 2003;44(6):1071–9.

21. Han X, Yang K, Gross RW. Multi-Dimensional Mass Spectrometry-based Shotgun Lipidomics and Novel Strategies for Lipidomic Analyses. Mass Spectrom Rev. 2012;31(1):134–78.

22. Lintonen TPI, Baker PRS, Suoniemi M, Ubhi BK, Koistinen KM, Duchoslav E, Campbell JL, Ekroos K. Differential Mobility Spectrometry-Driven Shotgun Lipidomics. Anal Chem. 2014;86(19):9662–9.

23. Buré C, Ayciriex S, Testet E, Schmitter J-M. A Single Run LC-MS/MS Method for Phospholipidomics. Anal Bioanal Chem. 2013;405(1):203–13.

24. Hsu F-F, Turk J. Electrospray Ionization with Low-energy Collisionally Activated Dissociation Tandem Mass Spectrometry of Glycerophospholipids: Mechanisms of Fragmentation and Structural Characterization. J Chromatogr B. 2009;877(26):2673–95.

25. Wasslen KV, Canez CR, Lee H, Manthorpe JM, Smith JC. Trimethylation Enhancement Using Diazomethane (TrEnDi) II: Rapid In-Solution Concomitant Quaternization of Glycerophospholipid Amino Groups and Methylation of Phosphate Groups via Reaction with Diazomethane Significantly Enhances Sensitivity in Mass Spectrometry Analyses via a Fixed, Permanent Positive Charge. Anal Chem. 2014;86(19):9523–32.

26. Canez CR, Shields SWJ, Bugno M, Wasslen KV, Weinert HP, Willmore WG, Manthorpe JM, Smith JC. Trimethylation Enhancement Using ^{13}C-Diazomethane (^{13}C-TrEnDi): Increased Sensitivity and Selectivity of Phosphatidylethanolamine, Phosphatidylcholine, and Phosphatidylserine Lipids Derived from Complex Biological Samples. Anal Chem. 2016;88(14):6996–7004.

27. Wang M, Palavicini JP, Cseresznye A, Han X. Strategy for Quantitative Analysis of Isomeric Bis(monoacylglycero)phosphate and Phosphatidylglycerol Species by Shotgun Lipidomics after One-Step Methylation. Anal Chem. 2017;89(16):8490–5.

28. Stutzman JR, Blanksby SJ, McLuckey SA. Gas-Phase Transformation of Phosphatidylcholine Cations to Structurally Informative Anions via Ion/Ion Chemistry. Anal Chem. 2013;85(7):3752–7.

29. Rojas-Betancourt S, Stutzman JR, Londry FA, Blanksby SJ, McLuckey SA. Gas-Phase Chemical Separation of Phosphatidylcholine and Phosphatidylethanolamine Cations via Charge Inversion Ion/Ion Chemistry. Anal Chem. 2015;87(22):11255–62.

30. Pulfer M, Murphy RC. Electrospray Mass Spectrometry of Phospholipids. Mass Spectrom Rev. 2003;22(5):332–64.

31. Hsu F-F, Turk J. Electrospray Ionization with Low-Energy Collisionally Activated Dissociation Tandem Mass Spectrometry of Glycerophospholipids: Mechanisms of Fragmentation and Structural Characterization. J Chromatogra B. 2009;877(26):2673–95.

32. Tomer KB, Crow FW, Gross ML. Location of Double-Bond Position in Unsaturated Fatty Acids by Negative Ion MS/MS. J Am Chem Soc. 1983;105(16):5487–8.

33. Thomas MC, Mitchell TW, Harman DG, Deeley JM, Nealon JR, Blanksby SJ. Ozone-Induced Dissociation: Elucidation of Double Bond Position within Mass-Selected Lipid Ions. Anal Chem. 2008;80(1):303–11.

34. Brown SHJ, Mitchell TW, Blanksby SJ. Analysis of Unsaturated Lipids by Ozone-Induced Dissociation. BBA-Mol Cell Bio Lipids. 2011;1811(11):807–17.

35. Pham HT, Maccarone AT, Thomas MC, Campbell JL, Mitchell TW, Blanksby SJ. Structural Characterization of Glycerophospholipids by Combinations of Ozone- and Collision-Induced Dissociation Mass Spectrometry: The Next Step towards "Top-Down" Lipidomics. Analyst. 2014;139(1):204–14.

36. Klein DR, Brodbelt JS. Structural Characterization of Phosphatidylcholines Using 193 nm Ultraviolet Photodissociation Mass Spectrometry. Anal Chem. 2017;89(3):1516–22.

37. Pham HT, Trevitt AJ, Mitchell TW, Blanksby SJ. Rapid Differentiation of Isomeric Lipids by Photodissociation Mass Spectrometry of Fatty Acid Derivatives: Photodissociation of Derivatized Fatty Acids. Rapid Commun Mass Spectrom. 2013;27(7):805–15.

38. Pham HT, Julian RR. Radical Delivery and Fragmentation for Structural Analysis of Glycerophospholipids. Int J Mass Spectrom. 2014;370:58–65.

39. Deimler RE, Sander M, Jackson GP. Radical-Induced Fragmentation of Phospholipid Cations using Metastable Atom-Activated Dissociation Mass Spectrometry (MAD-MS). Int J Mass Spectrom. 2015;390:178–86.

40. Li P, Hoffmann WD, Jackson GP. Multistage Mass Spectrometry of Phospholipids using Collision-Induced Dissociation (CID) and Metastable Atom-Activated Dissociation (MAD). Int J Mass Spectrom. 2016;403:1–7.

41. Campbell JL, Baba T. Near-Complete Structural Characterization of Phosphatidylcholines Using Electron Impact Excitation of Ions from Organics. Anal Chem. 2015;87(11):5837–45.

42. Baba T, Campbell JL, Le Blanc JCY, Baker PRS. Structural Identification of Triacylglycerol Isomers using Electron Impact Excitation of Ions from Organics (EIEIO). J Lipid Res. 2016;57(11):2015–27.

43. Stinson CA, Zhang W, Xia Y. UV Lamp as a Facile Ozone Source for Structural Analysis of Unsaturated Lipids Via Electrospray Ionization-Mass Spectrometry. J Am Soc Mass Spectr. 2018;29(3):481–9.

44. Harris RA, May JC, Stinson CA, Xia Y, McLean JA. Determining Double Bond Position in Lipids Using Online Ozonolysis Coupled to Liquid Chromatography and Ion Mobility-Mass Spectrometry. Anal Chem. 2018;90(3):1915–24.

45. Ma X, Xia Y. Pinpointing Double Bonds in Lipids by Paternò-Büchi Reactions and Mass Spectrometry. Angew Chem Int Ed. 2014;53(10):2592–6.

46. Stinson CA, Xia Y. A Method of Coupling the Paternò–Büchi Reaction with Direct Infusion ESI-MS/MS for Locating the C=C Bond in Glycerophospholipids. Analyst. 2016;141(12):3696–704.

47. Ma X, Chong L, Tian R, Shi R, Hu TY, Ouyang Z, Xia Y. Identification and Quantitation of Lipid C=C Location Isomers: A Shotgun Lipidomics Approach Enabled by Photochemical Reaction. Proc Natl Acad Sci U S A. 2016;113(10):2573–8.

48. Ren J, Franklin ET, Xia Y. Uncovering Structural Diversity of Unsaturated Fatty Acyls in Cholesteryl Esters via Photochemical Reaction and Tandem Mass Spectrometry. J Am Soc Mass Spectrom. 2017;28(7):1432–41.

49. Murphy RC, Okuno T, Johnson CA, Barkley RM. Determination of Double Bond Positions in Polyunsaturated Fatty Acids Using the Photochemical Paternò-Büchi Reaction with Acetone and Tandem Mass Spectrometry. Anal Chem. 2017;89(16):8545–53.

50. Liebisch G, Vizcaíno JA, Köfeler H, Trötzmüller M, Griffiths WJ, Schmitz G, Spener F, Wakelam MJO. Shorthand Notation for Lipid Structures Derived from Mass Spectrometry. J Lipid Res. 2013;54(6):1523–30.

51. Xia Y, Chrisman PA, Erickson DE, Liu J, Liang X, Londry FA, Yang MJ, McLuckey SA. Implementation of Ion/Ion Reactions in a Quadrupole/Time-of-Flight Tandem Mass Spectrometer. Anal Chem. 2006;78(12):4146–54.

52. Cao W, Ma X, Li Z, Zhou X, Ouyang Z. Locating Carbon–Carbon Double Bonds in Unsaturated Phospholipids by Epoxidation Reaction and Tandem Mass Spectrometry. Anal Chem. 2018;90(17):10286–92.

CHAPTER 3.   COUPLING HEADGROUP AND ALKENE SPECIFIC SOLUTION MODIFICATIONS WITH GAS-PHASE ION-ION REACTIONS FOR SENSITIVE GLYCEROPHOSPHOLIPID IDENTIFICATION AND CHARACTERIZATION

3.1   Abstract

Shotgun lipidomics provides sensitive and fast lipid identification without the need for chromatographic separation. Challenges faced by shotgun analysis of glycerophospholipids (GPs) include the lack of signal uniformity across GP classes and the inability to determine the carbon-carbon double bond (C=C) location within the radyl chains of an unsaturated species. Two distinct derivatization strategies were employed to both boost the sensitivity of GPs, via trimethylation enhancement using ^{13}C-diazomethane (^{13}C-TrEnDi), as well as determine location of double bonds within radyl chains, employing an in-solution photochemical reaction with acetone (Paternò–Büchi). The modified GPs were then subjected to positive ion mode ionization producing uniformed ionization efficiencies for GP species. The GPs were charge inverted via gas-phase ion/ion reactions and sequentially fragmented using ion trap collision-induced dissociation (CID). The CID of the species led to fragmentation producing diagnostic ions indicative of C=C bond location. The approach enabled enhanced ionization and the identification of GP species at the C=C level in a bovine lipid extract.

3.2   Introduction

Tandem mass spectrometry (MS) is a core tool in lipidomics research due to its high sensitivity and specificity. Lipid ions may be efficiently generated using electrospray ionization (ESI) and selectively fragmented via tandem MS (MS^2) to obtain structural details and enable unambiguous identification. Shotgun lipidomics is an MS-based approach that involves the direct-infusion of complex lipid extracts without prior separation, offering both speed and efficient coverage for lipid analysis. Glycerophospholipids (GPs) are the most abundant lipid class by mass in eukaryotic cells.[1] GP analysis benefits from different MS approaches that seek to improve the characterization of individual lipid species.[2] Although relatively low in molecular weight when compared to other biologically relevant molecules, GPs are structurally diverse. For example, over 100 species can exist within a single sample, each potentially possessing unique biological

activity.[3] A GP consists of a glycerol backbone with a polar head group attached at the *sn3* position[1,2] and acyl chains attached at the *sn1* and/or *sn2* positions. One of the challenges with the shotgun approach is that the ionization efficiency of GPs depends on the identity of the polar headgroup. For example, the headgroup of phosphatidylethanolamine (PE) consists of a basic primary amine that is readily protonated but susceptible to matrix effects during the ESI process leading to variation in sensitivity between samples. Several approaches to address this issue have been made including the installation of a fixed positive charge using sulfonium ions.[4,5] or through the generation of a fixed quaternary ammonium and methylated phosphate using trimethylation enhancement using diazomethane (TrEnDi).[6,7] Depending upon the headgroup identity, TrEnDi can improve ionization greater than 11-fold compared to unmodified lipids in the positive ion mode[6] and is compatible with the use of isotopically labelled diazomethane to differentiate modified lipid classes and enable quantification strategies (^{13}C-TrEnDi).[7] However, TrEnDi generally compromises ionization in the negative mode due to the complete methylation of functional groups with pKa values less than 11, disabling anions from being able to form in ESI. For this reason, fatty acyl analysis is no longer feasible as traditional negative ion ESI-MS^2 produces no ions and positive ion tandem mass spectra are strongly dominated by head group product ions. Gas-phase charge inversion of the TrEnDi modified cations followed by MS^2 has been shown to be an effective solution to this and enable full determination of fatty acyl chain composition.[8,9,10] This gas-phase charge inversion strategy indicates the number of carbon-carbon double bonds (C=C) that are present in a given lipid but does not yield any information as to their location. Several methods currently exist to probe the C=C location within fatty acyl chains,[11–21] however, most of them require instrument modifications or high energy collisions. Methods involving in-solution modification prior to ionization have been developed as means of obtaining C=C information without instrument modification[22–24] including the Paternò–Büchi (PB) reaction.[25–29] This UV-initiated reaction utilizes acetone as a reagent for a [2+2] cycloaddition to the unsaturation site(s) on a fatty acyl chain. Upon low-energy CID, signature fragments are formed that elucidate the C=C location. Charge inversion of PB reacted GPs has been applied for improved structural coverage of GPs allowing for C=C location to determined.[30] Herein, we demonstrate the utility of combining ^{13}C-TrEnDi, PB chemistry and gas-phase charge inversion to extend GP lipid structural characterization to also include the determination of C=C bonds.

3.3 Experimental

3.3.1 Materials.

All the phospholipid samples were purchased as chloroform solutions from Avanti Polar Lipid, Inc. (Alabaster, AL). The analytes were *1-palmitoyl-2-oleoyl-glycero-3-phosphocholine* (POPC), *1-palmitoyl-2-oleoyl-sn-glycero-3-phosphoethanolamine* (POPE), and bovine liver polar lipid extract (BLE). 1,4-phenylenedipropionic acid (PDPA) was purchased from Sigma Aldrich (St. Louis, MO). All solvents were HPLC-grade. ^{13}C-labeled N-methyl-N-nitroso-p-toluenesulfonamide and ^{13}C-diazomethane were prepared according to procedures by Shields et al.[31]

3.3.2 The ^{13}C-TrEnDi Modification of GPs.

The modification has previously been reported.[7] In short, 1 µL of freshly prepared tetrafluoroboric acid diethyl ether complex in diethyl ether was added to a solution of lipid standard or BLE in ethanol. To the lipid solution approximately 1 mL of freshly distilled ethereal ^{13}C-diazomethane was added, and allowed to react at room temperature for 5 min. Once the reaction was complete, the light-yellow solution was carefully dried down under a gentle stream of N_2(g) and sealed under an atmosphere of N_2(g) before shipping over dry ice.

3.3.3 The PB Reactions Setup.

The PB reaction was conducted using an offline flow microreactor as previously discussed.[30] The flow cell of the device was a UV transparent fused silica capillary (fluoropolymer-coated, 100 µm i.d. 363 µm o.d.; Polymicro Technologies/Molex; Phoenix, AZ). In order to control the reaction and as a safety precaution, the exposure of the cell to UV emission was limited to a 4 cm portion within an aluminum-coated box. A syringe pump was used to facilitate the flow of solution through the microreactor. The optimal yield of the product was obtained by a 4-5 second reaction time thus the flowrate was kept between 4 to 6 µL/min. After UV exposure, about 10 µL of the solution was collected by a pulled nanoESI borosilicate capillary and used for mass spectrometric analysis.

3.3.4 Mass Spectrometry

Standard solutions were analyzed on a TripleTOF 5600 triple quadrupole/time of flight (Sciex, Concord, ON, Canada) and the polar lipid extract and QTRAP 4000 systems (Sciex, Concord, ON, Canada) both modified to allow for mutual storage of cations and anions as reported.[32] Spray voltage was held at 1300 V for all experiments. Precursor ion scans (PIS) and neutral loss scans (NLS) were obtained for the mass range 700 Da to 900 Da with a collision energy of 35 eV. PIS at m/z 184, 199, and 202 profiled unmodified PC, tmPC, and tmPE, respectively while NLS of 141 Da profiled unmodified PE.

The PDPA anions ($[PDPA - 2H]^{2-}$) were mass selected with Q1 and injected for 0.2 s into the q2 collision cell. The modified lipid cations ($[^{PB}tmGP]^+$) subsequently followed the same procedure joining the anions in q2 where both ion populations were mutually stored for 0.5 s. LMCO for q2 to Q3 transfer was set as m/z 600 or 700, depending on the mass of the species of interest, to preclude low mass ions. A q-value of 0.2 was used to perform single frequency resonance excitation of all generations of ions produced throughout the experiments.

3.4 Results and Discussion

3.4.1 Structural characterization of synthetic GPs

Ionization enhancement of GPs is an attractive feature for lipidomics because it allows for the detection of less abundant species and improvement in identifying species that require protonation. The Smith group published methods of enhancing sensitivity of PE analysis via methylation using diazomethane and ^{13}C-labeled diazomethane, TrEnDi and ^{13}C-TrEnDi, respectively.[6,7] In both methods, functional groups with pKa values 11 or less will be readily permethylated and in the case of PE, the primary amine and phosphate functional groups become a quaternary ammonium and phosphoester. The resulting tetramethylated species contains a fixed charge and does not have signal splitting due to cationization competition between H^+, Na^+, and K^+. These new features combine to give a sensitivity gain of about 11-fold compared to unmodified PE species. However, TrEnDi using unlabeled diazomethane on a complex lipid matrix will convert all PEs to PCs, which precludes the distinction of these lipid classes. ^{13}C-TrEnDi modification of GPs uses labeled diazomethane to differentiate modified PEs and PCs by a mass shift of 3 Da, due to a difference of three labeled methyl groups installed on PE over PC lipid

classes (i.e. PC 36:2 vs PE 36:2).
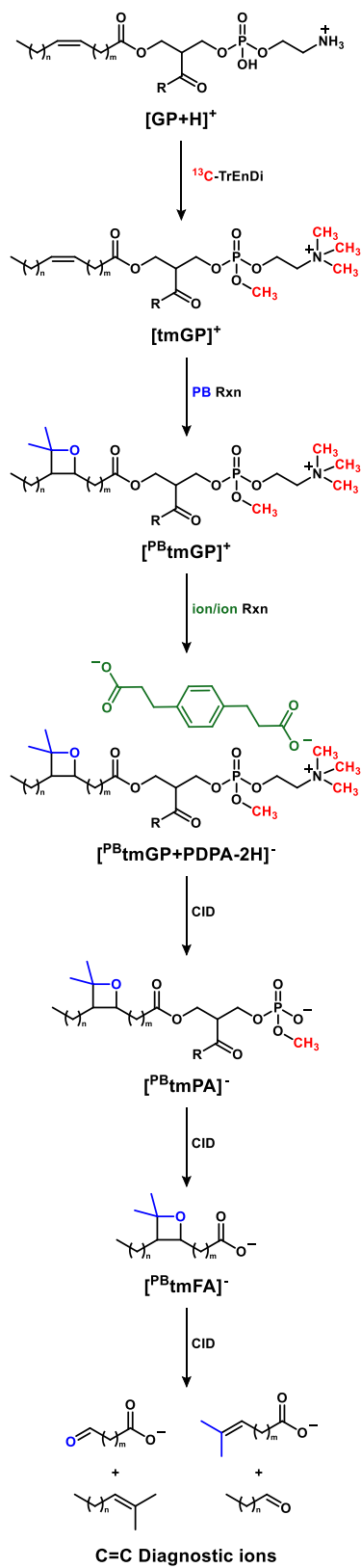
Figure 3.1. Sequence of events for lipid structure identification.

Structural characterization beyond subclass was not achieved using ^{13}C-TrEnDi modification alone. Positive ion mode fragmentation forming a neutral loss of a ketene that are normally in low abundance for unmodified species are absent using ^{13}C-TrEnDi. The phosphotriester formed during the modification eliminated the deprotonation pathway and diminishes negative ion mode ionization using an anion adduct. Charge inversion of tmGPs via gas phase ion/ion reactions has been described as a means of determining fatty acyl chain information in negative ion mode.[10] The modified lipid is introduced to the mass spectrometer and mutually stored with a dianion, doubly-deprotonated 1,4-phenylenedipropionic acid (PDPA), which is also used in this study. The ion/ion reaction results in an electrostatically bound complex, with an overall negative charge. After charge inversion of the tmGP, sequential CID steps yield the product ions corresponding to the sum composition of the fatty acyl chains. The combined methods, TrEnDi and charge inversion, show increased PE coverage in a complex sample as well as fatty acid composition. However, location in of alkenes in unsaturated GP fatty acyl chains is not forthcoming using the above approach. Structural characterization of lipid species is important for determining their biophysical properties,[33] thus probing C=C location is of great interest. Recently, the PB reaction was used to localize the C=C within charge inverted unsaturated GPs.[30] The PB reaction is a classic [2+2] photocycloaddition that forms a bond between an olefin and a carbonyl compound. This reaction is utilized for lipid structure characterization by selectively modifying alkene with photoactivated acetone to give a four membered oxetane ring, which, upon CID, collapses to dimethyl-alkene and aldehyde (Figure 3.1). Both dimethyl-alkene and aldehyde product ions can be used as diagnostic ions for double bond localization based on a neutral loss when compared to the original m/z of [^{PB}tmFA]$^-$. Combining gas-phase charge inversion with the PB reaction allowed for specific structural elucidation of unsaturated GPs. The method is efficient at characterizing PC, however, PEs ionization in mixtures can be suppressed in the positive ion mode leading to many species being left unidentified. Herein, we report the combination of in-solution modifications followed by charge inversion for sensitive and specific characterization of GPs with a focus on ^{13}C-TrEnDi modified PE species.
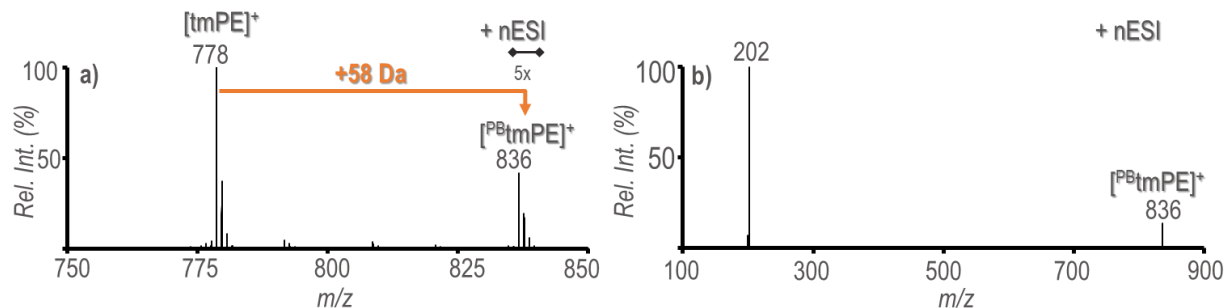
Figure 3.2. a) The PB reaction spectrum of 5 µM tm PE 16:0/18:1(9Z) after 5 seconds of UV exposure, b) Isolation followed by ion trap CID of [^{PB}tmPE]$^+$ collected in positive ion mode.

[13]C-TrEnDi modification was applied to PE 16:0/18:1(9Z) for the proof of concept experiments. The PB reaction was facilitated by an offline flow microreactor, which had a product yield of approximately 15%.[30] The reaction yield was calculated by normalizing the relative ion intensity of the PB product to that of the species before the photo-reaction. Figure 3.2a displays the PB reaction spectrum for the ^{13}C-TrEnDi modified PE. The tmPE species appeared at *m/z* 778 and the PB reaction yielded product ions with a neutral gain of 58 Da (*m/z* 836). The [^{PB}tmPE]$^+$ ion was isolated and activated via ion trap CID and shows an exclusive product ion at *m/z* 202 [(^{13}CH$_3$)$_4$C$_2$H$_2$NO$_4$P]$^+$, confirming the PE headgroup loss as shown in Figure 3.2b. Product ions from fragmentation at the oxetane ring for positive ion mode C=C location were not present; therefore, all structural information was collected in negative ion mode post charge inversion.
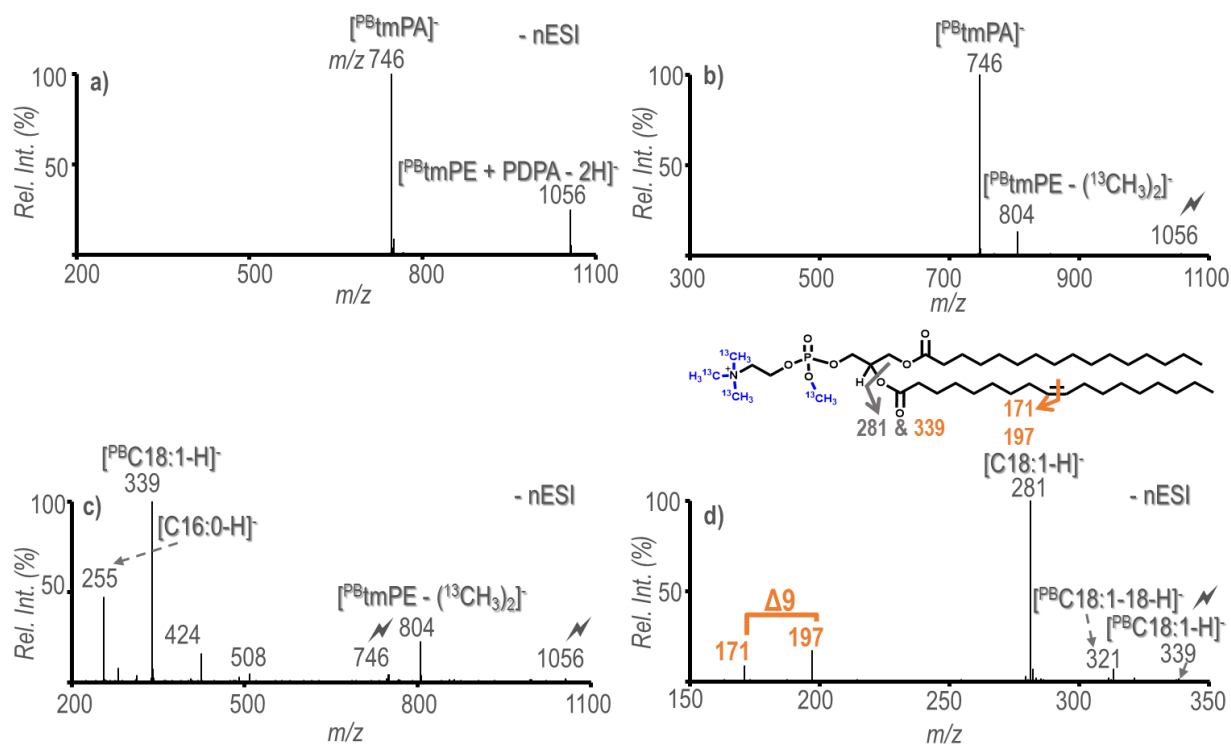
Figure 3.3. a) Isolation of the PB product ions at m/z 836 from Figure 3.1a and sequential charge inversion via gas-phase ion/ion reaction of [^{PB}tmPE]$^+$ and [PDPA - 2H]$^{2-}$, b) Ion trap CID of [^{PB}tmPE + PDPA - 2H]$^-$ at *m/z* 1056, c) Ion trap CID of [^{PB}tmPA]$^-$ at *m/z* 746, d) Ion trap CID of the PB product of C18:1(9Z) verifying the C=C position of PC 16:0/18:1(Δ9). CID of a target ion is depicted by alightning bolt (✎).

The in-solution modified PE ion, [^{PB}tmPE]$^+$, was subjected to ionization via direct nESI and mutually stored in q2 with doubly deprotonated PDPA, [PDPA - 2H]$^{2-}$. The mutual storage ion/ion reaction resulted in two major products, a complex formed between the two ions at *m/z* 1056 and an anionic ^{13}C-methylated phosphatic acid ([tmPA]$^-$) at *m/z* 746, as shown in Figure 3.3a. The tmPA formation was due to the loss of (^{13}CH$_3$)$_3$NCH$_2$CH$_2$ from the phosphate headgroup of the tmPE species leaving a ^{13}C-methylated phosphatic acid. These results are similar to what was observed for tmPE without PB reaction, further suggesting that the addition of the acetone does not affect the overall pathway for gas-phase charge inversion. In Figure 3.3b, the ion trap CID of the complex [^{PB}tmPE + PDPA - 2H]$^-$ resulted in the increase of [tmPA]$^-$ and also the minor loss of two ^{13}C-methyl groups ([^{PB}tmPE - (^{13}CH$_3$)$_2$]$^-$. The sequential fragmentation of the precursor at *m/z* 746 generates the spectrum in Figure 3.3c. Abundant product ions corresponding to unmodified C16:0 and PB reacted C18:1 at *m/z* 255 and 339, respectively, are obtained. Also present in lower

abundance is the neutral ketene loss (NL ketene) of both acyl chains at *m/z* 424 and *m/z* 508. The relatively more abundant NL ketene loss of ^{PB}C18:1 at *m/z* 424 corresponds with the C18:1 being at the *sn2* position relative to the C16:0 at the *sn1* position. Ultimately, the series of experiments verified that the method can be used for determining the species as PE 16:0/18:1.To further probe the structure of the tmPE, fragmentation of the ion population at *m/z* 339 was carried out as shown in Figure 3.3d. Diagnostic ions *m/z* 171 and 197 can be readily identified by the difference of 26 Da, and from NL of *m/z* 168 and 142 respectively from [^{PB}tmPA]$^-$ the location of C=C can be determined to be Δ9 in the synthetic PE 16:0/18:1 standard.
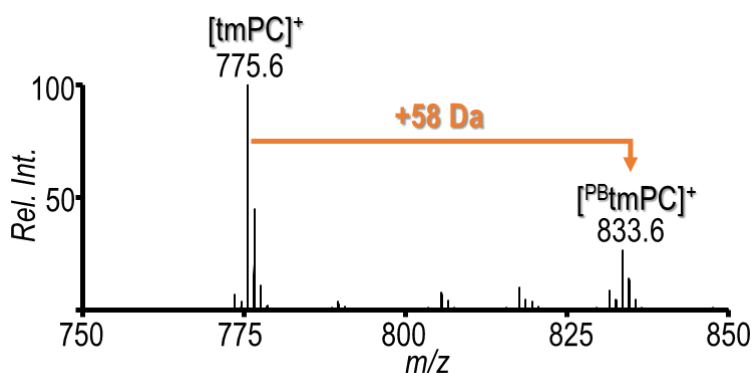
Figure 3.4. Positive ion mode mass spectrum of the PB reaction of [tmPC 16:0/18:1(9Z)]$^+$.
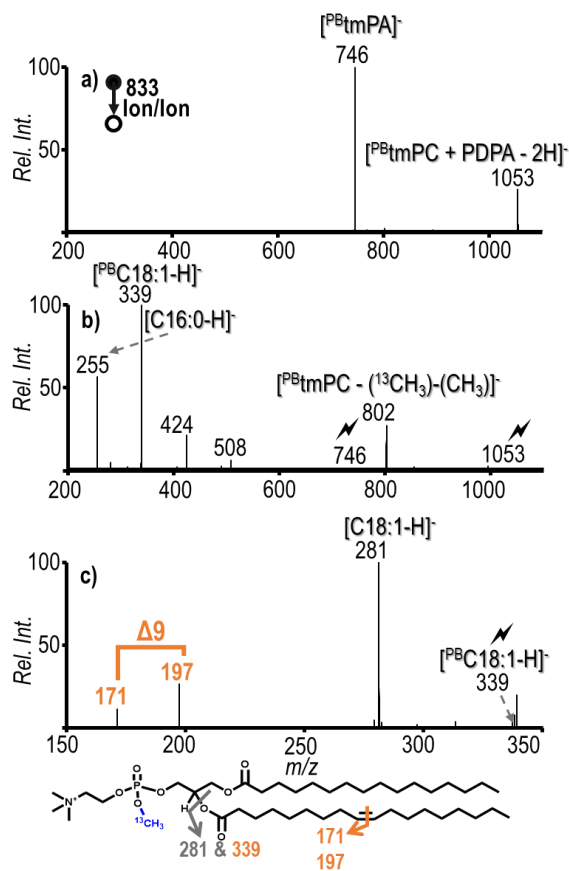
Figure 3.5. a) Post-ion/ion reaction between [PDPA - 2H]$^{2-}$ and [^{PB}tmPC 16:0/18:1(9Z)]$^{+}$; b) Ion trap CID of [^{PB}tmPC + PDPA - 2H]$^{-}$ followed by subsequent ion trap CID of [^{PB}tmPA]$^{-}$, c) Sequential steps of CID for the C=C localization.

The PB reaction was also applied to tmPC (*m/z* 775), which yielded a product at *m/z* 833. The results shown in Figure 3.4 show that PC lipid species also benefit from our derivatization and charge inversion strategy. Analysis of PC 16:0/18:1 was conducted in a similar fashion, yielding comparable results (Figure 3.5). The primary difference between PC and PE analysis is the 3 Da mass differences in the products due to the PC being ^{13}C-TrEnDi modified only at the phosphate group whereas the PE is modified with four ^{13}C-methyl groups (one on phosphate and 3 on primary amine). Based on these results, the method described herein can be applied to in-depth structural characterization of GPs, including unsaturation site identification. Figure 3.1 shows the overall workflow for our described method. The combination of the workflows represents a GP structural elucidation method that is both highly sensitive and specific.

3.4.2 Application of in-solution modification and gas-phase charge inversion

The PB reaction paired with charge inversion via ion/ion reactions is a method that provides sensitive and selective characterization. While effective, the PB reaction chemistry in conjunction with ion/ion reactions is limited by the ionization efficiency of the species present in the sample. By improving ionization efficiency of PEs, the number of identified PE species in the sample can theoretically increase. A NLS for 141 Da for detection of PEs in unmodified bovine liver extract is shown in Figure 3.6a with the most abundant ions in the spectrum labelled as m/z 744 (PE 36:2) and m/z 768 (PE 38:4). ^{13}C-TrEnDi modification bovine liver extract was also scanned for PEs using a PIS of m/z 202 as shown in Figure 3.6b. The findings were consistent with ^{13}C-TrEnDi studies in the past that show an increase in species identified with greater than 10-fold signal increase obtained with the modification. By comparing an equivalent number of scans, Figure 3.6 shows the potential for increased absolute identification of PEs using a combination of derivatization and charge inversion.
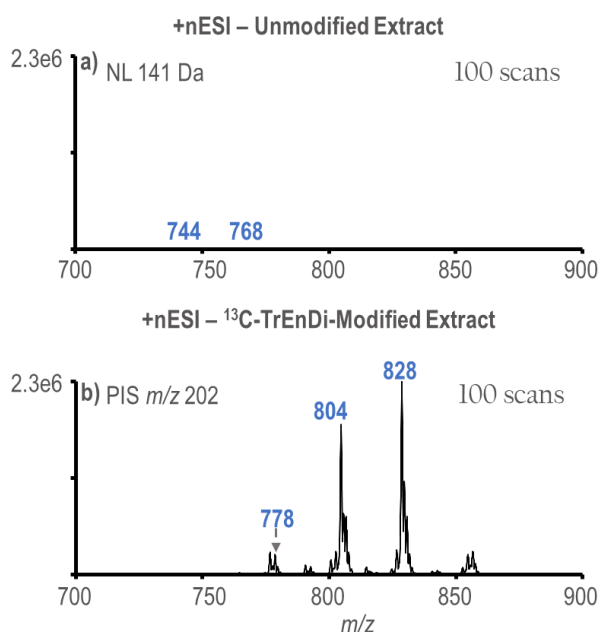
Figure 3.6. Bovine liver polar lipid extract (88 ug/mL) mass spectra for PE detection. a) Neutral loss scan for 141 of unmodified extract b) Precursor ion scan for 202 of the modified extract.

Bovine liver polar lipid extract was used to illustrate the utility of these combined methods for a complex mixture derived from a biological source. A primary goal for undertaking this work was to determine structural information for GPs present in biological extracts. Before the PB

77

reaction was applied in the positive ion mode, the ion population at *m/z* 778 (tmPE 34:1) was isolated and subsequently transformed in the gas-phase via the ion/ion charge inversion chemistry to generate a [tmPE + PDPA - 2H]⁻ complex. After the charge inversion to the negative polarity, CID of the [tmPE + PDPA - 2H]⁻ ion followed by CID of [tmPA]⁻ generated anions representative of the fatty acyl chains present in the selected lipid, as demonstrated with Figure 3.7a. After the sequential steps of CID just described, fragmentation products were formed at *m/z* 253, 255, 281 and 283, which correspond to fatty acyl chains C16:1, C16:0, C18:1 and C18:0, respectively. The appearance of these peaks indicates the presence of the isomers PE 16:0_18:1 and PE 18:0_16:1 in the ion population at *m/z* 778. The PB reaction of the sample was conducted producing a post-reaction product for *m/z* 778 58 Da greater in mass at *m/z* 836, which, following the analogous set of experiments described above, resulted in the fatty acyl chain ions shown in Figure 3.7b. The fatty acyl chains present in the spectrum are consistent with those of Figure 3.7a, which also suggests the presence of PE 16:0_18:1 and PE 18:0_16:1 after the addition of a 58 Da acetone modification to the unsaturated fatty acyl species. The abundant peak at *m/z* 339 represents [^{PB}18:1-H]⁻. The [^{PB}18:1 - H]⁻ ion was subjected to ion trap CID to generate further structural information and the resulting spectrum is shown in Figure 3.7c. The major fragment ion at *m/z* 281 arises from the loss of acetone. The diagnostic ions at *m/z* 171/197 and 199/225 correspond to a double bonds being present at the Δ9 and Δ11 positions of C18:1. The fragmentation of [^{PB}16:1 - H]⁻ ions produced diagnostic ions at 171/197 corresponding to the C=C position at the Δ9 position and identifies PE 18:0_16:1(Δ9) (Figure 3.8). The data showed that the methods are capable of being combined for structural characterization down to the C=C location of lipids in a biological sample and allows for the distinction between C=C positional isomers.
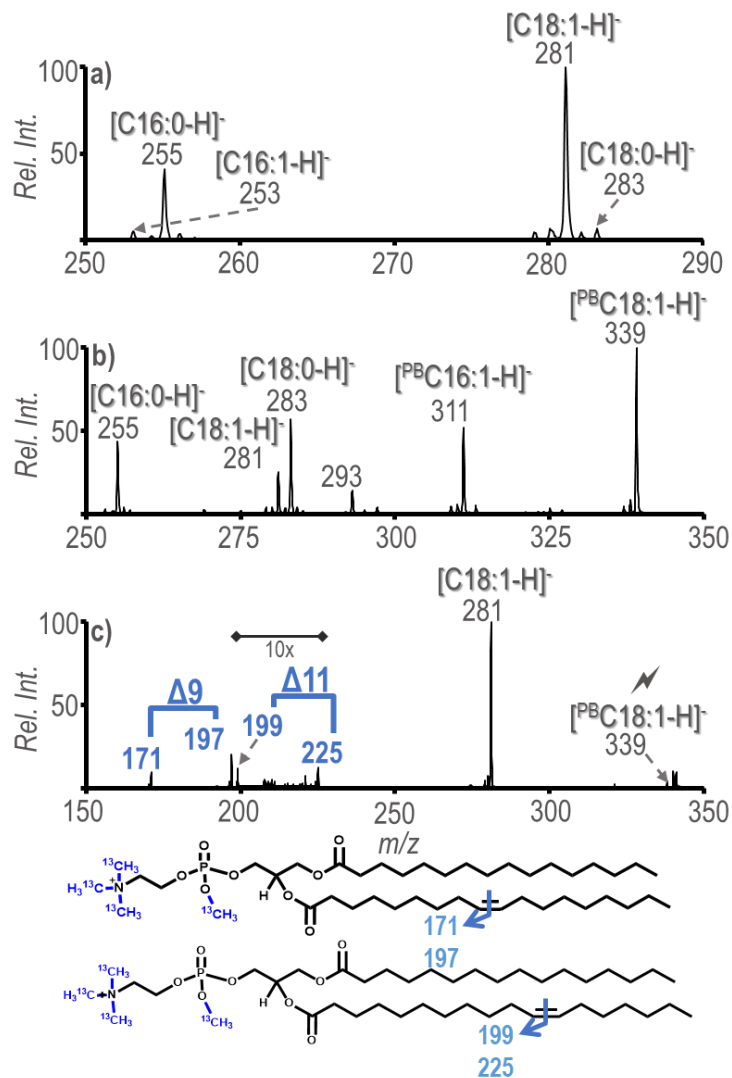
Figure 3.7. a) Charge inversion of positive ion mode *m/z* 778 followed by multiple steps of ion trap CID for fatty chain determination, b) Charge inversion of positive ion mode of ions at *m/z* 836 (PB product of *m/z* 778), c) Sequential CID spectrum of *m/z* 339 from panel b). ID: PE 16:0_18:1(Δ9) and PE 16:0_18:1(Δ11).
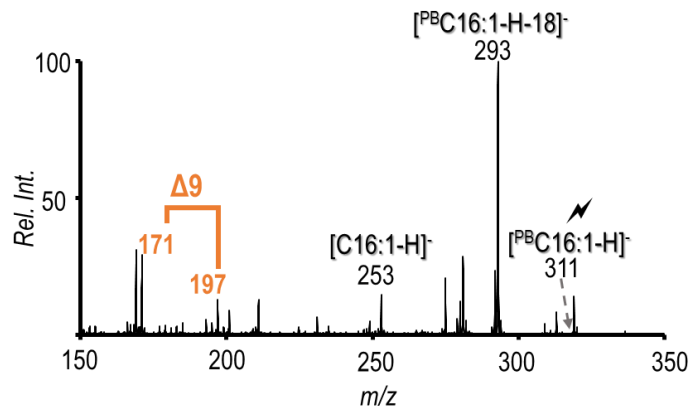
Figure 3.8. Charge inversion of positive ion mode m/z 836 (PB product of m/z 778) followed by multiple steps of ion trap CID and sequential CID spectrum of m/z 311 from Figure 3.7b.

3.4.3   Specific characterization of unsaturated fatty acyl chain isomers

The structural complexity of GPs can include unsaturation on both of the fatty acyl chains at the *sn1* and *sn2* glycerol positions. The origin of the C=C location has been challenged in the past in the PB reaction spectrum analysis from data acquired without recourse to the charge inversion MS^n procedure used in this work.[27] There could be overlap in diagnostic ions for different fatty acyl chains within a single GP subclass leading to ambiguity in analysis. Charge inversion of the PB reacted species followed by generation and isolation of each fatty acyl chain allows for the independent characterization of each specific fatty acyl chain thereby avoiding the ambiguity with analysis that may arise when identifying species in positive ion mode.
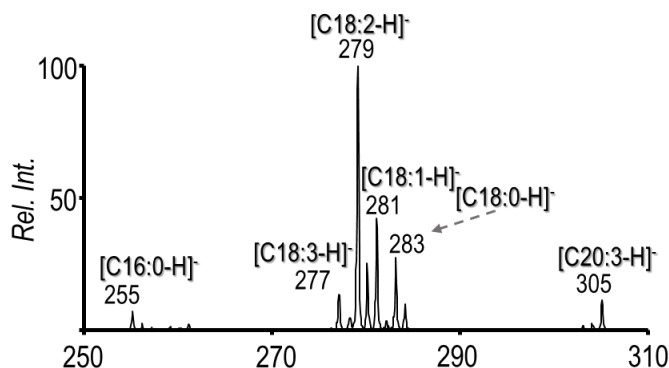
Figure 3.9. Charge inversion via ion/ion reaction with PDPA of ions at *m/z* 802 followed by sequential steps of CID for fatty chain determination.

An example of species presents at the lower end of our dynamic range (which is 50 times) without ^{13}C-TrEnDi modification was the subclass PE 36:3 (*m/z* 802 after ^{13}C-TrEnDi modification). In our previous work, PE 36:3 was not structurally characterized because of its relatively low abundance.[30] The tmPE 36:3 ions at *m/z* 802 were isolated, charge inverted and subjected to multiple steps of CID thereby generating the fatty acyl chains C16:0, C18:0, C18:1, C18:2, C18:3, and C20:3 (Figure 3.9). The PE 36:3 species were identified as PE 18:0_18:3, PE 18:1_18:2, and PE 16:0_20:3, exemplifying the structural diversity of the lipidome, particularly regarding the presence of GP species including two unsaturated fatty acyl chains. The sample underwent photochemical reaction and was subjected to ion/ion reaction followed by sequential CID steps resulting in Figure 3.10a showing that each unsaturated chain was modified. By fragmenting each individual chain separately, specific fatty acyl chain C=C localization can be achieved. As shown in Figure 3.10b, the less abundant chain [^{PB}C18:1 - H]$^-$ was probed and shows that there were C=C isomers present at Δ9 and Δ11 (i.e., isomers PE 18:1(Δ9)_18:2 and PE 18:1(Δ11)_18:2). Figure 3.10c shows results for the analogous experiments performed on C18:2 where the abundant fragment is the loss of the acetone (*m/z* 279) and there exist two sets of diagnostic ions that identify the species as C18:2(Δ9, Δ12). Identifying fatty acyl chains permits in-depth structural elucidation, as PE 36:3 can further be assigned as PE 18:1(Δ9)_18:2(Δ9, Δ12) and PE 18:1(Δ11)_18:2(Δ9, Δ12). These new species identified in BLE shows that the method has increased the sensitivity and can be beneficial for characterizing absolute lipids structure.
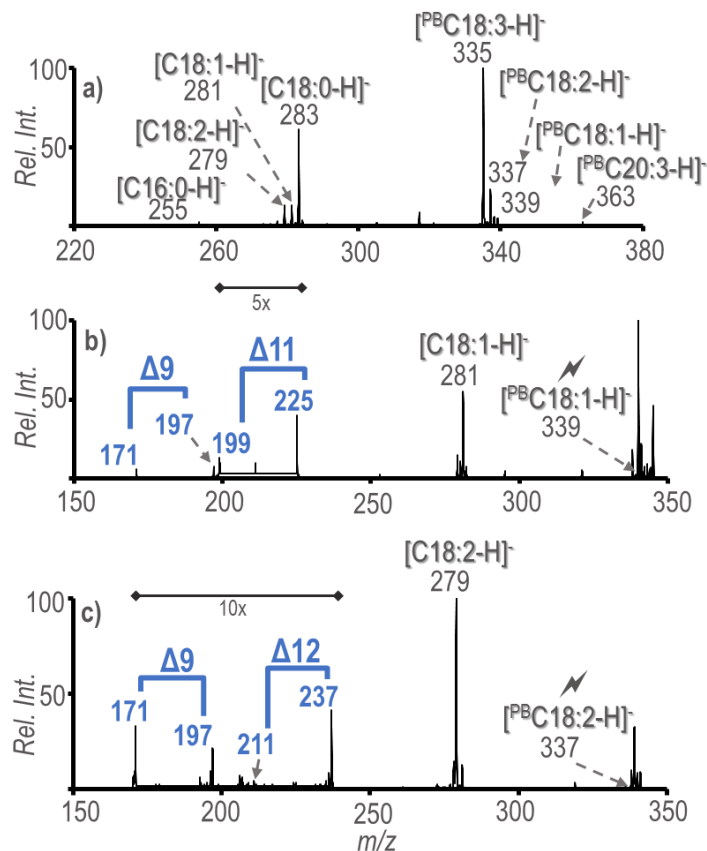
Figure 3.10. a) Charge inversion of positive ion mode m/z 860 (the PB product of 802) followed by sequential steps of CID for fatty chain determination, b) Sequential CID spectrum of *m/z* 339 from panel a), c) Sequential CID spectrum of *m/z* 337 from panel a). ID: PE 18:1(Δ9)_18:2(Δ9, Δ12), PE 18:1(Δ11)_18:2(Δ9, Δ12).

3.4.4 Determining C=C location isomers for polyunsaturated fatty acyl chains

Up until now, this report centralized the structural identification of mono- and di-unsaturated GPs species using a combination of ^{13}C-TrEnDi modification, the PB reaction, and gas-phase ion/ion charge inversion chemistries. Diagnostic ions of polyunsaturated (with three or more degrees of unsaturation) lipids have mainly been unexplored via the PB reaction for determining C=C location in negative ion mode due to the complexity of the spectra. In 2017, Murphy and co-workers, however, applied the PB reaction to polyunsaturated fatty acids and conducted subsequent MS/MS analysis in the negative ion mode.[29] Novel diagnostic ions were found after fragmentation, permitting C=C location distinction for polyunsaturated fatty acids possessing 18 or 20 carbons and three to four degrees of unsaturation. We have used insights

provided in that work for interpreting results from the workflow described herein for polyunsaturated species found in the complex lipid sample.
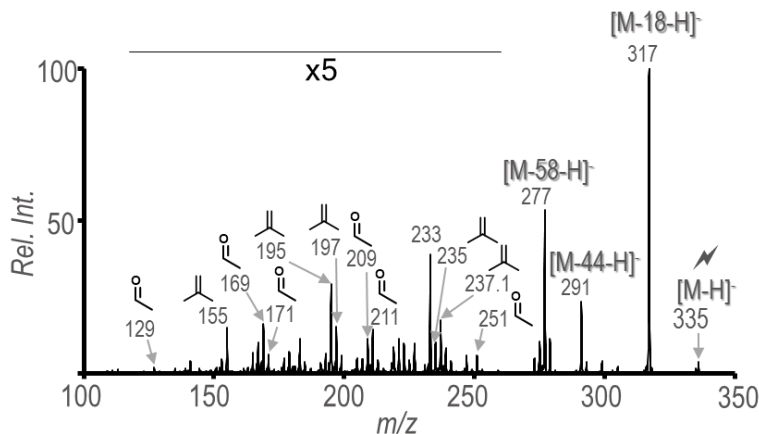
Figure 3.11. Sequential CID spectrum of *m/z* 335 from Figure 3.10a. ID: PE 18:0_18:3(Δ6, Δ9, Δ12), PE 18:0_18:3(Δ9, Δ12, Δ15).

The fragment ion at *m/z* 335 in Figure 3.10a was subjected to ion trap CID to determine the ability to distinguish the location of unsaturation along C18:3. The resulting spectrum is shown in Figure 3.11 and shows results matching Murphy's findings. The diagnostic ions at 129/155, 169/195, 209/235 indicate the presence of C18:3(Δ6, Δ9, Δ12), whereas the ions at *m/z* 171/197, 211/237, and 251/277 show the presence of C18:3(Δ9, Δ12, Δ15). The combination of TrEnDi/PB modification and charge inversion clearly shows that PE 36:3 bovine liver exists as a minimum of 4 species {PE 18:0_18:3(Δ6, Δ9, Δ12), PE 18:0_18:3(Δ9, Δ12, Δ15), PE 18:1(Δ9)_18:2(Δ9, Δ12), and PE 18:1(Δ11)_18:2(Δ9, Δ12)}. This is the first time to our knowledge of using negative ion mode for complex lipid species identification. The combination of using ^{13}C-TrEnDi, the PB reaction, and charge inversion allows for sensitive and specific structural characterization of GPs down to the C=C location (Table 3.1 and Table 3.2).

Table 3.1. Identified PCs in bovine liver polar lipid extract.

m/z	PB product	Fatty Acyl Diagnostic Ions	PB Reaction Diagnostics	Identified Species
747	805	225; 339	171, 197	PC 14:0_18:1(Δ9)
747	805	225; 339	199, 225	PC 14:0_18:1(Δ11)
747	805	255; 311	171, 197	PC 16:0_16:1(Δ9)
773	831	255; 337	171, 197 ; 211, 237	PC 16:0_18:2(Δ9,Δ12)
775	833	255; 339	171, 197	PC 16:0_18:1(Δ9)
775	833	255; 339	199, 225	PC 16:0_18:2(Δ11)
775	833	283; 311	171, 197	PC 16:1(Δ9)_18:0
801	859	283; 337	171, 197 ; 211, 237	PC 18:0_18:2(Δ9, Δ12)
801	859	339	171, 197	PC 18:1(Δ9)_18:1(Δ9)
801	859	339	199, 225	PC 18:1(Δ11)_18:1(Δ11)
801	859	255; 365	199, 225; 239, 265	PC 16:0_20:2(Δ11, Δ14)
803	861	283; 339	171, 197	PC 18:0_18:1(Δ9)
803	861	283; 339	199, 225	PC 18:0_18:1(Δ11)

Table 3.2. Identified PEs in bovine liver polar lipid extract.

m/z	PB product	Fatty Acyl Diagnostic Ions	PB Reaction Diagnostics	Identified Species
764	822	339; 241	171, 197	PE 18:1(Δ9)_15:0
774	832	255; 335	171, 197; 211, 237; 251, 277	PE 16:0_18:3(Δ9, Δ12, Δ15)
774	832	255; 336	129, 155; 169, 195; 209, 235	PE 16:0_18:3(Δ6, Δ9, Δ12)
776	834	255 ; 337	171, 197 ; 211, 237	PE 16:0_18:2(Δ9, Δ12)
778	836	255; 339	171, 197	PE 16:0_18:1(Δ9)
778	836	255; 339	199, 225	PE 16:0_18:1(Δ11)
778	836	253; 283	171, 197	PE 16:1(Δ9)_18:0
790	848	337; 269	171, 197; 211, 237	PE 17:0_18:2(Δ9, Δ12)
792	850	269; 339	171, 197	PE 17:0_18:1(Δ9)
802	860	339; 337	171, 197; 171, 197; 211, 237	PE 18:1(Δ9)_18:2(Δ9, Δ12)
802	860	339; 337	199, 225; 171, 197; 211, 237	PE 18:1(Δ11)_18:2(Δ9, Δ12)
802	860	335; 283	171, 197; 211, 237; 251, 277	PE 18:0_18:3(Δ9, Δ12, Δ15)
802	860	335; 283	129, 155; 169, 195; 209, 235	PE 18:0_18:3(Δ6, Δ9, Δ12)
804	862	337; 283	171, 197 ; 211, 237	PE 18:0_18:2(Δ9, Δ12)
804	862	339; 281	171, 197	PE 18:1(Δ9)_18:1(Δ9)
804	862	339; 281	199, 225	PE 18:1(Δ11)_18:1(Δ11)
806	864	339; 283	171, 197	PE 18:0_18:1(Δ9)
806	864	339; 283	199, 225	PE 18:0_18:1(Δ11)

3.5   Conclusion

The combination of ^{13}C-TrEnDi modification, the PB reaction and gas-phase charge inversion allows for analysis of GPs using a single ionization polarity and solvent composition. ^{13}C-TrEnDi modification improved the PE species sensitivity more than 10-fold, while the PB reaction probes the unsaturated fatty acyl chains. In the case of charge inversion of the PB reacted GPs without ^{13}C-TrEnDi, there was the improved sensitivity and selectivity in locating C=C bonds. However, using the method presented herein, the sensitivity of GP identification is limited by the ionization efficiency and relative abundances of each species.[13]C-TrEnDi markedly improves

identification of PE species via increased ionization efficiency of PE lipids in the positive ion mode. Gas-phase charge inversion enables the lipid species to the selected in the positive ion mode which is the best means of ionization and upon ion/ion reactions be converted into an anionic species for future structural analysis. Overall, the technique for sensitive and selective structural characterization of phospholipids was demonstrated. The limitation of this work is that not all polyunsaturated species can be currently analyzed due to indistinguishable characteristic of the negative ion mode PB reaction fragmentation spectrum. This is the first time that C=C location has been determined for ^{13}C-TrEnDi modified lipids.

This work demonstrates the combination of three techniques to improve the sensitivity and specificity in characterizing the structures of GPs. ^{13}C-trendi provides high signal responses for multiple lipid classes in the positive ion mode, gas-phase charge inversion allows for the generation of structurally diagnostic fatty acyl anions, and the PB reaction allows for the location of double bonds within the fatty acyl chain. This unique combination of techniques enables detailed structural characterization for lipid species that may not ionize efficiently in shotgun lipidomics (e.g., PEs) while retaining the ability to generating detailed fatty acid information (i.e., composition and double bond location).

3.6   References

1.   Han, X. & Gross, R. W. Shotgun lipidomics: Electrospray ionization mass spectrometric analysis and quantitation of cellular lipidomes directly from crude extracts of biological samples. *Mass Spectrom. Rev.* **24**, 367–412 (2005).

2.   Han, X. *Lipidomics: Comprehensive mass spectrometry of lipids*. (John Wiley & Sons, 2016).

3.   Quehenberger, O. *et al.* Lipidomics reveals a remarkable diversity of lipids in human plasma,. *J. Lipid Res.* **51**, 3299–3305 (2010).

4.   Fhaner, C. J., Liu, S., Ji, H., Simpson, R. J. & Reid, G. E. Comprehensive Lipidome Profiling of Isogenic Primary and Metastatic Colon Adenocarcinoma Cell Lines. *Anal. Chem.* **84**, 8917–8926 (2012).

5.   Ryan, E. & Reid, G. E. Chemical Derivatization and Ultrahigh Resolution and Accurate Mass Spectrometry Strategies for "Shotgun" Lipidome Analysis. *Acc. Chem. Res.* **49**, 1596–1604 (2016).

6. Wasslen, K. V., Canez, C. R., Lee, H., Manthorpe, J. M. & Smith, J. C. Trimethylation Enhancement Using Diazomethane (TrEnDi) II: Rapid In-Solution Concomitant Quaternization of Glycerophospholipid Amino Groups and Methylation of Phosphate Groups via Reaction with Diazomethane Significantly Enhances Sensitivity in Mass Spectrometry Analyses via a Fixed, Permanent Positive Charge. *Anal. Chem.* **86**, 9523–9532 (2014).

7. Canez, C. R. *et al.* Trimethylation Enhancement Using ^{13}C-Diazomethane (^{13}C-TrEnDi): Increased Sensitivity and Selectivity of Phosphatidylethanolamine, Phosphatidylcholine, and Phosphatidylserine Lipids Derived from Complex Biological Samples. *Anal. Chem.* **88**, 6996–7004 (2016).

8. Stutzman, J. R., Blanksby, S. J. & McLuckey, S. A. Gas-Phase Transformation of Phosphatidylcholine Cations to Structurally Informative Anions via Ion/Ion Chemistry. *Anal. Chem.* **85**, 3752–3757 (2013).

9. Rojas-Betancourt, S., Stutzman, J. R., Londry, F. A., Blanksby, S. J. & McLuckey, S. A. Gas-Phase Chemical Separation of Phosphatidylcholine and Phosphatidylethanolamine Cations via Charge Inversion Ion/Ion Chemistry. *Anal. Chem.* **87**, 11255–11262 (2015).

10. Betancourt, S. K. *et al.* Trimethylation Enhancement Using ^{13}C-Diazomethane: Gas-Phase Charge Inversion of Modified Phospholipid Cations for Enhanced Structural Characterization. *Anal. Chem.* **89**, 9452–9458 (2017).

11. Tomer, K. B., Crow, F. W. & Gross, M. L. Location of double-bond position in unsaturated fatty acids by negative ion MS/MS. *J. Am. Chem. Soc.* **105**, 5487–5488 (1983).

12. Klein, D. R. & Brodbelt, J. S. Structural Characterization of Phosphatidylcholines Using 193 nm Ultraviolet Photodissociation Mass Spectrometry. *Anal. Chem.* **89**, 1516–1522 (2017).

13. Pham, H. T. *et al.* Structural characterization of glycerophospholipids by combinations of ozone- and collision-induced dissociation mass spectrometry: the next step towards "top-down" lipidomics. *The Analyst* **139**, 204–214 (2014).

14. Brown, S. H. J., Mitchell, T. W. & Blanksby, S. J. Analysis of unsaturated lipids by ozone-induced dissociation. *Biochim. Biophys. Acta BBA - Mol. Cell Biol. Lipids* **1811**, 807–817 (2011).

15. Thomas, M. C. *et al.* Ozone-Induced Dissociation: Elucidation of Double Bond Position within Mass-Selected Lipid Ions. *Anal. Chem.* **80**, 303–311 (2008).

16. Pham, H. T., Trevitt, A. J., Mitchell, T. W. & Blanksby, S. J. Rapid differentiation of isomeric lipids by photodissociation mass spectrometry of fatty acid derivatives: Photodissociation of derivatized fatty acids. *Rapid Commun. Mass Spectrom.* **27**, 805–815 (2013).

17. Pham, H. T. & Julian, R. R. Radical delivery and fragmentation for structural analysis of glycerophospholipids. *Int. J. Mass Spectrom.* **370**, 58–65 (2014).

18. Campbell, J. L. & Baba, T. Near-Complete Structural Characterization of Phosphatidylcholines Using Electron Impact Excitation of Ions from Organics. *Anal. Chem.* **87**, 5837–5845 (2015).

19. Baba, T., Campbell, J. L., Le Blanc, J. C. Y. & Baker, P. R. S. Structural identification of triacylglycerol isomers using electron impact excitation of ions from organics (EIEIO). *J. Lipid Res.* **57**, 2015–2027 (2016).

20. Deimler, R. E., Sander, M. & Jackson, G. P. Radical-induced fragmentation of phospholipid cations using metastable atom-activated dissociation mass spectrometry (MAD-MS). *Int. J. Mass Spectrom.* **390**, 178–186 (2015).

21. Li, P., Hoffmann, W. D. & Jackson, G. P. Multistage mass spectrometry of phospholipids using collision-induced dissociation (CID) and metastable atom-activated dissociation (MAD). *Int. J. Mass Spectrom.* **403**, 1–7 (2016).

22. Stinson, C. A., Zhang, W. & Xia, Y. UV Lamp as a Facile Ozone Source for Structural Analysis of Unsaturated Lipids Via Electrospray Ionization-Mass Spectrometry. *J. Am. Soc. Mass Spectrom.* **29**, 481–489 (2018).

23. Harris, R. A., May, J. C., Stinson, C. A., Xia, Y. & McLean, J. A. Determining Double Bond Position in Lipids Using Online Ozonolysis Coupled to Liquid Chromatography and Ion Mobility-Mass Spectrometry. *Anal. Chem.* **90**, 1915–1924 (2018).

24. Cao, W., Ma, X., Li, Z., Zhou, X. & Ouyang, Z. Locating Carbon–Carbon Double Bonds in Unsaturated Phospholipids by Epoxidation Reaction and Tandem Mass Spectrometry. *Anal. Chem.* **90**, 10286–10292 (2018).

25. Ma, X. & Xia, Y. Pinpointing Double Bonds in Lipids by Paternò-Büchi Reactions and Mass Spectrometry. *Angew. Chem. Int. Ed.* **53**, 2592–2596 (2014).

26. Stinson, C. A. & Xia, Y. A method of coupling the Paternò–Büchi reaction with direct infusion ESI-MS/MS for locating the C☐C bond in glycerophospholipids. *The Analyst* **141**, 3696–3704 (2016).

27. Ma, X. *et al.* Identification and quantitation of lipid C=C location isomers: A shotgun lipidomics approach enabled by photochemical reaction. *Proc. Natl. Acad. Sci.* **113**, 2573–2578 (2016).

28. Ren, J., Franklin, E. T. & Xia, Y. Uncovering Structural Diversity of Unsaturated Fatty Acyls in Cholesteryl Esters via Photochemical Reaction and Tandem Mass Spectrometry. *J. Am. Soc. Mass Spectrom.* **28**, 1432–1441 (2017).

29. Murphy, R. C., Okuno, T., Johnson, C. A. & Barkley, R. M. Determination of Double Bond Positions in Polyunsaturated Fatty Acids Using the Photochemical Paternò-Büchi Reaction with Acetone and Tandem Mass Spectrometry. *Anal. Chem.* **89**, 8545–8553 (2017).

30. Franklin, E. T., Betancourt, S. K., Randolph, C. E., McLuckey, S. A. & Xia, Y. In-depth structural characterization of phospholipids by pairing solution photochemical reaction with charge inversion ion/ion chemistry. *Anal. Bioanal. Chem.* (2019) doi:10.1007/s00216-018-1537-1.

31. Shields, S. W. J. & Manthorpe, J. M. Efficient, scalable and economical preparation of tris(deuterium)- and ^{13}C-labelled *N* -methyl- *N* -nitroso- *p* -toluenesulfonamide (Diazald®) and their conversion to labelled diazomethane: Efficient preparation of bis(deuterium)- and [13] C-labelled diazomethane. *J. Label. Compd. Radiopharm.* **57**, 674–679 (2014).

32. Xia, Y. *et al.* Implementation of Ion/Ion Reactions in a Quadrupole/Time-of-Flight Tandem Mass Spectrometer. *Anal. Chem.* **78**, 4146–4154 (2006).

33. Dowhan, W. Molecular genetic approaches to defining lipid function. *J. Lipid Res.* **50**, S305–S310 (2009).

CHAPTER 4.   TRIACYLGLYCEROL ANALYSIS BY PAIRING PHOTOCHEMICAL REACTIONS WITH REVERSE-PHASE LIQUID CHROMATOGRAPHY TANDEM MASS SPECTROMETRY

4.1   Abstract

Triacylglycerol (TG) is a class of lipids that is responsible for energy storage in biological systems and appears large in number in biological fluids such as human plasma. Due to structural complexity, analyzing TGs using shotgun lipidomic method is a challenge because of presence of compositional isomers. Reverse phase liquid-chromatography (RPLC) is a tool used for separation of TG molecular species for improved identification. RPLC paired with electrospray ionization (ESI) and tandem mass spectrometry (MS/MS) more accurately identifies species. Although long retention times will separate TGs with different locations of unsaturation, RPLC-MS/MS does not structural informative information for the location of carbon-carbon double-bond (C=C) without using synthesized standards. The Paternò–Büchi (PB) reaction has been employed to confidently characterize the location of C=C within lipid species via photo-initiated modification of the alkene group with an acetone, which was later subjected to MS/MS to formed signature fragmentation peaks. In this work, an online RPLC-PB-MS/MS system was developed for the analysis of TGs at C=C location level. The systems allowed for the identification of 46 TG species in human plasma at C=C location at a limit of detection of 50 nM.

4.2   Introduction

Prokaryotic and eukaryotic cells are composed of a substantial number of triacylglycerols (TGs) molecular species. A major role of TGs is energy storage as they are the key component of adipose cells, however, these neutral lipids are important for the delivery of fatty acids to cellular processes. [1] TG composition within human plasma is as a result of both internal biosynthesis but also food ingestion, which can contribute to increased complexity in the TG composition with a sample. Fish oils and milk fat, which both contribute to the Standard American Diet, have the most complex TG mixture.[2] TG molecular species have shown promise in acting as predictors to obesity and type II diabetes (T2D), while also strongly correlating with body-mass index (BMI).[3–5] For example, Ståhlman and co-workers found that there is an increase in vaccenic acid within human

90

plasma TG species in type 2 diabetes patients versus a control group.[6] Seeing as both vaccenic and oleic acid can be present in TG composition alongside many other carbon-carbon double bond (C=C) being able to distinguish these isomers will help improve the understanding of the roles of lipid species.

TGs structures are composed of three esterified fatty acids onto a glycerol backbone. Each fatty acyl chain has varying lengths, degrees of unsaturation, and location of unsaturation that are important for its overall physical properties. Mass spectrometry is an important tool for the characterization of TG molecular species. Shotgun analysis is the injection of a crude sample for direct analysis without prior separation and has the advantages of speed and high sensitivity. Methods such as multiple reaction monitoring (MRM) utilizes a shotgun approach for rapidly profiling of large sample set (1000 samples in less than 5 day).[7] The matrix effect and species overlapping is prevalent in shotgun analysis leading to limited capability of TG characterization due to ion suppression and complex mass spectra. Chromatography paired with mass spectrometry is a means of overcoming these challenges for the improved resolution of molecular species

In the past, gas chromatography was used for the separation of intact TG but was inefficient at providing characterization due to degradation of some species because of their low volatility and thermal instability.[8] Another separation technique is liquid chromatography (LC) which has multiple modes such as normal-phase, and reverse-phase (RP). Molecular species separation is possible with RPLC and allows for the separation of isomeric and isobaric species.[9–12] The separation of C=C isomers is possible with long retention times. However, it is difficult to determine differences in unsaturation site in a high throughput manner due to complexity in TG fatty acyl composition and lack on synthesized standards for retention time comparison. Although many methods for structural elucidation at C=C location exist, there is a lack of methods available for localization of C=C in a high-throughput manner. Electron impact excitation of ions from organics (EIEIO) paired with differential mobility spectrometry (DMS) revealed key structural information of TGs in Portuguese olive oil by reacting the species with a beam of electrons creating informative fragment ions.[13] Ozone-induced dissociation (OzID) uses gas-phase ion-molecule reaction between unsaturated lipids and ozone to localize the C=C.[14–16] The Paternò–Büchi (PB) reaction is a [2+2] cycloaddition of a ketone group to an alkene resulting in an oxetane ring. The PB reaction has when applied to unsaturated lipids to give C=C location upon low-energy collision-induced dissociation (CID). Activation of the product results in fragmentation at the

91

oxetane ring leading to C=C specific peaks. The PB reaction has been successfully applied to TGs using benzophenone and undergo RPLC-MS/MS for analysis.[17] This work shows the pairing of the PB reaction with RPLC for the detailed characterization of TG species. This online RPLC-PB-MS/MS system allowed for TG separation and characterization at C=C position. The lipid sample undergoes RPLC separation, then goes to a microreactor to undergo the PB reaction. The PB reacted sample was probed for structural character and a table of identified species was built. The method allowed for distinction of positional isomers without the need for fine tuning of each isomeric species.

4.3   Experimental Section

4.3.1   Chemicals

Triolein, triα-linolenic acid, and 1-Palmitoyl-2-oleoyl-3-linoleoyl-rac-glycerol were purchased from Sigma Aldrich. SPLASH Lipidomix Mass Spectrometry Standard was purchased from Avanti Polar Lipids. Pooled human plasma (Anticoagulant: Li Heparin) was purchased from Innovative Research. Acetone, methanol, ethyl acetate, acetonitrile, 2-propanol, and ammonium acetate were purchased from Fisher Chemical. Isooctane and chloroform were purchased from Beijing Tong Guang Fine Chemicals Company. A purification system at 0.03 µS cm (model: Micropure UV; Thermo Scientific; San Jose, CA, USA) was used to obtain the deionized water.

4.3.2   Sample preparation

The human plasma lipid extraction was based on the Folch protocol followed by a silica solid phase extraction (SPE) column method[18] for glycerol lipid isolation. In summary, 50 µL of human plasma as combined with 1.5 mL chloroform/methanol/water (v/v/v, 2/1/0.75), vortexed and centrifuged at 10,000 RPM for 10 minutes. The chloroform layer was collected and dried down using nitrogen gas. The sample was reconstituted in 0.5 mL of isooctane/ethyl acetate (80:1, v/v) and applied to a silica SPE column pretreated with 1 mL of isooctane/ethyl acetate (80:1, v/v). Three 5 mL fractions were collected using isooctane/ethyl acetate (80:1, 20:1, 75:25, v/v). The second and third fractions contained TGs and DGs, respectively. The eluant was dried and the samples were stored in a -80˚C freezer until analysis.

4.3.3 LC-PB-MS(/MS) Experiments

Glycerolipid samples were dissolved in methanol and place in an autosampler, which injected 2 µL of solution into an ExionLC AC system (Sciex) equipped with an Ascentis Express C8- HPLC column (150 x 3.0 mm, 2.7 µm, Sigma-Aldrich). The separation was performed isocratically at 90% mobile phase A for 50 minutes with a temperature of 55˚ C using mobile containing predominately acetone (A: 70/29/1, v/v/v, acetone/acetonitrile/2-propanol; B: 10 mM aqueous ammonium acetate, A/B 90/10, flowrate 0.3 mL/min). A homebuilt microreactor designed similarly to the previously described[19] conducted the online PB reaction and was connected to the electrospray ionization (ESI) source for analysis using a X500R Q-TOF (Sciex). MS parameters were as follows: ESI voltage: 5000 V; ion source gas: 33 psi; curtain gas: 30 psi; declustering potential: 80 V; accumulation time 0.25 s for MS experiments and 0.1 s for MS/MS experiments; temperature 450˚ C; collision energy: 35 V (beam-type CID).

4.3.4 RPLC-PB-MS/MS of Synthetic Glycerol Lipids.

The species TG 18:1(9Z)/18:1(9Z)/18:1(9Z), TG 18:3(9Z, 12Z, 15Z)/18:3(9Z, 12Z, 15Z)/18:3(9Z, 12Z, 15Z), and TG 16:0/18:1(9Z)/18:2(9Z, 12Z) were used to establish the method. Our group has shown the online HILIC-LC-PB-MS setup separation for identification of polar lipids however the protocol does not have the optimal conditions for GL analysis.[19] HILIC separation is helpful for interclass separation but does not support the full power of LC to be utilized as it does not allow for intraclass separation of TG species for improved lipidome coverage. A traditional method for TG species separation is RPLC. This method has allowed for separation of synthetic and naturally occurring TG molecular species. In order to obtain more accurately defined molecular species, TG standards are required for calibration of the separation and longer elution times are necessary for separation of species at C=C location. These parameters make it difficult to analyze C=C location in a high-throughput manner.[2] Herein, we show the optimized conditions for TG analysis for structural characterization at C=C location level using the PB reaction integrated into a RPLC-MS system without the need for standards of each molecular species C=C position.
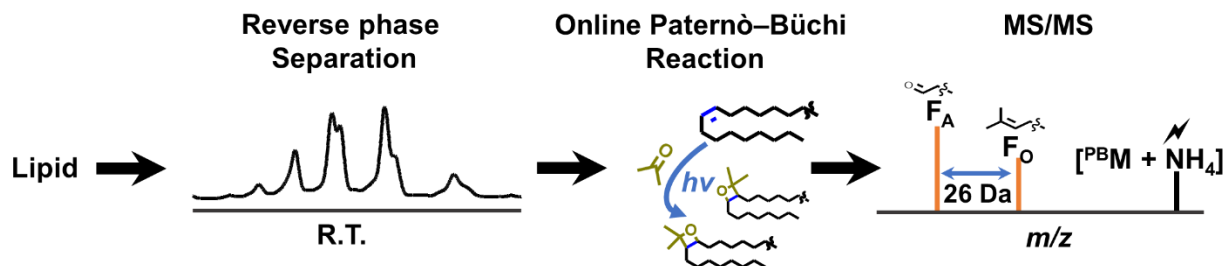
Figure 4.1. The RPLC-PB-MS/MS workflow for the analysis of unsaturated TG species. Lipid samples are injected into the LC system for reverse-phase separation and post-column the PB reaction is applied for an acetone modification which fragments to give C=C location.

In order to facilitate the PB reaction, solvent conditions for reaction optimization is necessary for efficient C=C localization. Typical solvent conditions for RPLC-separation of TGs may include high concentrations of 2-propanol, acetonitrile and/or methanol. 2-propanol and methanol have shown to slow down the PB reaction between a lipid olefin group and acetone resulting in a decreased product yield.[20] Acetone containing solvent were used as an eluent and reaction reagent in this workflow. A representation of the online RPLC-PB-MS/MS setup is shown in Figure 4.1. A RPLC-column is used for the distinct separation of TG species based on equivalent carbon numbers (ECNs).[21] The separated lipids flow through a microreactor to undergo the PB reaction modifying the TG with an acetone. The reaction time was 18 seconds based on the flowrate 0.3 mL/min used for HPLC separation and optimized reaction conditions. The PB reacted species are then subjected to ESI and undergo tandem MS for structural analysis. The resulting spectrum presents ions that differ by 26 Da and allow for the distinct determination of molecular species at C=C position.

As shown in Figure 4.1a, TG 54:9 eludes from the column first followed by TG 52:3 and species TG 54:3, respectively, as expected due to their ECNs 36, 46, 48, respectively. The spectrum highlights that the solvent conditions show to be reliable for separation of species. The PB reaction is applied post-column and this allows for the PB products to share similar RT as the unmodified species are shown with the blue trace in Figure 4.2a. The black and blue traces show the overlaying XICs of the unreacted species and reacted species, respectively. Figure 4.2a shows that the PB reaction product share similar peak shape as the unmodified species and can be directly linked by mass and RT.

The incorporation of ammonium acetate to the mobile phase allowed for intact and modified TG species to be readily adducted by a single ammonium and produce an abundant signal. TG 54:9 perceives to have a higher product yield than the other two species based on the relative intensity of XIC of the PB product at time 11 minutes. This is expected to be because of the presence of more double bonds creating a higher reaction efficiency. In Figure 4.2b, TG 54:9 formed an ammonium adducted species at m/z 890. The post PB reaction spectra for the species is shown in Figure 4.2c exposing that there is an increase in mass for the PB product peak at 58 Da higher than the intact species at m/z 948 corresponding to the acetone reagent attaching to the species. The PB reaction also initiated the addition of more than a single acetone onto the TG species. Due to the presence of nine double bonds, also present is the doubly and triply acetone-adducted species in smaller abundances. The PB reactions can lead to the acetone modifying any of the unsaturation sites, which further shows how TG 54:9 had a greater product yield.
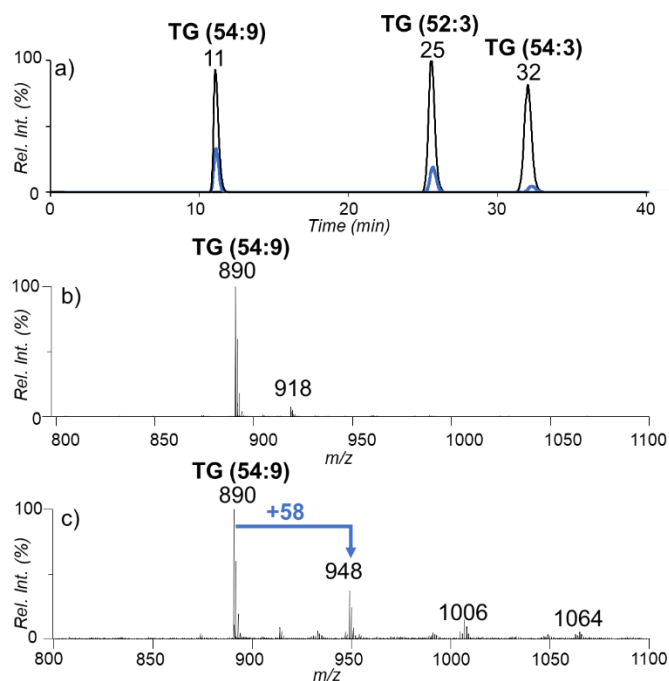
Figure 4.2. a) The overlaying XICs of masses corresponding to TG 54:9, TG 52:3, and TG 54:3 before and after the PB reaction, the black trace is before the reaction and the blue trace is after the reaction (zoomed 10x). b) An averaged mass spectrum for the ions present at 11 minutes before the PB reaction c) The post PB reaction spectrum of the ions present at 11 minutes.

The PB reaction was applied to TG 54:3 at RT 32 min (Figure 4.2a) and it shows that an acetone modified species is present at *m/z* 960 in Figure 4.3a. There is also the presence of a double adducted species at *m/z* 1018 as a minor product. For the fragmentation of the unmodified species, the fragment ions present are the neutral loss of 18:1 as a carboxylic acid and ammonia at *m/z* 603, 18:1 acylium ion plus 74 at *m/z* 339, and 18:1 as an acylium ion as expressed in Figure 4.3b. These fragment peaks are consistent with past work and the predicted MS/MS spectrum information provided by LipidMaps.[1] The ions at *m/z* 603 verify that the standard consist of three 18:1 fatty acyl chains based on the lack of any other fragment ions corresponding to an fatty acyl chains loss identifying the species as TG (18:1/18:1/18:1).

However, to get more coverage of the structure the PB product was applied and Figure 4.3c is the resulting CID spectrum of the ions at *m/z* 960 from Figure 4.3a. The fragmentation of the PB product shows a single set of diagnostic ions that are 26 Da apart at *m/z* 493 and 519 that can be used for structural characterization. The diagnostic peaks show that the fragmentation at the C=C location happens after the fatty acyl chain loss resulting in diagnostic peaks less than the mass of the fatty acyl chain losses. It is not evident that there is a secondary fragmentation pathway of the PB products before the fatty acyl chain loss forming the DG-like species. There is the presence of the fatty acyl chain loss from the PB reacted species at *m/z* 661 and its water loss at *m/z* 643. The 18:1 acylium ion and acylium + 74 are still present for the PB reacted species. There is also a population of ions at m/z 305, which may be as a result to the water loss of a PB reacted acylium ion. The signature 26 Da separation of the PB product is shown and can be used to verify the C=C locations at the Δ9 position upon the 18:1 fatty acyl chains identifying the species as TG 18:1(Δ9)/18:1(Δ9)/18:1(Δ9).
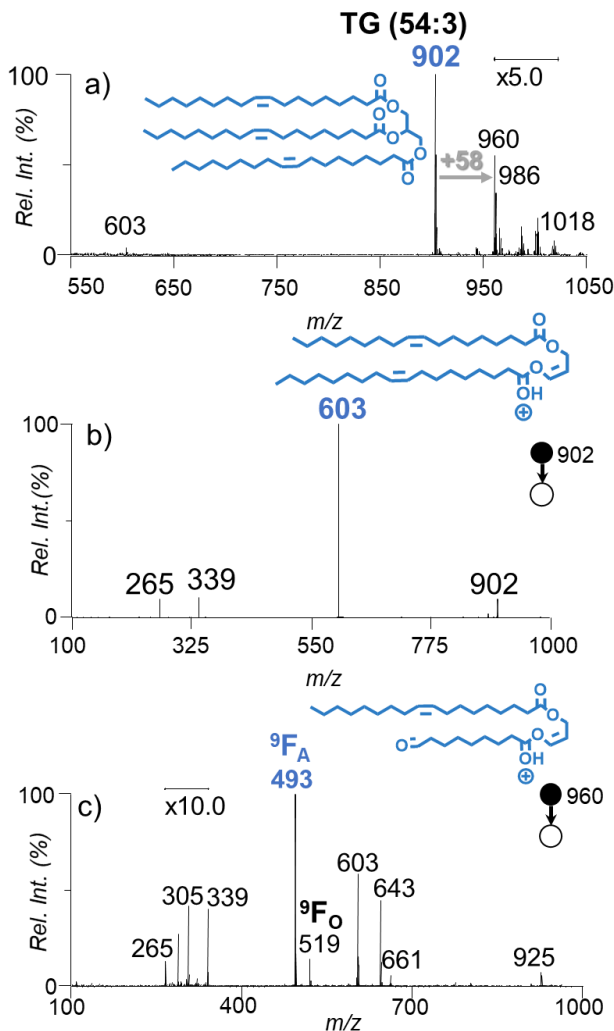
Figure 4.3. a) An averaged mass spectrum for the ions present at 32 minutes after the PB reaction. b) the CID spectrum of the ions population at *m/z* 902 at time 32 minutes c) the CID spectrum the ions population at *m/z* 960 at time 32 minutes.

When using our solvent conditions for RPLC-MS/MS to determine the species identity at fatty acyl chain level, TG 18:1/18:1/18:1 can be distinguished at a detection limit of 10 pM based on the presence of the 18:1 loss (*m/z* 603) three times the noise level in the CID spectrum. When applying the PB reaction the ability to determine TG 18:1(Δ9)/18:1(Δ9)/18:1(Δ9) has a limit of detection of 50 nM based on the C=C diagnostic ion (*m/z* 493 and *m/z* 519) signal-to-noise ratio being at least 3. The diagnostic ion at *m/z* 519 is the fragment ion that reduces the limit of detection due to the fragment forming less than 30% of the signal formed by the diagnostic ions at *m/z* 493. This limit of detection is 1 order of magnitude less than that of detecting the C=C location using

shotgun analysis of PC.[20] The hinderance of the LOD may be due to the difference in ionization efficient and due to the difference in smaller abundance of the diagnostic ions.
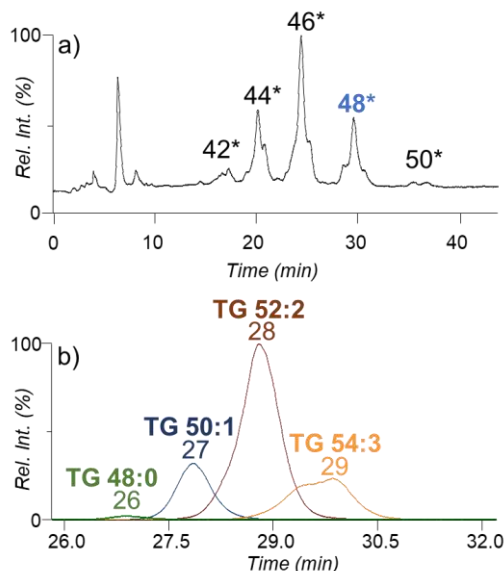
Figure 4.4. a) Total ion chromatograph of the reverse phase separation of pooled human plasma in positive ionization mode. b) The overlaying XIC of the masses corresponding to the species with an ECN of 48 (*m/z* 824, *m/z* 850, *m/z* 876, *m/z* 902).

4.3.5   Analysis of TGs in Human Plasma.

Obtaining abundant lipidome coverage is difficult without modification or separation prior to MS detection. The signal for TG is suppressed in the presence of polar lipids that readily ionized due to basic sites or fixed charges. TGs are neutral species that require an adduct for ionization resulting in the matrix effect in LC-MS/MS analysis.[22] A silica SPE column prior to RPLC separation was used for the removal of polar lipids from the extracts. TGs are highly abundant and complex in structure allowing for structural diversity. For C=C isomer separation, it may require long separation or analysis using GC-MS.[12] Herein we show the separation of TG species in human plasma in under 40 minutes followed by the C=C localization. Figure 4.4a shows the separation of human plasma TG species by ECN. RPLC is used here for separating species within a modest time frame compared to other LC methods geared at full separation. The peak shapes for a given ECN is non-gaussian due to the presence of multiple species eluting at slightly different times within the span of about 4 minutes. The species with an ECN of 48 are highlighted in Figure 4.4b where

the XIC of *m/z* 824, *m/z* 850, *m/z* 876, and *m/z* 902 are shown which correspond to TG 48:0, TG 50:1, TG 52:2, and TG 54:3, respectively. It is worth noting that the species elute in ascending mass order which is relative to the number of C=Cs present with the ions at *m/z* 824 having 0 and *m/z* 902 having 3 degrees of unsaturation. The TGs identified at subclass level in this work is consistent with the interlaboratory exercise.[23] Although improved separation can be achieved in future work, this method proves to be efficient at partially separating subclasses of TGs and the goal herein is not complete separation, but instead modest separation that allows for efficient lipid characterization at C=C level.
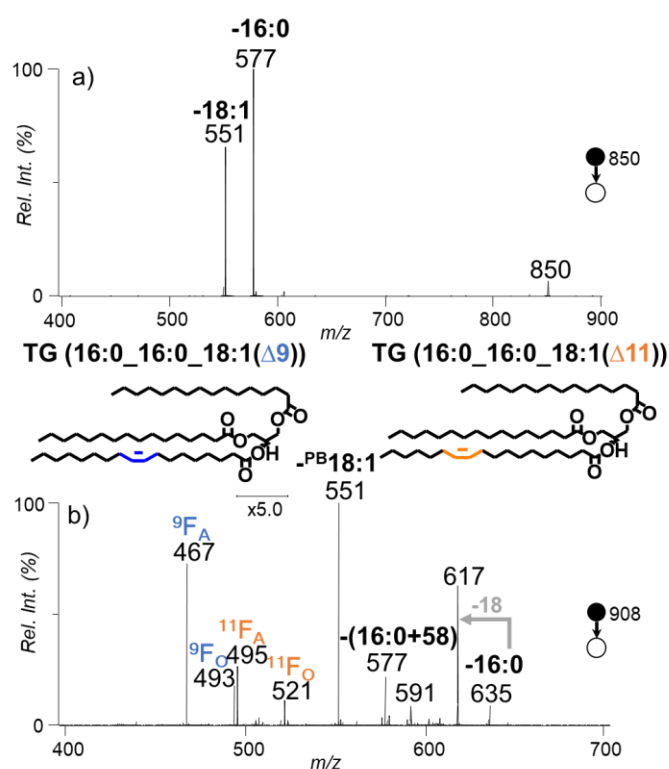
Figure 4.5. a) The averaged CID spectrum of the ions at *m/z* 850 shown as the blue trace at time 27 minutes in Figure 4.3b. b) The CID spectrum of the mass corresponding to the PB product of *m/z* 850 at *m/z* 908.

Further characterization was performed by applying CID as shown Figure 4.5a where the ions at *m/z* 850 corresponding to TG 50:1 (from Figure 4.3c) were probed. The CID spectrum shows two abundant peaks at *m/z* 551 and *m/z* 577 which represent the neutral loss of 18:1 and 16:0, respectively, from the glycerol backbone. The presence of the mentioned acyl chain losses

helped identify the species at fatty acyl chain level as TG (16:0_16:0_18:1). The PB reaction was applied to the sample and the post reaction CID spectrum of TG (16:0_16:0_18:1) is shown in Figure 4.5b. After fragmentation, the PB reacted 18:1, [PB]18:1, and 16:0 are loss forming a DG-like species. The reacted species was also fragmented at the oxetane ring forming two pairs of diagnostic species. The pairs correspond to diagnostic species being formed after the loss of a 16:0 forming fragmentation ions at *m/z* 467/493 and *m/z* 495/521 congruent with an 18:1(Δ9) and an 18:1(Δ11), respectively. The species are identified as TG (16:0_16:0_18:1(Δ9)) and TG (16:0_16:0_18:1(Δ11)). This is an example of how confident C=C location isomers can be distinguished using this method at modest RT without the requirement of a standard sample for RT comparison.

Another challenge with human plasma analysis is due to the high amounts of TG species within the complex mixtures such as human plasma extracts. A zoom in (m/z 895 – m/z 907) of the averaged total ion chromatography spectrum is shown in Figure 4.6a showing there can be much isotopic interference hindering the ability to identify species and suppression of low abundant species. The XIC for *m/z* 904 in Figure 4.6b emphasizes that the $[M+2]^+$ isotope of the ions at m/z 902 significantly contributes to the signal at *m/z* 904. The CID of the full XIC spectrum shows that there are interference peaks and species at *m/z* 904 cannot be clearly determined at fatty acyl chain level which is a previously reported phenomenon.[24] The averaged CID spectrum for the peak at retention time 35 minute (Figure 4.6b), Figure 4.6c shows that the peak consists of TG 18:0_18:1_18:1 based on the presence of ions at *m/z* 603 and m/z 605 which are the losses of 18:0 and 18:1, respectively. Fragmentation of the PB reacted TG (18:0_18:1_18:1) yields even greater information showcasing the power of obtaining a more in-depth characterization of the species as presented in Figure 4.6d. Four sets of diagnostic ions are yielded upon CID of the PB product corresponding to the 18:1(Δ9) and 18:1(Δ11). It is possible to identify the species as TG (18:0_18:1(Δ9)_18:1(Δ9)), (TG 18:0_18:1(Δ11)_18:1(Δ11)) and/or TG (18:0_18:1(Δ9) _18:1(Δ11)). Ammonium-adducted TG species readily lose all three of the fatty acyl chains thus in the case of TG 18:0_18:1_18:1 the diagnostic peaks can be produced after the loss of 18:1 or 18:0. There are two sets of diagnostic ions per C=C location for 18:1(Δ9) as a result of the loss of 18:0 at *m/z* 493/519 and m/z 495/521 and for 18:1(Δ11) *m/z* 521/547 and m/z 523/549, respectively. The diagnostic ions for the aldehyde fragment of 18:1(Δ9) and the dimethyl fragment of 18:1(Δ11) appear at the same nominal mass. By using high resolution MS, the isobars were resolved at 6 ppm

thus the MS/MS spectra can be used for confident determination of isobaric overlap. However, a limitation of our method is that when molecular species with two of the same unsaturated fatty acyl chains exist it cannot always be determined the whether the C=C location isomers exist within the same molecular species or as different molecules.
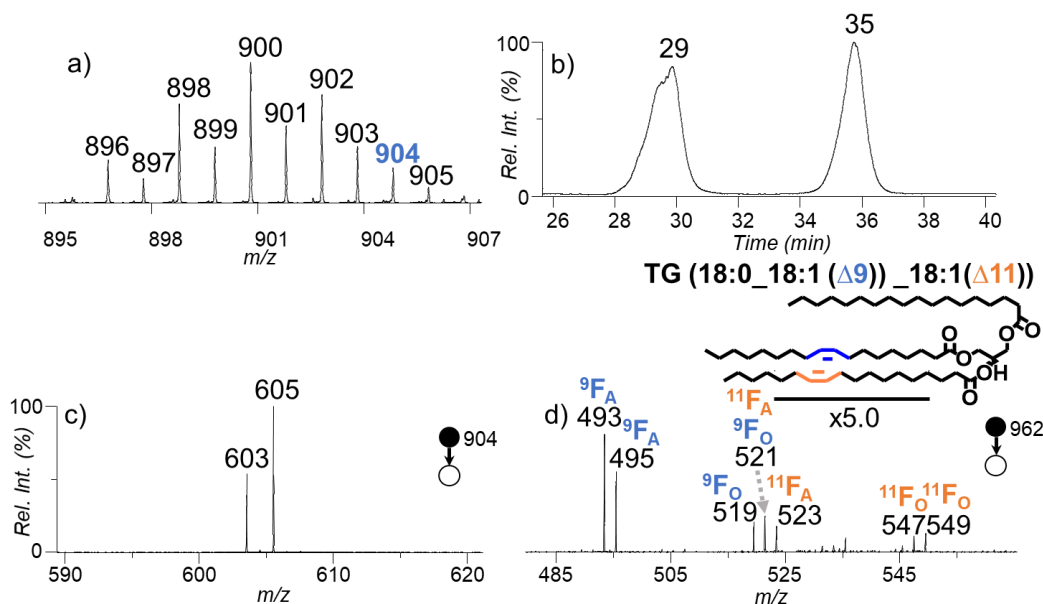
Figure 4.6. a) The zoomed in averaged MS spectrum of the total ion chromatograph b) XIC of m/z 904 c) The CID spectrum of the ions at *m/z* 904 eluted at 34 minutes from b). d) The CID spectrum of the ions at *m/z* 962 eluted at 34 minutes.

There has been a push in literature to use new PB reagents as a means of eliminating the overlap of the PB product mass from unmodified species that share the same mass.[17] This RPLC-PB-MS/MS method separates the isobaric species. The XICs of *m/z* 820 and m/z 880 after the PB reaction are presented in Figure 4.7a showing that the PB product can be traced back to its unmodified species to help with identification. The XIC of *m/z* 880 demonstrates the presence of multiple species which are highly abundant at the mass. The most abundant species is at a retention time of 33 minutes and corresponds to the $[M+2]^+$ isotope of the monoisotopic species at *m/z* 878.The CID spectrum of the ions present at retention time 39 is shown in Figure 4.7b as the intact species at *m/z* 880 and consists of TG (18:0_18:0_16:0). Fragmentation of *m/z* 822 results in the loss of 18:1, 16:0, and 14:0 identifying TG (18:1_16:0_14:0). Figure 4.7c shows the fragmentation of the ions at retention time 22 corresponding to the PB product of TG (18:1_16:0_14:0). There

are two sets of diagnostic ions at m/z 439/465 and m/z 467/493 representing the presence of 18:1(Δ9). Another set of diagnostic ions are present at m/z 495/521 corresponding to the present of 18:1(Δ11). The species present are TG 18:1(Δ9)_16:0_14:0 and a minor abundance of TG 18:1(Δ11)_16:0_14:0. In this case, there is the ability to identify the species of interest without the concern of preexisting species and this allows for fatty acyl chain and C=C location information to be obtained within the same run.
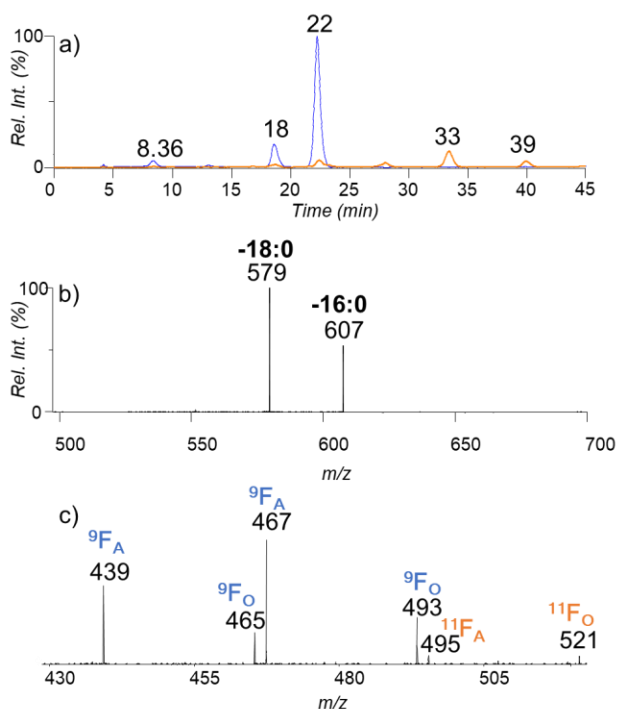
Figure 4.7. a) The overlaying XIC of m/z 822 and m/z 880 traced in blue and orange, respectively, b) The CID spectrum of the ions at *m/z* 880 eluted at 39 minutes from panel a). c) The CID spectrum of the ions at *m/z* 880 eluted at 22 minutes.

Separating fatty acyl compositional isomers is beneficial for confident characterization of TG species because it is possible to have up to 12 fatty acyl chain fragments in a single CID spectrum. Further modifications such as the PB reaction make the MS/MS spectra even more complex and it makes identification a challenge. The major component of the species that have an ECN of 44 (Figure 4.4a) is TG 52:4 at m/z 872. The CID spectrum of the ions at m/z 872 losses 16:1, 18:1, 18:2, 18:4, 16:0, and 20:4 however the presences of the fragments for different fatty acyl chain losses depend on the RT range being averaged suggesting that this group consist of

multiple isomeric molecular species and are retained at different RT. Figure 4.8a shows the overlaying XICs for the loss of 18:2, 18:3 and 20:4 after the CID of the ions at m/z 872. The fatty chain losses are not fully resolved because some species are composed of the same fatty acyls and better separation would be necessary for full resolving power. The average of scans at different fatty acyl chain peaks were used for spectrum collection and show that there were at least 4 different fatty acyl chain isomers present TG 16:1_18:1_18:2, TG 16:0_18:2_18:2, TG 16:0_18:1_18:3, and TG 16:0_16:0_20:4 The PB reaction was applied to the sample and fragmentation of the product resulted in the presence of diagnostic peaks which can be separated for identification of each species at C=C location.
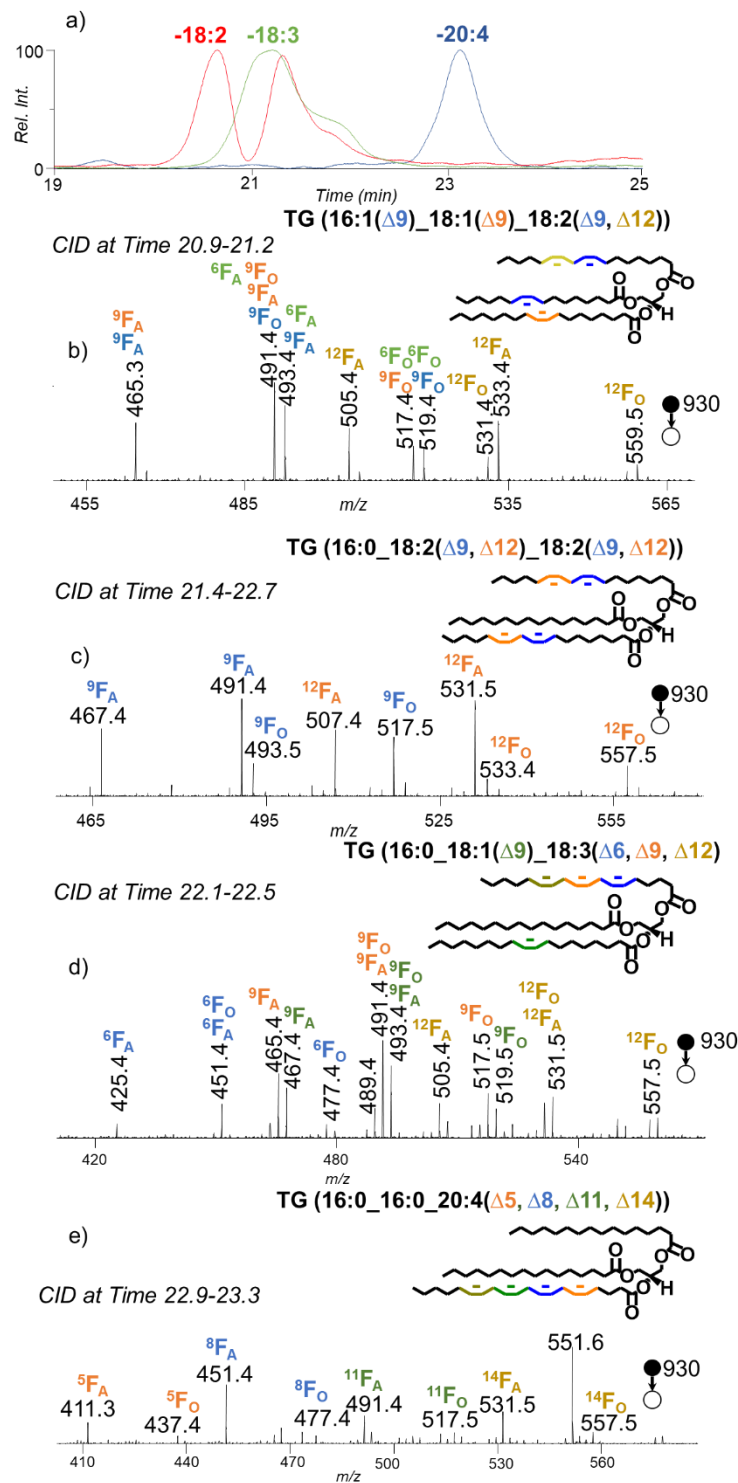
Figure 4.8. a) The overlaying XIC of the masses corresponding to the losses of the fatty acyl chains 18:2, 18:3, and 20:4. b) The CID spectrum of the ions at *m/z* 930 eluted from time 20.9-21.2 minutes, c) The CID spectrum of the ions at *m/z* 930 eluted from time 21.4-22.7 minutes, d) The CID spectrum of the ions at *m/z* 930 eluted from time 22.1-22.5 minutes, e) The CID spectrum of the ions at *m/z* 930 eluted from time 22.9-23.3 minutes.

Figure 4.8b shows that CID spectrum post PB reaction of the first species to elude within this subclass, TG (16:1_18:1_18:2). The two pairs of diagnostic ions at m/z 465/491 and m/z 493/519 correspond to the Δ9 position on the 18:2. There is another set of pairs at m/z 505/531 and m/z 533/559 corresponding to the Δ12 position on the 18:2 identifying TG (16:1_18:1_18:2(Δ9, Δ12)) leading to one of the limitation of this method. The diagnostic ions for 18:1(Δ9), 16:1(Δ9), and the Δ9 of 18:2 have isomeric overlap. This makes it challenging to determine which unsaturation site leads to the signal. TG (16:0_18:2_18:2) is the second molecular species that eludes. Figure 4.8c shows two sets of distinct diagnostic ions per C=C position help with identifying the species as TG (16:0_18:2(Δ9, Δ12)_18:2(Δ9, Δ12)). The other two molecular species were identified as TG (16:0_18:1_18:3) and TG 16:0_16:0_20:4. In Figure 4.8d, there are two sets of diagnostic ions for 18:3(Δ6, Δ9, Δ12) and there are two pairs of diagnostic ions for 18:1(Δ9) identifying the species as TG (16:0_18:1(Δ9)_18:3(Δ6, Δ9, Δ12). The last species to elude was TG 16:0_16:0_20:4 and 1 set of diagnostic ions are formed (Figure 4.8e) because only one of the fatty acyl chains is unsaturated so only the loss of 16:0 will produce diagnostic ions identifying TG (16:0_16:0_20:4(Δ5, Δ8, Δ11, Δ14)). This shows that subclasses of TG the complexity of TG composition with a sample.

Table 4.1. TG molecular species identified at C=C level in pooled human plasma using RPLC-PB-MS/MS.

m/z	Subclass	Molecular Species
794.7	46:1	TG(16:0_14:0_16:1(Δ9))
816.7	48:4	TG(12:0_18:2(Δ9, Δ12)_18:2(Δ9, Δ12))
818.7	48:3	TG(12:0_18:1(Δ9)_18:2(Δ9, Δ12))
820.7	48:2	TG(16:0_16:1(Δ9)_16:1(Δ9))
822.7	48:1	TG(14:0_16:0_18:1(Δ9))
822.7	48:1	TG(14:0_16:0_18:1(Δ11))
844.7	50:4	TG (14:0_18:2(Δ9, Δ12)_18:2(Δ9, Δ12))
846.7	50:3	TG (14:0_18:1(Δ9)_18:2(Δ9, Δ12))
846.7	50:3	TG (16:0_16:1(Δ9)_18:2(Δ9, Δ12))
846.7	50:3	TG (16:0_16:0_18:3(Δ6, Δ9, Δ12))
848.8	50:2	TG (14:0_18:1(Δ9)_18:1(Δ9))
848.8	50:2	TG (16:0_16:1(Δ9)_18:1(Δ9))
848.8	50:2	TG (16:0_16:0_18:2(Δ9, Δ12))
850.8	50:1	TG 16:0_16:0_18:1(Δ9)
850.8	50:1	TG 16:0_16:0_18:1(Δ11)
860.8	51:3	TG(18:2(Δ9, Δ12_18:1(Δ9)_15:0)
862.8	51:2	TG(18:1(Δ9)_18:1(Δ9)_15:0)
864.8	51:1	TG(18:1(Δ9)_16:0_17:0)
870.7	52:5	TG (16:1(Δ9)_18:2(Δ9, Δ12)_18:2(Δ9, Δ12))
870.7	52:5	TG (16:0_18:2(Δ9, Δ12)_18:3(Δ6, Δ9, Δ12))
872.8	52:4	TG (16:0_18:2(Δ9, Δ12)_18:2(Δ9, Δ12))
872.8	52:4	TG (16:0_18:1(Δ9)_18:3(Δ6, Δ9, Δ12)
872.8	52:4	TG (16:0_16:0_20:4(Δ5, Δ8, Δ11, Δ14))
872.8	52:4	TG (16:1(Δ9)_18:1(Δ9)_18:2(Δ9, Δ12))
874.8	52:3	TG(16:1(Δ9)_18:1(Δ9)_18:1(Δ9))
874.8	52:3	TG(16:1(Δ9)_18:1(Δ9)_18:1(Δ11))
874.8	52:3	TG(16:0_18:1(Δ9)_18:2(Δ9, Δ12))
874.8	52:3	TG(16:0_18:1(Δ11)_18:2(Δ9, Δ12))
876.8	52:2	TG (16:0_18:1(Δ9)_18:1(Δ9))
876.8	52:2	TG (16:0_18:1(Δ11)_18:1(Δ11))
876.8	52:2	TG (16:0_18:0_18:2(Δ9, Δ12))
878.8	52:1	TG (16:0_18:0_18:1(Δ9))
878.8	52:1	TG (16:0_18:0_18:1(Δ11))
890.8	53:2	TG(18:1(Δ9)_17:0_18:1(Δ9))
896.8	54:6	TG (18:2(Δ9, Δ12)_18:2(Δ9, Δ12)_18:2(Δ9, Δ12)
896.8	54:6	TG (16:0_18:2(Δ9, Δ12)_20:4(Δ5, Δ8, Δ11, Δ15))

Table 4.1. (continued)

m/z	Subclass	Molecular Species
898.8	54:5	TG (18:1(Δ9)_18:2(Δ9, Δ12)_18:2(Δ9, Δ12))
898.8	54:5	TG (16:0_18:1(Δ9)_20:4(Δ5, Δ8, Δ11, Δ14))
900.8	54:4	TG (18:1(Δ9)_18:1(Δ9)_18:2(Δ9, Δ12)
900.8	54:4	TG (18:1(Δ11)_18:1(Δ11)_18:2(Δ9, Δ12)
902.8	54:3	TG (18:1 (Δ9)_18:1(Δ9)_18:1 Δ9))
902.8	54:3	TG (18:1 (Δ11)_18:1(Δ11)_18:1 Δ11))
902.8	54:3	TG (18:0_18:1(Δ9)_18:2(Δ9, Δ12))
902.8	54:3	TG (18:0_18:1(Δ11)_18:2(Δ9, Δ12))
904.8	54:2	TG (18:0_18:1(Δ9)_18:1(Δ9))
904.8	54:2	TG (16:0_20:1(Δ9)_18:1(Δ9))

Over 120 molecular species were identified in human plasma using RPLC-MS/MS at fatty acyl chain composition 15 of which were unsaturated and 46 were identified at C=C location level (Table available in Appendix A). The species that were analyzed using RPLC-PB-MS/MS for C=C localization are presented in Table 4.1. Figure 4.9 shows the overall summary of the capability of using this system. A limitation to improving C=C level identification compositional isomer interference leading to fatty acyl chain ambiguity although C=C diagnostic ions are present after the reaction. Even so, this method has the potential for further application such as biomarker detection in human plasma. Using this method, we found 16 molecular species which contain 18:1 meaning there is a possibility to probe 16 species for oleic vs vaccenic acid composition which has been the aim in literature for biomarker detection.
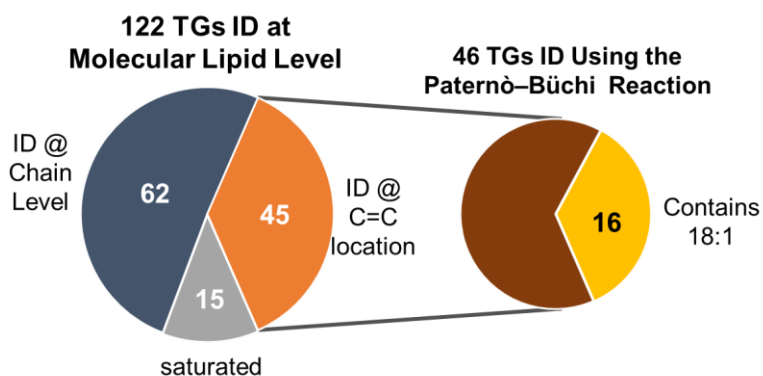
Figure 4.9. Pie charts representing the amount of TG species found in pooled human plasma.

4.4   Conclusion

In this work a solvent system for pairing the online PB reaction with RPLC-MS/MS is introduced which allows for the separation of species based on their ECN. Sum compositional isomers were partially separated and over 120 lipids were identified at fatty acyl chain level. Upon application of the PB reaction, tandem mass spectra allowed for the confident identification of C=C position and the determination isomers that differ in unsaturation site. The molecular species are better defined upon application of the PB reaction. TGs with 1 or 2 doubles have been shown to be the most promising for biomarker detection and this method could be useful for further characterization of unsaturation information. This method has been applied for the analysis of the human plasma for T2D patients compared to a control group. The overall outcome was that the RPLC-MS approach showed an increase in the presence of TG 50:1 for T2D human plasma sample versus that of a control group which is consistent with previous work. It was found using RPLC-PB-MS/MS that there is not a statistical difference between the ratio of vaccenic acid versus oleic acid in TG 16:0_16:0_18:1 for the control and T2D samples. This finding was not consistent with previous work that found an increase in the vaccenic composition in T2D samples. The method may not process results found in literature because the limit of detection may be too high for the capability of efficient ion statistics to complete consistent quantitative work

4.5   References

1. Murphy, R. C. Chapter 4. Glyceryl Esters. in *Tandem Mass Spectrometry of Lipids: Molecular Analysis of Complex Lipids* 105–129 (Royal Society of Chemistry, 2014). doi:10.1039/9781782626350-00105.

2. Řezanka, T., Pádrová, K. & Sigler, K. Regioisomeric and enantiomeric analysis of triacylglycerols. *Analytical Biochemistry* **524**, 3–12 (2017).

3. Balgoma, D. Common Fatty Markers in Diseases with Dysregulated Lipogenesis. 3.

4. Quehenberger, O. The Human Plasma Lipidome. *The New England Journal of Medicine* 12 (2011).

5. Suvitaival, T. *et al.* Lipidome as a predictive tool in progression to type 2 diabetes in Finnish men. *Metabolism* **78**, 1–12 (2018).

6. Ståhlman, M. *et al.* Clinical dyslipidaemia is associated with changes in the lipid composition and inflammatory properties of apolipoprotein-B-containing lipoproteins from women with type 2 diabetes. *Diabetologia* **55**, 1156–1166 (2012).

7. Yannell, K. E., Ferreira, C. R., Tichy, S. E. & Cooks, R. G. Multiple reaction monitoring (MRM)-profiling with biomarker identification by LC-QTOF to characterize coronary artery disease. *The Analyst* **143**, 5014–5022 (2018).

8. Mareš, P. High temperature capillary gas liquid chromatography of triacylglycerols and other intact lipids. *Progress in Lipid Research* **27**, 107–133 (1988).

9. Malone, M. & Evans, J. J. Determining the relative amounts of positional isomers in complex mixtures of triglycerides using reversed-phase high-performance liquid chromatography-tandem mass spectrometry. *Lipids* **39**, 273–284 (2004).

10. Bird, S. S., Marur, V. R., Sniatynski, M. J., Greenberg, H. K. & Kristal, B. S. Serum Lipidomics Profiling Using LC–MS and High-Energy Collisional Dissociation Fragmentation: Focus on Triglyceride Detection and Characterization. *Analytical Chemistry* **83**, 6648–6657 (2011).

11. Nagy, K., Sandoz, L., Destaillats, F. & Schafer, O. Mapping the regioisomeric distribution of fatty acids in triacylglycerols by hybrid mass spectrometry. *J. Lipid Res.* **54**, 290–305 (2013).

12. Cvačka, J. *et al.* Analysis of triacylglycerols in fat body of bumblebees by chromatographic methods. *Journal of Chromatography A* **1101**, 226–237 (2006).

13. Baba, T., Campbell, J. L., Le Blanc, J. C. Y. & Baker, P. R. S. Structural identification of triacylglycerol isomers using electron impact excitation of ions from organics (EIEIO). *Journal of Lipid Research* **57**, 2015–2027 (2016).

14. Thomas, M. C. *et al.* Ozone-Induced Dissociation: Elucidation of Double Bond Position within Mass-Selected Lipid Ions. *Analytical Chemistry* **80**, 303–311 (2008).

15. Marshall, D. L. *et al.* Sequential Collision- and Ozone-Induced Dissociation Enables Assignment of Relative Acyl Chain Position in Triacylglycerols. *Analytical Chemistry* **88**, 2685–2692 (2016).

16. Marshall, D. L. *et al.* Mapping Unsaturation in Human Plasma Lipids by Data-Independent Ozone-Induced Dissociation. *J. Am. Soc. Mass Spectrom.* **30**, 1621–1630 (2019).

17. Xu, T., Pi, Z., Song, F., Liu, S. & Liu, Z. Benzophenone used as the photochemical reagent for pinpointing C=C locations in unsaturated lipids through shotgun and liquid chromatography-mass spectrometry approaches. *Analytica Chimica Acta* **1028**, 32–44 (2018).

18. Ingalls, S. T. *et al.* Method for isolation of non-esterified fatty acids and several other classes of plasma lipids by column chromatography on silica gel. *Journal of Chromatography B: Biomedical Sciences and Applications* **619**, 9–19 (1993).

19. Zhang, W. *et al.* Online photochemical derivatization enables comprehensive mass spectrometric analysis of unsaturated phospholipid isomers. *Nature Communications* **10**, (2019).

20. Stinson, C. A. & Xia, Y. A method of coupling the Paternò–Büchi reaction with direct infusion ESI-MS/MS for locating the C☐C bond in glycerophospholipids. *The Analyst* **141**, 3696–3704 (2016).

21. Hvattum, E. Analysis of triacylglycerols with non-aqueous reversed-phase liquid chromatography and positive ion electrospray tandem mass spectrometry. *Rapid Communications in Mass Spectrometry* **15**, 187–190 (2001).

22. Pucci, V., Di Palma, S., Alfieri, A., Bonelli, F. & Monteagudo, E. A novel strategy for reducing phospholipids-based matrix effect in LC–ESI-MS bioanalysis by means of HybridSPE. *Journal of Pharmaceutical and Biomedical Analysis* **50**, 867–871 (2009).

23. Bowden, J. A. *et al.* Harmonizing lipidomics: NIST interlaboratory comparison exercise for lipidomics using SRM 1950–Metabolites in Frozen Human Plasma. *Journal of Lipid Research* **58**, 2275–2288 (2017).

24. Holčapek, M., Liebisch, G. & Ekroos, K. Lipidomic Analysis. *Analytical Chemistry* **90**, 4249–4257 (2018).

CHAPTER 5.   CONCLUSION AND FUTURE DIRECTION

Mass spectrometry (MS) is a powerful tool for lipid analysis. In particular, lipid samples are admitted to a mass spectrometer directly (i.e., shotgun lipidomics) or via liquid chromatography (i.e, LC-MS). MS can be paired with multiple technologies for the improved characterization of lipid molecular species. As demonstrated, gas-phase ion/ion reactions enable cationic glycerophospholipid (GP) species to be charge inverted and structurally characterized at fatty acyl composition level via low-energy collision induced dissociation (CID). To enhance lipid structural identification, GPs were PB reacted before ionization. Following ionization in positive ion mode, PB-derivatized GPs can be charged inverted to negative ion mode, where CID of the charge inverted GP ion enables carbon-carbon double bond (C=C) localization. Unfortunately, the matrix effect resulted in phosphatidylethanolamines (PEs) ion suppression . To combat this challenge, trimethylation enhancement using ^{13}C-diazomethane (^{13}C-TrEnDi) modification was exploited, greatly improving PEs ionization efficiency. More so, even after ^{13}C-TrEnDi modification, GPs can be reacted in solution with acetone to form a PB product. The dually modified species are ionized, and charge inverted giving the C=C location of the species. The combination of these three methods (charge inversion, the PB reaction, and ^{13}C-TrEnDi) empowered the analysis of GPs species such that confident molecular species identification was obtained for lipids in bovine liver.

TGs are very complex species of lipids and each species can have a plethora of structural isomers. These isomers can consist of differences in fatty acyl chain components, *sn*-position, or C=C position. The use of reverse-phase LC (RPLC) allowed for the separation of TGs based on equivalent carbon number (ECN, ECN = number of fatty acyl chain carbons - 2(number of C=C)) for increased species identification. Combining RPLC with an CID approach gives fatty acyl chain position, however C=C location cannot be determined using this method. The PB reaction can be put in tandem with an LC system and mass spectrometer for the modification of TGs. The TG species were activated in gas-phase to produce mass spectra that contain diagnostic species that are structurally informative. There are pairs of peaks corresponding to each C=C location within a probed TG species that gives more details about the molecule. The RPLC-PB-MS/MS platform has the potential to be used for high-throughput TG analysis for possible biomarker detection.

The PB reaction is an UV-activated reaction which can synthesize an oxetane ring and can be executed in the gas-phase at 3 kTorr.[1] Future work could go into the synthesis of the oxetane ring within an ion trap mass analyzer. Specifically, an unsaturated PC species could be introduced into an ion trap stored and met with an anionic reagent containing a ketone. When the electrostatic bond is formed, a UV-laser may initiate the formation of an oxetane ring by excitation of the ketone and alkene group. Further activation of the gas-phase product may lead to C=C localization. This would be an ideal reaction because it eliminates solvent effects. The challenge of this experiment may be finding a ketone containing reagent that can form an electrostatic complex with the quaternary ammonium group on the PC and interacted with the unsaturation site within the fatty acyl chain.

Gas-phase charge inversion for structural characterization could also be applied to other classes of lipids such as glycerolipids. Randolph *et. al.* showed that gas-phase ion/ion reactions of fatty acid anions with metal-containing complex dications effectively derivatize fatty acids in the gas-phase. Furthermore, CID of the charge inverted fatty acid complex cation leads to charge remote fragmentation and the generation of product ions indicative of C=C location(s).[2] Adhikari *et. al.* shows that thiol-containing reagents can modify the unsaturation site within a glycerol lipid and improve ionization.[3] A thiol-containing reagent which forms an anion can be used to modify the glycerolipid. The modified lipid can then be sprayed as an anion, activated to produce fatty acyl chains and the chains can be charge inverted to show the C=C location. Further exploration of gas-phase ion/ion reactions between more lipid classes and different reagents can be further explored to characterize lipids.

More work for the RPLC-PB-MS/MS approach may go into simplifying lipid extraction steps for a greater extraction recovery. Future work should explore the separation of overlapping fatty acyl chain isomers such that the post PB reaction CID spectra are cleaner. In particular, this separation could be improved using a longer RPLC column or 2D LC. Another possible promise is the use of a sodium or lithium adduct instead of ammonium followed by MS^3 experiments such that the alkali adducted PB product forms the modified fatty acyl chains and the MS^3 spectrum reveals individual fatty acyl chain C=C information. This method would be useful in longer separations such that the PB reaction can be applied for characterization instead of finding standard for each C=C isomer especially when looking at complex mixture.

The limitation of separation techniques including LC and ion mobility (IM) is that there are not enough synthetic standards available for the verification of species that are present in a complex mixture. It may be possible to synthesize GPs such as sphingomyelin in gas-phase such that species that contain a C18:1(Δ11) can be produced. Amide bond formation is possible via ion/ion reactions between a primary amine group and a carboxyl group activated by sulfoNHS.[4–7] A fatty acid can be modified with a sulfoNHS, injected into the mass spectrometer, and stored in an ion trap. LysoSM can then be introduced into the trap and an ion/ion reaction between the ions will form a complex that can be later activated to produce a SM species with a fatty acyl chain bond to the primary amine. For the reaction to occur, the lysoSM must be sprayed as doubly charged cation such that when complexed with the modified fatty acid, it does not neutralize. This may look like the lysoSM adducted with Fe^{2+}.

While lipids are a category of metabolites, the field of lipidomics is evolving independent of metabolomics and is helpful for understanding the phenotype of organisms. There is a growing interest in the lipid analysis based on the annual increase in publications on the topic. Seeing that MS is the leading tool for lipidomic studies, it is expected that in order to push the field forward effort should go into developing new MS-based techniques. It is important that attention is paid to each lipid class and that research dives into characterizing novel lipid species. Although lipidomics was established as a field less than 20 years ago, it has made great strides and it shows promise to continue developing as a useful interdisciplinary tool.

5.1   References

1. Brogaard, R. Y. et al. The Paternò–Büchi reaction: importance of triplet states in the excited-state reaction pathway. Phys. Chem. Chem. Phys. 14, 8572 (2012).

2. Randolph, C. E., Foreman, D. J., Betancourt, S. K., Blanksby, S. J. & McLuckey, S. A. Gas-Phase Ion/Ion Reactions Involving Tris-Phenanthroline Alkaline Earth Metal Complexes as Charge Inversion Reagents for the Identification of Fatty Acids. Analytical Chemistry 90, 12861–12869 (2018).

3. Adhikari, S., Zhang, W., Xie, X., Chen, Q. & Xia, Y. Shotgun Analysis of Diacylglycerols Enabled by Thiol–ene Click Chemistry. Analytical Chemistry 90, 5239–5246 (2018).

4. Mentinova, M. & McLuckey, S. A. Covalent Modification of Gaseous Peptide Ions with N - Hydroxysuccinimide Ester Reagent Ions. J. Am. Chem. Soc. 132, 18248–18257 (2010).

5. Mentinova, M., Barefoot, N. Z. & McLuckey, S. A. Solution Versus Gas-Phase Modification of Peptide Cations with NHS-Ester Reagents. J. Am. Soc. Mass Spectrom. 23, 282–289 (2012).

6. Mentinova, M. & McLuckey, S. A. Intra- and Inter-Molecular Cross-Linking of Peptide Ions in the Gas Phase: Reagents and Conditions. J. Am. Soc. Mass Spectrom. 22, 912–921 (2011).

7. McGee, W. M. & McLuckey, S. A. Efficient and directed peptide bond formation in the gas phase via ion/ion reactions. Proceedings of the National Academy of Sciences 111, 1288–1292 (2014).

APPENDIX A. TABLE OF TRIACYLGLYCEROL SPECIES IDENTIFIED IN HUMAN PLASMA

TG molecular species identified at fatty acyl compositional level in pooled human plasma using RPLC-MS/MS.

m/z	Subclass	Species
708.6	40:2	TG (18:2_16:0_6:0)
710.6	40:1	TG (18:1_16:0_6:0)
712.6	40:0	TG (12:0_12:0_16:0)
724.6	41:1	TG (12:0_18:1_11:0)
734.6	42:3	TG (12:0_18:3_12:0)
734.6	42:3	TG (8:1_16:0_18:2)
736.7	42:2	TG (8:1_16:0_18:1)
736.7	42:2	TG (18:2_12:0_12:0)
738.7	42:1	TG (12:0_18:1_12:0)
740.7	42:0	TG (16:0_14:0_12:0)
750.7	43:3	TG (9:0_16:0_18:2)
760.6	44:4	TG (18:2_18:2_8:0)
762.6	44:3	TG (10:1_18:2_16:0)
764.7	44:2	TG (18:2_16:0_10:0)
766.7	44:1	TG (18:1_16:0_10:0)
768.7	44:0	TG (14:0_14:0_16:0)
780.7	44:1	TG (16:1_14:0_15:0)
782.7	45:0	TG (16:0_15:0_14:0)
786.7	46:5	TG (18:2_10:0_18:3)
788.7	46:4	TG (18:2_10:0_18:2)
794.7	46:1	TG (16:0_14:0_16:1)
796.7	46:0	TG (16:0_14:0_16:0)
806.7	47:2	TG (18:2_15:0_14:0)
808.7	47:1	TG (16:0_15:0_16:1)
810.7	47:0	TG (16:0_15:0_16:0)
814.7	48:5	TG (12:0_18:2_18:3)
816.7	48:4	TG (12:0_18:2_18:2)
818.7	48:3	TG (12:0_18:1_18:2)
820.7	48:2	TG (16:0_16:1_16:1)
822.7	48:1	TG (14:0_16:0_18:1
824.8	48:0	TG (16:0/16:0/16:0)
824.8	48:0	TG (14:0_16:0_18:0)
834.7	49:2	TG (16:0_18:2_15:0)

Table continued

m/z	Subclass	Species
836.8	49:1	TG (16:0_18:1_15:0)
838.8	49:0	TG (16:0_16:0_17:0)
842.7	50:5	TG (18:2_18:3_14:0)
844.7	50:4	TG (14:0_18:2_18:2)
846.7	50:3	TG (14:0_18:1_18:2)
846.7	50:3	TG (16:0_16:1_18:2)
846.7	50:3	TG (16:0_16:0_18:3)
848.8	50:2	TG (14:0_18:1_18:1)
848.8	50:2	TG (16:0_16:1_18:1)
848.8	50:2	TG (16:0_16:0_18:2)
850.8	50:1	TG 16:0_16:0_18:1
852.8	50:0	TG (16:0_18:0_16:0)
856.7	51:5	TG (18:2_18:3_15:0)
856.7	51:5	TG (15:1_18:2_18:2)
858.8	51:4	TG (18:2_18:2_15:0)
860.8	51:3	TG (18:2_18:1_15:0)
862.8	51:2	TG (18:1_18:1_15:0)
864.8	51:1	TG (18:1_16:0_17:0)
866.8	51:0	TG (16:0_18:0_17:0)
866.8	51:0	TG (19:0_16:0_16:0)
870.7	52:5	TG (16:1_18:2_18:2)
870.7	52:5	TG (16:0_18:2_18:3)
872.8	52:4	TG (16:0_18:2_18:2)
872.8	52:4	TG (16:0_18:1_18:3)
872.8	52:4	TG (16:0_16:0_20:4)
872.8	52:4	TG (16:1_18:1_18:2)
874.8	52:3	TG (16:1_18:1_18:1)
874.8	52:3	TG (16:0_18:1_18:2)
876.8	52:2	TG (16:0_18:1_18:1)
876.8	52:2	TG (16:0_18:0_18:2)
878.8	52:1	TG (16:0_18:0_18:1)
880.8	52:0	TG (18:0_18:0_16:0)
884.8	53:5	TG (18:2_17:1_18:2)
888.8	53:3	TG (18:1_18:2_17:0)
888.8	53:3	TG (18:1_17:1_18:1)
890.8	53:2	TG (18:1_17:0_18:1)
892.8	53:1	TG (16:0_19:0_18:1)
892.8	54:8	TG (18:3_18:3_18:2)

Table continued

m/z	Subclass	Species
894.8	54:7	TG (18:3_18:2_18:2)
896.8	54:6	TG (18:2_18:2_18:2)
896.8	54:6	TG (16:0_18:2_20:4)
898.8	54:5	TG (18:1_18:2_18:2
898.8	54:5	TG (16:0_18:1_20:4)
900.8	54:4	TG (18:1_18:1_18:2)
900.8	54:4	TG (16:0_18:0_20:3)
902.8	54:3	TG (18:1_18:1_18:1)
902.8	54:3	TG (18:0_18:1_18:2)
902.8	54:3	TG (18:0_18:1_18:2)
904.8	54:2	TG (18:0_18:1_18:1)
904.8	54:2	TG (16:0_20:1_18:1)
906.8	54:1	TG (18:1_18:0_18:0)
908.8	54:0	TG (18:0_18:0_18:0)
912.8	55:5	TG (18:2_19:2_18:1)
914.8	55:4	TG (18:1_18:2_19:1)
916.8	55:3	TG (18:1_19:1_18:1)
922.9	56:7	TG (16:0_22:5_18:2)
924.8	56:6	TG (20:4_18:1_18:1)
926.8	56:5	TG (20:4_18:1_18:0)
928.8	56:4	TG (20:4_18:0_18:0)
930.8	56:3	TG (18:1_18:1_20:1)
932.9	56:2	TG (18:1_18:1_20:0)
936.9	57:7	TG (22:5_18:2_17:0)
938.8	57:6	TG (18:1_17:0_22:5)
940.8	57:5	TG (22:4_18:1_17:0)
944.9	58:10	TG (20:4_20:4_18:2)
944.9	58:10	TG (22:6_18:2_18:2)
946.9	58:9	TG (22:6_18:1_18:2)
948.9	58:8	TG (22:5_18:2_18:1)
948.9	58:8	TG (22:6_18:1_18:1)
950.9	58:7	TG (22:4_18:1_18:2)
950.9	58:7	TG (24:5_16:0_18:2)
952.8	58:6	TG (18:1_22:4_18:0)
958.9	58:3	TG (18:2_18:1_22:0)
960.9	58:2	TG (18:1_22:0_18:1)
962.9	58:1	TG (16:0_18:1_24:0)
962.9	58:1	TG (18:0_22:0_18:1)

Table continued

m/z	Subclass	Species
986.9	60:3	TG (24:0_18:1_18:2)
986.9	60:3	TG (24:1_18:0_18:2)
988.9	60:2	TG (24:0_18:1_18:1)
990.9	60:1	TG (24:0_18:0_18:1)
992.9	60:0	TG (22:0_20:0_18:0)

VITA

Elissia Franklin was born in Chicago, Illinois to Erica Killingham and James Franklin. Elissia always showed interest in academic achievements graduating at the top of her class at Colin Powell Middle School in Matteson, Illinois as the school's first student body president. She graduated from Gwendolyn Brooks College Preparatory Academy. In 2010, she worked as pharmacy technician at CVS pharmacy where she was responsible for filling prescription orders and servicing customers who were picking up medication. She also worked at the Special Supplemental Nutrition Program for Women, Infants, and Children (WIC) from 2008 until 2011 then she continued to Urbana-Champaign to pursue a Bachelor of Science at the University of Illinois.

While at the University of Illinois, Elissia worked with Ted Hymowitz as a laboratory assistant and help organize and maintain both the research lab and greenhouse soybean species. From 2013 until 2015, Elissia conducted research under the direction of Professor Steven Zimmerman where her experiments focused on drug discovery for myotonic dystrophy. She studied abroad in Heredia, Costa Rica, Kaohsiung, Taiwan, Hong Kong, P. R. China, and Shanghai, China while at the University of Illinois. She was awarded multiple scholarships and honors including making the Dean's List in the Spring of 2015.

In 2015, she moved on to Purdue University to pursue a Doctor of Philosophy in chemistry. She joined the research group of Professor Yu Xia where she studied photochemical reactions for the structural elucidation of lipids. In 2017, she became co-advised by Professor Scott McLuckey where she paired gas-phase charge inversion with photochemical reactions for in-depth structural analysis of glycerophospholipids. After receiving PhD candidacy, she visited Tsinghua University as a senior research scholar and developed a liquid chromatography mass spectrometry approach for structural analysis of triacylglycerol.

PUBLICATIONS

1. Franklin, E. T., Triacylglycerol analysis by pairing photochemical reactions with reverse-phase liquid chromatography tandem mass spectrometry. *Manuscript in Preparation.*

2. Franklin, E. T., Shields S. W. J., Smith, J. C., Xia, Y., McLuckey, S. A. Coupling Headgroup and Alkene Specific Solution Modifications with Gas-Phase Ion-Ion Reactions for Sensitive Phospholipid Identification and Characterization. *Manuscript in Preparation.*

3. Franklin, E. T.; Betancourt, S. K.; Randolph, C. E.; McLuckey, S. A.; Xia, Y. In-Depth Structural Characterization of Phospholipids by Pairing Solution Photochemical Reaction with Charge Inversion Ion/Ion Chemistry. *Anal. Bioanal. Chem.* **2019**. https://doi.org/10.1007/s00216-018-1537-1.

4. Ren, J.; Franklin, E. T.; Xia, Y. Uncovering Structural Diversity of Unsaturated Fatty Acyls in Cholesteryl Esters via Photochemical Reaction and Tandem Mass Spectrometry. *J. Am. Soc. Mass Spectrom.* **2017**, *28* (7), 1432–1441. https://doi.org/10.1007/s13361-017-1639-6.

FOCUS: BIO-ION CHEMISTRY: INTERACTIONS OF BIOLOGICAL IONS WITH IONS, MOLECULES, SURFACES, ELECTRONS, AND LIGHT - RESEARCH ARTICLE

Uncovering Structural Diversity of Unsaturated Fatty Acyls in Cholesteryl Esters via Photochemical Reaction and Tandem Mass Spectrometry

Jia Ren, Elissia T. Franklin, Yu Xia

Department of Chemistry, Purdue University, West Lafayette, IN 47907-2084, USA
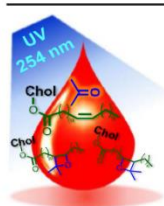
Abstract. Mass spectrometry analysis of cholesteryl esters (CEs) faces several challenges, with one of them being the determination of the carbon–carbon double bond (C=C) locations within unsaturated fatty acyl chains. Paternò-Büchi (PB) reaction, a photochemical reaction based on the addition of acetone to C=C, is capable of C=C location determination when coupled with tandem mass spectrometry (MS/MS). In this study, the PB reaction conditions were tailored for CEs and subsequent nanoelectrospray ionization (nanoESI). A solvent system containing acetone/methanol/dichloromethane/water (40/30/20/10, volume ratios) and 100 μM LiOH was determined to be optimal, resulting in reasonable PB reaction yield (~30%) and good ionization efficiency (forming lithium adduct of CEs). Collision-induced dissociation (CID) of the PB reaction products produced characteristic fragment ions of CE together with those modified by the PB reactions, such as lithiated fatty acyl ([FA + Li]$^-$) and its PB product ([FA – PB + Li]$^-$). MS^3 CID of [FA – PB + Li]$^-$ led to abundant C=C diagnostic ion formation, which was used for C=C location determination and isomer quantitation. A PB-MS^3 CID approach was developed and applied for CE analysis from human plasma. A series of unsaturated CEs was identified with specific C=C locations within fatty acyl chains. Absolute quantitation for each CE species was achieved including coexisting C=C location isomers, such as Δ9 and Δ11 isomers of CE 18:1 and ω-6 and ω-3 isomers of CE 18:3. These results show that PB-MS/MS is useful in uncovering structural diversity of CEs due to unsaturation in fatty acyls, which is often undetected from current lipid analysis approach.
Keywords: C=C determination, Cholesteryl esters, Paternò-Büchi reaction, Lipidomics, Tandem mass spectrometry

Introduction

In all types of cells, the balance between the biologically active free sterols and the inactive storage form as sterol esters, viz. sterol homeostasis, is important [1, 2]. Cholesterol esters (CEs) have long fatty acid chains attached to the 3-hydroxyl group of cholesterol (Figure 1) and function as a biologically inert storage form of cholesterol [3]. They are less polar than free cholesterol; therefore, they are a preferred form within lipoprotein particles for transportation. CEs are bio-

synthesized in two different pathways. One relies on acyl-CoA cholesterol acyltransferase (ACAT) to esterify sterols inside the cell [4, 5]. The other one occurs in the extracellular space (i.e., bloodstream), catalyzed by lecithin cholesterol acyl transferase (LCAT) [6]. In this process, fatty acyls at *sn*-2 position of phosphatidylcholines are transferred to cholesterols and produce CEs. Plasma CE concentrations can be as high as 1–3 mmol L^{-1}, and they tend to contain relatively high proportions of polyunsaturated fatty acyl (PUFA) chains [7]. Recent studies show that LCAT also serves in reverse cholesterol transport and polyunsaturated CE synthesis, whereas, ACAT2 [8] (one isoform of ACAT) promotes accumulation of mono-unsaturated and saturated CE in lipoprotein particles containing apolipoprotein B [9]. Given the importance of cholesterol homeostasis for normal functions of cells, abnormal CE levels are often linked with various pathological conditions, including
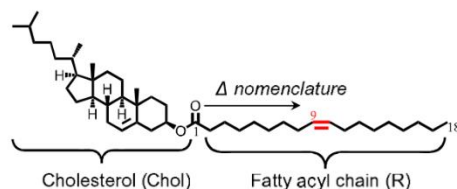
Figure 1. Nomenclature of cholesteryl ester. The C=C double bond is indicated as cis-Δ^9 in Δ^x nomenclature system for CE 18:1 (9Z)

metabolic disorders [10], heart disease [11], and cancer [12, 13]. CE profiling, a subset study of metabolomics and lipidomics, has been frequently used as a means to discover biomarkers for disease monitoring or diagnosis [14].

Mass spectrometry (MS)-based lipid analysis has been established as a powerful tool for the identification and quantitation of a variety of lipid classes from biological matrixes, offering a combined advantage of high sensitivity, speed, and detailed structural information [15]. Many different MS techniques have been applied to CE analysis with both successes and limitations. Conventionally, the fatty acyl composition of CE is analyzed by gas chromatography (GC)-MS via electron ionization (EI) or chemical ionization (CI). Because of limited volatility, CEs need to be hydrolyzed and the methylated fatty acyls are subjected to GC-MS, the process of which requires relatively long analysis time (in hours) [16]. The development of electrospray ionization (ESI) [17] has greatly expanded the spectrum of lipids that can be analyzed by MS. Han and Gross were amongst the first to recognize the potential of ESI-MS for global lipid analysis from biological systems [18]. Soon thereafter, two techniques based on ESI-MS were established as the main methods for current lipidomics studies: shotgun lipid analysis of crude lipid extract [19, 20] and ESI-MS coupled with liquid chromatography (LC) separations [21, 22].

Given the nonpolar nature of CE, adduct ion formation is employed to enhance ionization efficiency of CE in ESI, with NH_4^+, Li^+, and Na^+ being frequently used as adduct ions for positive ion mode. Tandem mass spectrometry (MS/MS) via low energy collision-induced dissociation (CID) of CE adduct ions has been developed for the identification and quantitation of CEs from mixtures [23]. For instance, CID of the ammonium adduct of CE generates a dominant fragment ion at m/z 369 (cholestene cation), allowing the use of product ion scan (PIS) for quantitation of CEs from lipid mixtures [24]. Collisional activation of lithiated or sodiated CE ions results in an abundant neutral loss of cholesterene (368 Da) and forms Li^+ or Na^+ adduct of fatty acyl ions [25, 26]. This fragmentation channel allows fatty acyl composition determination, viz. the number of carbons and degrees of unsaturation, while neutral loss scan (NLS) of 368 Da renders sensitive detection and quantitation of CEs. The above ESI-MS/MS techniques, however, have a major limitation of not being able to provide carbon–carbon double bond (C=C) location information within fatty acyls of

CEs. Given that unsaturation in lipids play critical roles in their biochemical and biophysical properties, and many unsaturated fatty acids have multiple C=C location isomers fulfilling distinct biological roles, it is of great importance to characterize unsaturated CEs at the structural level of C=C locations [27–29].

The need to determine a specific lipid structure from coexisting isomers and isobars has drawn increasing awareness in the field of lipidomics [30, 31]. Some notable MS methods that are suitable for the analysis of different classes of lipids and provide C=C location information include charge-remote fragmentation induced by high energy CID [32], ozone-induced dissociation (OzID) [33–35], radical directed dissociation (RDD) [36, 37], helium metastable atom-activated dissociation (He-MAD) [38, 39], and electron impact excitation of ions from organics (EIEIO) [40, 41]. Recently, our group has demonstrated that the Patern -Büchi (PB) reaction [42], a photochemical reaction via the addition of electronically excited acetone to a C=C, can be applied to C=C location determination and location isomer quantitation for fatty acids and phospholipids when coupled with ESI-MS/MS [43–46]. In this study, we aim to expand the scope of the PB reaction to neutral lipids, such as CEs, which tend to have high composition of unsaturated fatty acyls. The factors that are key to this development have been identified, including proper solvent system that allows both good PB reaction yield and ionization for CE using ESI, and MS/MS methods that can allow confident structural determination and C=C location isomer quantitation. Commercially available CE standards were used for method development and optimization. The analytical capability of PB-MS/MS was further tested for analyzing CEs in human plasma.

Experimental

Nomenclature

Shorthand notation for CEs is taken from LIPID MAPS [47]. For example, CE 18:1(9Z) detonates a cholesteryl ester containing an 18-carbon fatty acyl chain. The numeral "1" after the carbon number refers to the degree of unsaturation of the fatty acyl. The location(s) of the C=C bond(s) is defined in Δ^x nomenclature by counting from the alpha carbon of the fatty acyl and is indicated with the number(s) in parentheses. For polyunsaturated fatty acyl chains, the ω-nomenclature is also used for simplicity in which the location of the first C=C is counted from the methyl end of the fatty acyl chain. Cis- or trans-configuration of C=C bond is denoted with Z and E nomenclature, respectively. For CE analysis from biological extract, the Z/E stereo-configurations are not assigned.

Materials

CE standards, including CE 18:1 (9Z), CE 18: 1 (11Z), CE 18:2 (9Z, 12Z), CE 18:3 (9Z, 12Z, 15Z), CE 18:3 (6Z, 9Z, 12Z), CE 20:4 (5Z, 8Z, 11Z, 14Z), and CE 22:5 (7Z, 10Z, 13Z, 16Z, 19Z), and lithium hydroxide (LiOH) were purchased from

Sigma-Aldrich (St. Louis, MO USA). Pooled normal human plasma with anticoagulant lithium heparin was obtained from Innovative Research, Inc. (Novi, MI, USA). Organic solvents were all LC grade and ultrapure water was obtained from a purification system at 0.03 μS cm. CEs were extracted from 20 μL of plasma following methyl-*tert*-butyl ether (MTBE) method with an extraction efficiency of 71.0% ± 0.6% obtained (from three replicates) [48].

PB-MS/MS for CE Analysis

All samples were analyzed in positive ion mode using a 4000 QTRAP mass spectrometer (Sciex, Toronto, ON, CA) equipped with a home-built nanoESI source and a low pressure mercury lamp (primary emission at 254 nm; BHK Inc., Ontario, CA). CE standards (0.1–10 μM) were dissolved in acetone/methanol/dichloromethane/water = 40/30/20/10 (volume ratios) containing 100 μM LiOH. The PB reaction was facilitated by UV irradiation of a pulled borosilicate glass capillary nanoESI tip, which contained a solution of CE. A scheme of the reaction setup is shown in Supporting Information (SI), Figure S1. Multiple modes of MS/MS, including neutral loss scan (NLS), MS^2 via beam-type CID, and MS^3 via sequential beam-type CID and on-resonance ion trap CID were employed in CE analysis. For NLS, collision energy (CE) was optimized at 40 eV. In beam-type CID, the precursor ions were isolated by Q1 and accelerated to q2 for collisional activation with collision energy defined by the DC potential difference between Q0 and q2, which was typically within the range 35–40 V. Ion trap CID was carried out in Q3 linear ion trap, where a dipolar excitation was used for on-resonance collisional activation. The activation amplitudes were within the range 40–50 mV for 200 ms. The characteristic parameters of the mass spectrometer during this study were set as follows: spray voltage, 1200–1500 V; curtain gas, 10 psi; and declustering potential, 180 V. Data acquisition, processing, and instrument control were performed using Analyst 1.5 software.

Results and Discussions

Online Coupling of the PB Reaction and NanoESI-MS for CE Analysis

A simple binary mixture of acetone/water solvent system has been used for the analysis of fatty acids and phospholipids with acetone serving as both the PB reaction reagent and co-solvent in subsequent online ESI-MS or nanoESI-MS [43, 45]. This condition works well for both PB reaction and ionization since the above two classes of lipids have reasonable solubility in such polar solvent system. It is worth noting that organic solvent other than acetone is minimized in the solvent system to reduce possible side reactions involving radical intermediates formed from Norrish Type I cleavage of acetone [45]. CEs have very limited solubility in water and they are typically dissolved in methanol/chloroform (4:1 volume ratio) for ESI-MS analysis [23, 25]. Consequently, acetone/water solvent

system developed for polar lipids cannot be directly applied for the PB reaction and nanoESI-MS of CEs. Our first task was targeted to developing a solvent system that could provide good PB reaction of CE. Pure acetone was evaluated as the solvent for a model CE compound, CE 18:1(9Z) (5 μM), for various lengths of reaction time (10 s to 3 min) before reconstituting in methanol/chloroform (4:1 volume ratio, 100 μM LiOH) for nanoESI. The PB reaction yield was found low and was accompanied by a large extent of side reactions. It was hypothesized that because of the nonpolar nature of CE molecules, the fatty acyls might prefer strong interactions with their own cholesteryl moieties and therefore have reduced interactions with the more polar acetone solvent molecules. We suspected that the addition of less polar organic solvent into acetone might be necessary to enhance effective interaction between acetone and CE fatty acyls. A series of organic solvents (10%–50% volume ratio relative to acetone) including chloroform ($CHCl_3$), dichloromethane (CH_2Cl_2), and hexane were examined. Dichloromethane was found as the best solvent to provide reasonable reaction yield and limited degree of side reactions among all organic solvents tested. An example of reaction spectrum involving $CHCl_3$ as a co-solvent is shown in SI, Figure S2, which suffers from a high degree of CE ion signal loss and limited formation of the PB products.

The binary mixture of acetone/dichloromethane, however, was not miscible with even 10% of aqueous solution of salts, i.e., LiOH, the addition of which was necessary to enhance CE adduct ion formation and detection in ESI. Upon various tests, we found that methanol could be added as a co-solvent leading to a homogenous solution and ensuring stable ionization during nanoESI. The commonly used adduct ions for ESI analysis of CE, including lithium (Li^+), ammonium (NH_4^+), and sodium (Na^+) were evaluated for their compatibility with PB-MS/MS. Li^+ adduct of CE had combined advantages of relatively high ionization efficiency (relative to Na^+ adduct) and forming abundant fatty acyl fragment ion (relative to NH_4^+ adduct) under CID, and was used for further studies. After optimizations, a solvent system composed of acetone/methanol/dichloromethane/water (40/30/20/10) and 100 μM LiOH was identified as the best solvent condition for conducting online PB-nanoESI-MS for CE analysis.

Data in Figure 2 show typical mass spectra of CE 18:1(9Z) before and after the PB reaction using such a solvent system. Before reaction (Figure 2a), only intact CE at *m/z* 657.4 ([CE + Li]$^+$) was observed as the dominant species. The peak at *m/z* 673.4 is oxidized CE 18:1 (oxidation likely at the cholesteryl ring), existed in the original sample received. The PB reaction became stable after 1.5 min UV irradiation and the PB products, consisting of two structural isomers (structures shown in the inset of Figure 2), were detected at *m/z* 715.6 ([CE – PB + Li]$^+$) (Figure 2b). The PB products have a characteristic mass increase of 58 Da from intact CE due to acetone addition to a C=C bond. Under such reaction condition, the PB reaction was achieved with 20%–30% yield. A small degree of side reaction was observed at *m/z* 687.5, showing a mass increase of 30 Da from intact CE 18:1 ions. When CD_3OH was used in the
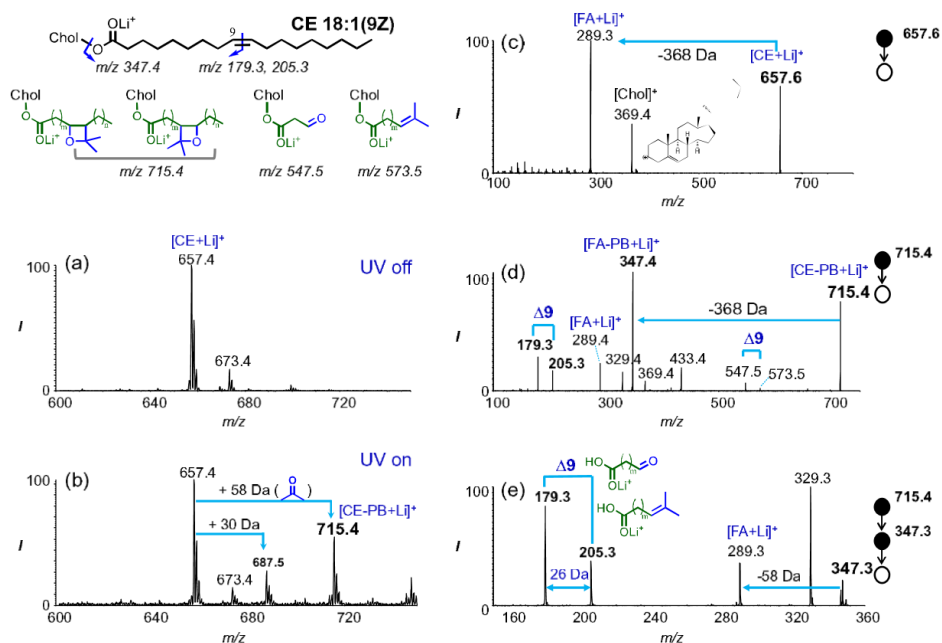
Figure 2. PB -MS/MS of CE 18:1 (9Z) 5 μM in acetone/methanol/dichloromethane/water (40/30/20/10) containing100 μM LiOH. NanoESI MS[1] spectra in positive ion mode: **(a)** before reaction and **(b)** after the PB reaction. MS[2] beam-type CID of **(c)** intact CE ions ($[CE+Li]^+$) at m/z 657.6 and **(d)** the PB product ($[CE - PB+ Li]^+$) at m/z 715.4. **(e)** MS[3] ion trap CID of $[FA + 58 + Li]^+$ (m/z 347.3)

reaction, this side reaction product was detected at m/z 689.5. The 2 Da mass shift suggests that hydroxyl methyl radical ($\bullet CH_2OH$) is formed and added to CE (likely to a C=C). This process might involve the formation of Norrish Type I products of acetone, such as methyl radical ($\bullet CH_3$) and acetyl radical ($CH_3(O)C\bullet$), which is concomitant under the PB reaction condition [49]. These radical intermediates further react with methanol and form hydroxyl methyl radical via hydrogen abstraction. Hydroxyl methyl radical adds on to a C=C bond; upon loss of a hydrogen atom, the hydroxyl methyl modified product is formed, having a mass 30 Da higher than the intact CE molecule.

Figure 2c and d compare MS[2] CID of intact CE 18:1(9Z) lithium adduct ($[CE + Li]^+$) versus its PB reaction product ($[CE - PB + Li]^+$). Intact CE ions (m/z 657.6) produce two complementary fragment ions: lithiated fatty acyl ion ($[FA + Li]^+$) at m/z 289.4 and cholestene cation ($[Chol]^+$) at m/z 369.4. These two characteristic fragment ions are also detected, however, with significantly reduced relative intensities in MS[2] CID of the PB reaction products (Figure 2d). Instead, ions at m/z 347.4 corresponding to acetone addition to the fatty acyl chain ($[FA - PB + Li]^+$) is the most abundant fragment peak. Interestingly, the fragment containing acetone addition to cholesterol ring

(m/z 433.4) is detected at 20% intensity relative to $[FA - PB + Li]^+$ peak. It is worth noting that CE 18:1(9Z) consists of one C=C bond within the cholesteryl ring and one in its fatty acyl chain. The above results suggest that the PB reaction is preferred at a C=C with less steric hindrance. Two pairs of fragments related to the location of C=C in fatty acyl are also detected: ions at m/z 547.5 and 573.5 and ions at m/z 179.3 and 205.3 (structures shown in the inset of Figure 2). The characteristic 26 Da mass difference within each pair of ions clearly suggests that they each result from rupture of the four-membered oxatane rings of the two PB products formed. The former pair consists of intact cholesteryl moiety, whereas the latter pair are likely produced from sequential fragmentation of $[FA - PB + Li]^+$ ions. Indeed, MS[3] CID of $[FA - PB + Li]^+$ (m/z 347.4, Figure 2e) leads to abundant formation of ions at m/z 179.3 and 205.3. Although the location of C=C in fatty acyl chain can be readily deduced from MS[2] CID as shown in Figure 2d, these C=C diagnostics are much more dominant in MS[3] CID, which is later found to be useful in mixture analysis.

Acetone/methanol/dichloromethane/water (40/30/20/10) solvent system was also applied to standard CEs containing multiple C=C bonds to test its performance for the PB reaction. Figure 3a and b compare nanoESI-MS spectra of
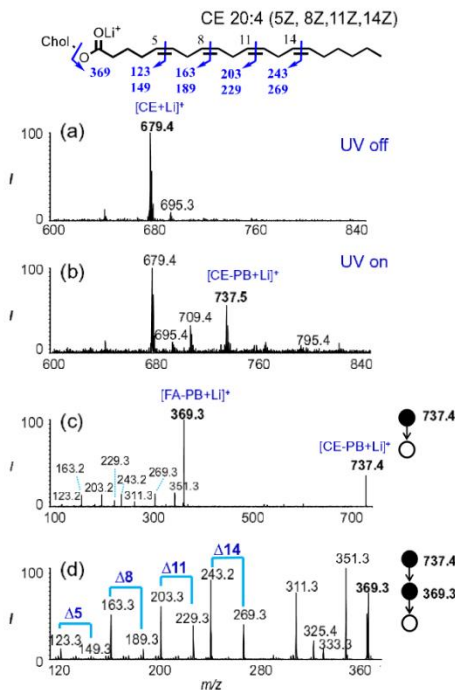
Figure 3. PB-MS/MS of CE 20:4 (5Z, 8Z, 11Z, 14Z). NanoESI MS^1 spectra in positive ion mode: **(a)** before reaction and **(b)** after the PB reaction. **(c)** MS^2 beam-type CID of the PB reaction product ([CE −PB + Li]$^+$) at m/z 737.4, **(d)** MS^3 ion trap CID of [FA − PB + Li]$^+$ (m/z 369.3) The fragmentation map of CE 20:4 is shown as an inset in Figure 3

5 μM CE 20:4 (5Z, 8Z, 11Z, 14Z) before and after the PB reaction. The single acetone addition product ([CE − PB + Li]$^+$, m/z 737.5) is the most abundant product peak after the PB reaction with very limited sequential acetone addition product, i.e., peak at m/z 795.4 observed (Figure 3b). Previous studies on the PB reactions of fatty acids and phospholipids suggest that the formation of single acetone addition PB product is most desirable in terms of generating easy-to-interpret C=C diagnostic ions for structural analysis. Ethanol at 10%–40% volume% has been added to acetone/water reaction solvent to suppress sequential PB reaction product formation for polyunsaturated fatty acyls, which have faster reactions than mono-unsaturated fatty acyls [46]. Since 30% of methanol is already used in the solvent system for CE analysis, it explains why single acetone addition product is the most abundant product. Unfortunately, a side reaction due to hydroxyl methyl radical addition to C=C bond, such as the peak at m/z 709 in Figure 3b is also formed.

Figure 3c shows MS^2 beam-type CID of [CE − PB + Li]$^+$ ions at m/z 737.4, the single acetone addition PB product of CE 20:4. [FA + 58 + Li]$^+$ (m/z 369.3) is the most abundant fragment peak, consistent with that observed from PB-MS/MS of CE 18:1. Due to sequential fragmentation of [FA −PB + Li]$^+$, C=C diagnostic ions corresponding to the four C=C bonds in the fatty acyl chain are also present in the MS^2 CID spectrum, however, with relatively low ion intensities. These C=C diagnostic ions (m/z 123/149, 163/189, 203/229, 243/269) are more prominent in MS^3 ion trap CID (Figure 3d), leading to unambiguous assignment of C=C bond locations at Δ5, 8, 11, and 14, respectively (fragmentation map shown in the inset of Figure 3).

PB-MS^3 CID for CE C=C Location Isomer Analysis

Many unsaturated lipids coexist with one or multiple C=C location isomers in their biological environments and fulfill distinct functions [28, 50, 51]. Our previous studies demonstrate that PB-MS/MS can be readily coupled with shotgun lipid analysis and provide C=C location information as well as C=C location isomer composition information without prior separation [44]. The key step in these experiments is to generate distinct C=C diagnostic ions in PB-MS/MS. Their m/z information leads to C=C location determination, whereas the relative ion intensities of the diagnostic ions provide quantitative information. The earlier experiments on CE standards show that MS^3 CID of the PB reaction modified fatty acyl chain ions ([FA − PB + Li]$^+$) provides stronger C=C diagnostic ion signals together with easy-to-interpret spectrum compared with MS^2 CID of the PB reaction product ([CE − PB + Li]$^+$). Therefore, a PB-MS^3 CID approach outlined in Scheme 1 was further tested for C=C location isomer analysis of unsaturated CEs.

Figure 4a demonstrates PB-MS^3 CID of [FA − PB + Li]$^+$ (m/z 347) derived from an equal molar mixture of CE 18:1 (9Z) and CE 18:1 (11Z) at total concentration of 10 μM. Their corresponding C=C diagnostic ions, viz. m/z 179/205 for Δ9 isomer and m/z 207/233 for Δ11 isomer are formed abundantly in the MS^3 spectrum, allowing confident determination of C=C location for each isomer. In order to obtain rigorous quantitative information, a series of mixtures of CE 18:1(9Z) and CE18:1 (11Z) with total concentration kept at 10 μM but varying molar ratios was prepared and subjected to PB-MS^3 CID. Peak areas of the two C=C diagnostic ions of each isomer were summed and their ratios were plotted against molar ratios (Figure 4b). Good linearity ($R^2 = 0.992$) was obtained in a wide dynamic range (molar ratios from 15:1 to 1:15) for such a calibration curve. We then evaluated PB-MS^3 for quantitative analysis of mixtures containing two common CE 18:3 isomers: ω-6 (C=C at 6Z, 9Z, 12Z) and ω-3(C=C at 9Z, 12Z, 15Z). Figure 4c shows MS^3 CID of [FA − PB + Li]$^+$ ions resulting from single acetone addition to CE 18:3 with the ω-6 and ω-3 isomers each at 5 μM. Because each isomer contains three C=C bonds, six pairs of C=C diagnostic ions are produced in the range m/z 130–260 (fragmentation maps for both isomers

125
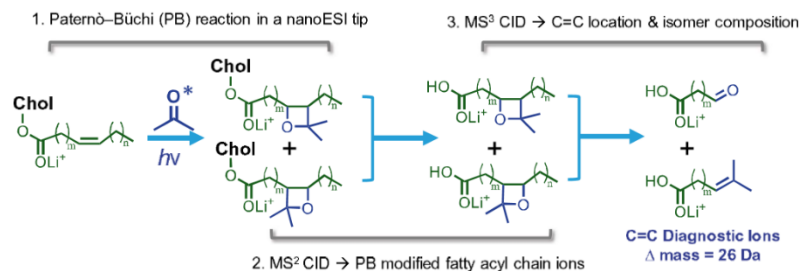
Scheme 1. A PB-MS^3 CID strategy for the determination of C=C location in fatty acyl chains of CEs and their C=C location isomer quantitation

shown in Figure 4d). The peak areas of the three pairs of C=C diagnostic ions derived from each isomer were summed up and used for quantitation in the same fashion as described for CE 18:1 isomer analysis. The calibration curve showed good linearity and dynamic range. We also tried simplifying this process by only using one C=C diagnostic peak from each isomer. In fact, calibration curves with good linearity were obtained from choosing different combinations of C=C diagnostic ions. Figure 4e demonstrates an example of such a calibration curve based on plotting peak area ratios of m/z 137 of ω-6 isomer to m/z 259 of ω-3 isomer against molar ratios of ω-6 versus ω-3. Again, good linearity is achieved in a wide dynamic range (molar ratio from 1:15 to15:1). These two peaks were found to suffer the least interference from chemical noises in the analysis of CEs from human plasma and, therefore, they were chosen for isomer quantitation. The experiments on standard CEs and CE C=C location isomers clearly support that the PB-MS^3 CID approach is successful in providing C=C location information and achieving relative quantitation for C=C location isomers if they coexist. This method is then further applied to CE extracts from human plasma to test its analytical utility in mixture analysis.

Analysis CE Extract from Human Plasma

CEs are relatively abundant species in human plasma and quantitative analyses of CE species in human plasma have been reported using either shotgun or LC-MS methods; the C=C double bond location isomer identification and relative composition have not been determined [7]. We are interested in providing C=C location information for unsaturated CE species, especially detecting coexisting C=C location isomers in human plasma by applying PB-MS^3 CID approach (Scheme 1) in the context of shotgun lipid analysis. CEs were extracted from human plasma (20 μL) based on the MTBE method and an extraction efficiency of 71.0% ± 0.6% was achieved, comparable to literature report [48]. The extract was dried and reconstituted into 1 mL acetone/methanol/dichloromethane/water (40/30/20/10) containing 100 μM LiOH for nanoESI-MS analysis.

Figure 5a shows the CE profile obtained via NLS of 368 Da (cholesterene, $C_{27}H_{44}$) before applying the PB reaction. Consistent with literature report, CE 18:2 (m/z 655.7) is the most abundant spices, followed by CE 18:1 (m/z 657.8) and CE 20:4 (m/z 679.8), whereas CE 16:1 (m/z 629.6), CE 16:0 (m/z 631.8),
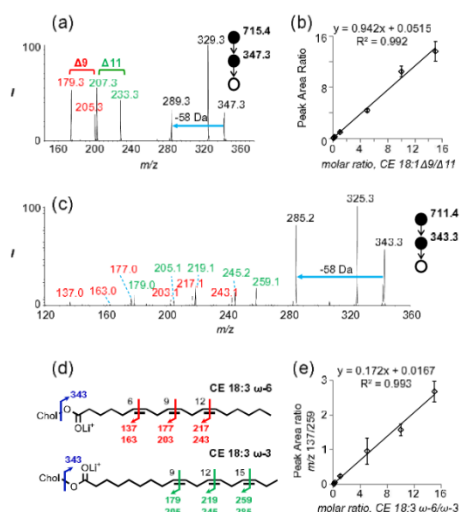
Figure 4. A PB-MS^3 CID approach to identify and quantify CE C=C location isomers. **(a)** PB-MS^3 CID of m/z 347.3 from the PB reaction product of 1/1 molar ratio of CE 18:1 (9Z)/(11Z) at a total concentration of 10 μM. **(b)** Linear relationship established from plotting C=C diagnostic ion peak area ratio and molar ratio of CE 18:1 C=C location isomers. **(c)** PB-MS^3 CID of m/z 343.3 from PB reaction product of 1/1 molar ratio of CE 18:3 (6Z, 9Z, 12Z) (ω-6)/(9Z, 12Z, 15Z) (ω-3) at a total concentration of 10 μM. **(d)** Fragmentation maps of CE 18:3 ω-6 and ω-3 isomers. **(e)** Linear relationship established from plotting peak area ratios of m/z 137 of ω-6 isomer to m/z 259 of ω-3 isomer against molar ratios of CE 18:3 isomers

126
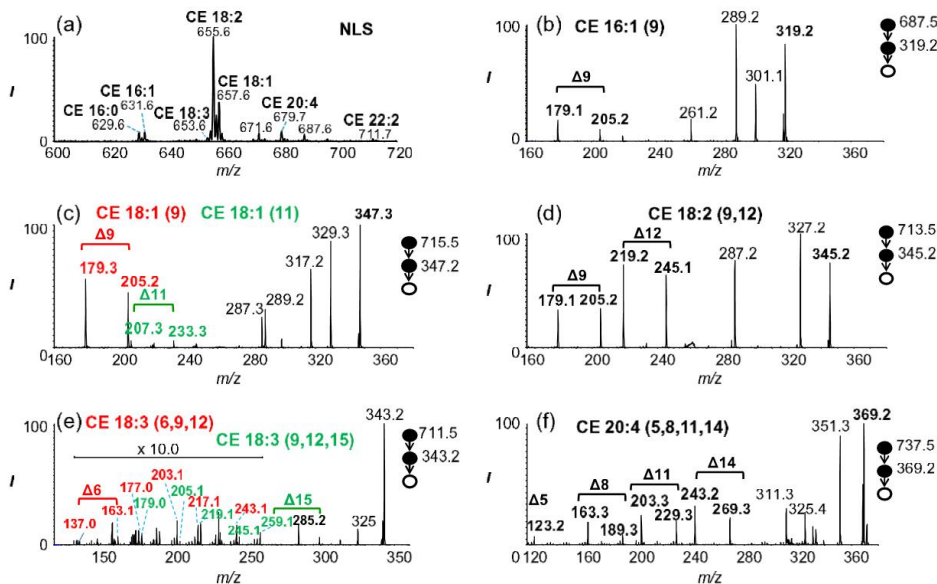
Figure 5. Identification of major unsaturated CE species from human plasma using PB-MS/MS. **(a)** Profile of CEs from human plasm based on NLS of 368 Da (cholesterene, $C_{27}H_{44}$). PB-MS^3 CID of [FA-PB+Li]$^-$ ions of **(b)** CE 16:1, **(c)** CE 18:1, **(d)** CE 18:2, **(e)** CE 18:3, and **(f)** CE 20:4

and CE 18:3 (*m/z* 653.8) are detected as less abundant species [7]. Unsaturated CE species were further subjected to PB-MS^3 CID for C=C location determination. Corresponding PB-MS^3 CID data are shown Figure 5b–f with C=C diagnostic ions labeled in each spectrum. Fragmentation maps of all identified unsaturated CEs are listed in SI, Figure S3. Due to fast cis-trans isomerization of C=C under PB reaction conditions [42], the stereo-configurations of C=C cannot be determined from PB-MS/MS; therefore, only the locations of C=C within CE fatty acyls are reported here. Among them, CE 16:1(9), CE 18:2 (9, 12), and CE 20:4 (5, 8, 11, 14) existed as pure compounds. For CE 18:1, Δ9 and Δ11 isomers were both detected and their molar ratio was determined to be 12/1 based on the calibration curve shown in Figure 4b. CE 18:3 is a relatively low concentration species, only accounting for 2% relative intensity of CE 18:2 (Figure 5a). Given the capability of performing MS^3 CID, diagnostic ions of the two isomers of CE 18:3: ω-6 (C=C at Δ6, 9, 12) and ω-3 (C=C at Δ9, 12, 15) are still detected (Figure 5f). The presence of C=C diagnostic ions in pairs with a signature separation of 26 Da greatly enhances the level of confidence in C=C location identification even though they have relatively low signal-to-noise ratios (S/N). For isomeric composition determination, C=C diagnostic peaks at *m/z* 259 of CE 18:3 ω-6 isomer and *m/z* 137 of the ω-3 isomers were chosen for relative quantitation because these ions experienced the least interference from chemical noises.

Using the calibration curve established in Figure 4e, we successfully determined molar ratio of ω-6/ω-3 isomers to be 3/5.

Use of internal standard (IS) helps to correct for errors associated with nanoESI spray instability, matrix effect, loss of analyte during sample preparation, and CID conditions. An appropriate IS should have similar physical property and ionization efficiency as CE analytes. In this study, CE 22:5 (7Z, 10Z, 13Z, 16Z, 19Z), which was not detected in human plasma, was chosen to be the internal IS. A fixed amount of IS (2 μM) was added into solutions containing different concentrations of reference standards (RS). Then a neutral loss scan (NLS) of 368 Da (cholesterene, $C_{27}H_{44}$) was used for quantitation of different CE species. The calibration curves for CE 16:1 (9Z), CE 18:1(9Z), CE 18:2 (9Z, 12Z), CE 18:3 (9Z, 12Z, 15Z), and CE 20:4 (5Z, 8Z, 11Z, 14Z) are shown in SI, Figure S4. Good linear relationship was obtained and the limit of quantitation (LOQ) was 0.1 μM achieved for all CE species. For pure unsaturated CEs, viz. CE 16:1, CE 18:2, CE 20:4, their concentrations were directly obtained based on NLS and established calibration curves. For CE species containing C=C location isomers, such as CE 18:1 and CE 18:3, the sum concentrations were determined from NLS and then each isomer's concentration was calculated using its composition ratio obtained from PB-MS^3 experiments. Table 1 summarizes quantitative information of the above five unsaturated CEs

Table 1. Quantitative Analysis of Major Unsaturated CE Species in Human Plasma

Unsaturated CE	Concentration (μM)	MW Da	$[M + Li]^+$ m/z
CE 16:1 (9)	98 ± 13	622.6	629.6
CE 18:1 (total)	414 ± 48		
CE 18:1 (9)	382 ± 44	650.6	657.6
CE 18:1 (11)	32 ± 4		
CE 18:2 (9, 12)	$(1.30 \pm 0.11) \times 10^3$	648.6	655.6
CE 18:3 (total)	24.0 ± 1.6		
CE 18:3 (6, 9, 12)/ω-6	9.0 ± 0.6	646.6	653.6
CE 18:3 (9, 12, 15)/ω-3	15.0 ± 1.0		
CE 20:4 (5, 8, 11, 14)	127 ± 4	672.6	679.6

* Ionic species detected in NLS (368 Da) for CE quantitation.

from human plasma. It is worth pointing out that the identification and quantitation of CE 18:1 and CE 18:3 isomers are reported for the first time without prior separations. Moreover, the capability of performing quantitative analysis on C=C location isomers of relatively low abundance CEs, such as CE 18:3, is enabled by high specificity and sensitivity innate in the PB-MS^3 CID approach.

Free FAs of the same human plasma sample were analyzed by PB-MS/MS and reported previously [46]. Comparing to CE data collected from this study, we notice that the C=C locations within fatty acyls are conserved no matter if they are in free FAs or in more complicated lipid molecules, such as CEs. For instance, CE 18:2 is a pure form with C=C located at Δ9 and Δ12, and the same is detected for FA 18:2. CE 18:1 has Δ9 and Δ11, two location isomers, and their molar ratio (12/1) is very close to that of free FA 18:1 (Δ9/Δ11 = 11/1). Similarly, the same ω-6 and ω-3 isomers of FA 18:3 are detected for CE 18:3. The conservation of fatty acyl identities in different classes of lipids reflects them being common building blocks in lipid biosynthesis. More importantly, this type of information could be used as a guide for the identification of unsaturated lipids of different classes.

Conclusions

In this study, an approach based on PB-MS^3 CID has been developed for the analysis of CEs containing unsaturated fatty acyl chains from mixtures. An important step of the development is to determine a proper solvent system that allows for both good PB reaction and ionization via nanoESI. Since CE is nonpolar, adding a nonpolar co-solvent, such as CH_2Cl_2 (20%), to acetone (40%) is necessary for achieving good yields in the PB reactions, while adding another relatively polar co-solvent, MeOH (30%) helps in forming homogenous solution and maintaining stable nanoESI upon the addition of 10% of LiOH aqueous solution. The PB products of CEs in the form of lithium adduct ions ($[CE - PB + Li]^+$) can be detected abundantly after reaction. Collisional activation of $[CE - PB + Li]^+$ results in prominent formation of PB modified fatty acyl ions ($[FA - PB + Li]^+$), while MS^3 CID of $[FA - PB + Li]^+$ leads to C=C diagnostic ion formation, which are

employed in the determination of C=C location and of C=C location isomer composition. The analytical utility of PB-MS^3 CID was demonstrated with CE analysis from human plasma. A series of CEs containing unsaturated fatty acyl chains was identified and quantified at structural level of the C=C locations, unveiling several coexisting C=C location isomers of CEs. Such detailed information is generally not obtainable using conventional lipid analysis methods. Overall, the PB-MS^3 CID approach is simple, fast, and compatible with shotgun lipid analysis workflow. It also offers a distinct advantage of high molecular specificity due to coupling C=C site specific derivatization and MS^3. These advantages would be especially attractive for discovering composition changes of CE C=C location isomers related to diseases or physiological changes. Undesirable aspects associated with the current method include low PB reaction yield and unwanted side reactions due to the use of MeOH as a co-solvent, both of which limit sensitivity of the PB-MS^3 CID approach. Future studies will focus on developing an improved reaction system for CE and other non-polar lipids.

Acknowledgements

References

1. Horton, J.D., Goldstein, J.L., Brown, M.S.: Srebps: Activators of the complete program of cholesterol and fatty acid synthesis in the liver. J. Clin. Invest. **109**, 1125–1131 (2002)

2. Brown, M.S., Ho, Y.K., Goldstein, J.L.: The cholesteryl ester cycle in macrophage foam cells. Continual hydrolysis and re-esterification of cytoplasmic cholesteryl esters. J. Biol. Chem. **255**, 9344–9352 (1980)

3. Schwartz, C.C., VandenBroek, J.M., Cooper, P.S.: Lipoprotein cholesteryl ester production, transfer, and output in vivo in humans. J. Lipid Res. **45**, 1594–1607 (2004)

4. Suckling, K.E., Stange, E.F.: Role of Acyl-CoA: cholesterol acyltransferase in cellular cholesterol metabolism. J. Lipid Res. **26**, 647–671 (1985)

5. Yang, H., Bard, M., Bruner, D.A., Gleeson, A., Deckelbaum, R.J., Aljinovic, G., Pohl, T.M., Rothstein, R., Sturley, S.L.: Sterol esterification in yeast: a two-gene process. Science **272**, 1353–1356 (1996)

6. Francone, O.L., Gurakar, A., Fielding, C.: Distribution and functions of lecithin: cholesterol acyltransferase and cholesteryl ester transfer protein in plasma lipoproteins. Evidence for a functional unit containing these activities together with apolipoproteins *a-i* and *d* that catalyzes the esterification and transfer of cell-derived cholesterol. J. Biol. Chem. **264**, 7066–7072 (1989)

7. Quehenberger, O., Armando, A.M., Brown, A.H., Milne, S.B., Myers, D.S., Merrill, A.H., Bandyopadhyay, S., Jones, K.N., Kelly, S., Shaner, R.L., Sullards, C.M., Wang, E., Murphy, R.C., Barkley, R.M., Leiker, T.J., Raetz, C.R.H., Guan, Z., Laird, G.M., Six, D.A., Russell, D.W., McDonald, J.G., Subramaniam, S., Fahy, E., Dennis, E.A.: Lipidomics reveals a remarkable diversity of lipids in human plasma. J. Lipid Res. **51**, 3299–3305 (2010)

8. Nishikawa, Y., Quittnat, F., Stedman, T.T., Voelker, D.R., Choi, J.-Y., Zahn, M., Yang, M., Pypaert, M., Joiner, K.A., Coppens, I.: Host cell lipids control cholesteryl ester synthesis and storage in intracellular toxoplasma. Cell. Microbiol. **7**, 849–867 (2005)

9. Lee, R.G., Kelley, K.L., Sawyer, J.K., Farese, R.V., Parks, J.S., Rudel, L.L.: Plasma cholesteryl esters provided by lecithin:Cholesterol acyltransferase and acyl-coenzyme A: cholesterol acyltransferase 2 have opposite atherosclerotic potential. Circ. Res. **95**, 998–1004 (2004)

10. Crowe, F.L., Skeaff, C.M., Green, T.J., Gray, A.R.: Serum fatty acids as biomarkers of fat intake predict serum cholesterol concentrations in a population-based survey of New Zealand adolescents and adults. Am. J. Clin. Nutr. **83**, 887–894 (2006)

11. Harkewicz, R., Hartvigsen, K., Almazan, F., Dennis, E.A., Witztum, J.L., Miller, Y.I.: Cholesteryl ester hydroperoxides are biologically active components of minimally oxidized LDL. J. Biol. Chem. **283**, 10241–10251 (2008)

12. Yue, S., Li, J., Lee, S.-Y., Lee, H.J., Shao, T., Song, B., Cheng, L., Masterson, T.A., Liu, X., Ratliff, T.L., Cheng, J.-X.: Cholesteryl ester accumulation induced by PTEN loss and pi3k/akt activation underlies human prostate cancer aggressiveness. Cell Metab. **19**, 393–406 (2014)

13. Peck, B., Schulze, A.: Cholesteryl esters: fueling the fury of prostate cancer. Cell Metab. **19**, 350–352 (2014)

14. German, J.B., Gillies, L.A., Smilowitz, J.T., Zivkovic, A.M., Watkins, S.M.: Lipidomics and lipid profiling in metabolomics. Curr. Opin. Lipid. **18**, 66–71 (2007)

15. Shevchenko, A., Simons, K.: Lipidomics: coming to grips with lipid diversity. Nat. Rev. Mol. Cell Biol. **11**, 593–598 (2010)

16. Murphy, R.C., Fiedler, J., Hevko, J.: Analysis of nonvolatile lipids by mass spectrometry. Chem. Rev. **101**, 479–526 (2001)

17. Fenn, J., Mann, M., Meng, C., Wong, S., Whitehouse, C.: Electrospray ionization for mass spectrometry of large biomolecules. Science **246**, 64–71 (1989)

18. Han, X., Gross, R.W.: Electrospray ionization mass spectroscopic analysis of human erythrocyte plasma membrane phospholipids. Proc. Natl. Acad. Sci. U. S. A. **91**, 10635–10639 (1994)

19. Han, X.L., Gross, R.W.: Global analyses of cellular lipidomes directly from crude extracts of biological samples by esi mass spectrometry: a bridge to lipidomics. J. Lipid Res. **44**, 1071–1079 (2003)

20. Han, X.L., Gross, R.W.: Shotgun lipidomics: Electrospray ionization mass spectrometric analysis and quantitation of cellular lipidomes directly from crude extracts of biological samples. Mass Spectrom. Rev. **24**, 367–412 (2005)

21. Bird, S.S., Marur, V.R., Sniatynski, M.J., Greenberg, H.K., Kristal, B.S.: Lipidomics profiling by high-resolution LC-MS and high-energy collisional dissociation fragmentation: focus on characterization of mitochondrial cardiolipins and monolysocardiolipins. Anal. Chem. **83**, 940–949 (2010)

22. Nygren, H., Seppänen-Laakso, T., Castillo, S., Hyötyläinen, T., Orešič, M.: Liquid chromatography-mass spectrometry (LC-MS)-based lipidomics for studies of body fluids and tissues. Springer (2011)

23. Murphy, R.C., Leiker, T.J., Barkley, R.M.: Glycerolipid and cholesterol ester analyses in biological samples by mass spectrometry. Biochim. Biophys. Acta Mol. Cell Biol. Lipids **1811**, 776–783 (2011)

24. Murphy, R.C.: Tandem mass spectrometry of lipids: molecular analysis of complex lipids. Royal Soc. Chem. (2014)

25. Bowden, J.A., Albert, C.J., Barnaby, O.S., Ford, D.A.: Analysis of cholesteryl esters and diacylglycerols using lithiated adducts and electrospray ionization-tandem mass spectrometry. Anal. Biochem. **417**, 202–210 (2011)

26. Bowden, J.A., Shao, F., Albert, C.J., Lally, J.W., Brown, R.J., Procknow, J.D., Stephenson, A.H., Ford, D.A.: Electrospray ionization tandem mass spectrometry of sodiated adducts of cholesteryl esters. Lipids **46**, 1169–1179 (2011)

27. Martinez-Seara, H., Róg, T., Pasenkiewicz-Gierula, M., Vattulainen, I., Karttunen, M., Reigada, R.: Interplay of unsaturated phospholipids and cholesterol in membranes: effect of the double-bond position. Biophys. J. **95**, 3295–3305 (2008)

28. Johnson, D.W., Beckman, K., Fellenberg, A.J., Robinson, B.S., Poulos, A.: Monoenoic fatty acids in human brain lipids: isomer identification and distribution. Lipids **27**, 177–180 (1992)

29. Rustan, A.C., Drevon, C.A.: Fatty acids: Structures and properties. John Wiley and Sons (2005)

30. Hancock, S.E., Poad, B.L.J., Batarseh, A., Abbott, S.K., Mitchell, T.W.: Advances and unresolved challenges in the structural characterization of isomeric lipids. Anal. Biochem. (2016). doi:10.1016/j.ab.2016.1009.1014

31. Ryan, E., Reid, G.E.: Chemical derivatization and ultrahigh resolution and accurate mass spectrometry strategies for "shotgun" lipidome analysis. Acc. Chem. Res. **49**, 1596–1604 (2016)

32. Tomer, K.B., Crow, F.W., Gross, M.L.: Location of double-bond position in unsaturated fatty acids by negative ion MS/MS. J. Am. Chem. Soc. **105**, 5487–5488 (1983)

33. Thomas, M.C., Mitchell, T.W., Harman, D.G., Deeley, J.M., Nealon, J.R., Blanksby, S.J.: Ozone-induced dissociation: elucidation of double bond position within mass-selected lipid ions. Anal. Chem. **80**, 303–311 (2007)

34. Brown, S.H.J., Mitchell, T.W., Blanksby, S.J.: Analysis of unsaturated lipids by ozone-induced dissociation. Biochim. Biophys. Acta Mol. Cell Biol. Lipids **1811**, 807–817 (2011)

35. Pham, H.T., Maccarone, A.T., Thomas, M.C., Campbell, J.L., Mitchell, T.W., Blanksby, S.J.: Structural characterization of glycerophospholipids by combinations of ozone- and collision-induced dissociation mass spectrometry: the next step towards "top-down" lipidomics. Analyst **139**, 204–214 (2014)

36. Pham, H.T., Trevitt, A.J., Mitchell, T.W., Blanksby, S.J.: Rapid differentiation of isomeric lipids by photodissociation mass spectrometry of fatty acid derivatives. Rapid Commun. Mass Spectrom. **27**, 805–815 (2013)

37. Pham, H.T., Julian, R.R.: Radical delivery and fragmentation for structural analysis of glycerophospholipids. Int. J. Mass Spectrom. **370**, 58–65 (2014)

38. Deimler, R.E., Sander, M., Jackson, G.P.: Radical-induced fragmentation of phospholipid cations using metastable atom-activated dissociation mass spectrometry (MAD-MS). Int. J. Mass Spectrom. **390**, 178–186 (2015)

39. Li, P., Hoffmann, W.D., Jackson, G.P.: Multistage mass spectrometry of phospholipids using collision-induced dissociation (cid) and metastable atom-activated dissociation (MAD). Int. J. Mass Spectrom. **403**, 1–7 (2016)

40. Campbell, J.L., Baba, T.: Near-complete structural characterization of phosphatidylcholines using electron impact excitation of ions from organics. Anal. Chem. **87**, 5837–5845 (2015)

41. Baba, T., Campbell, J.L., Le Blanc, J.C.Y., Baker, P.R.S.: Structural identification of triacylglycerol isomers using electron impact excitation of ions from organics (EIEIO). J. Lipid Res. **57**, 2015–2027 (2016)

42. Büchi, G., Inman, C.G., Lipinsky, E.S.: Light-catalyzed organic reactions. I. The reaction of carbonyl compounds with 2-methyl-2-butene in the presence of ultraviolet light. J. Am. Chem. Soc. **76**, 4327–4331 (1954)

43. Ma, X., Xia, Y.: Pinpointing double bonds in lipids by Paternò-Büchi reactions and mass spectrometry. Angew. Chem. Int. Ed. **126**, 2592–2596 (2014)

44. Ma, X., Chong, L., Tian, R., Shi, R., Hu, T.Y., Ouyang, Z., Xia, Y.: Identification and quantitation of lipid C=C location isomers: A shotgun lipidomics approach enabled by photochemical reaction. Proc. Natl. Acad. Sci. U. S. A. **113**, 2573–2578 (2016)

45. Stinson, C.A., Xia, Y.: A method of coupling the Paternò-Büchi reaction with direct infusion esi-ms/ms for locating the C=C bond in glycerophospholipids. Analyst **141**, 3696–3704 (2016)

46. Ma, X., Zhao, X., Li, J., Zhang, W., Cheng, J.-X., Ouyang, Z., Xia, Y.: Photochemical tagging for quantitation of unsaturated fatty acids by mass spectrometry. Anal. Chem. **88**, 8931–8935 (2016)

47. Liebisch, G., Vizcaíno, J.A., Köfeler, H., Trötzmüller, M., Griffiths, W.J., Schmitz, G., Spener, F., Wakelam, M.J.O.: Shorthand notation for lipid structures derived from mass spectrometry. J. Lipid Res. **54**, 1523–1530 (2013)

48. Matyash, V., Liebisch, G., Kurzchalia, T.V., Shevchenko, A., Schwudke, D.: Lipid extraction by methyl-tert-butyl ether for high-throughput lipidomics. J. Lipid Res. **49**, 1137–1146 (2008)

49. Norrish, R.G.W., Bramford, C.H.: Photodecomposition of aldehydes and ketones. Nature **138**, 1016 (1936)

50. Wijendran, V., Hayes, K.C.: Dietary *n*-6 and *n*-3 fatty acid balance and cardiovascular health. Annu. Rev. Nutr. **24**, 597–615 (2004)

51. Simopoulos, A.P.: The importance of the omega-6/omega-3 fatty acid ratio in cardiovascular disease and other chronic diseases. Exp. Biol. Med. **233**, 674–688 (2008)

RESEARCH PAPER

CrossMark

In-depth structural characterization of phospholipids by pairing solution photochemical reaction with charge inversion ion/ion chemistry

Elissia T. Franklin[1] · Stella K. Betancourt[1] · Caitlin E. Randolph[1] · Scott A. McLuckey[1] · Yu Xia[1,2]

Abstract

Shotgun lipid analysis based on electrospray ionization-tandem mass spectrometry (ESI-MS/MS) is increasingly used in lipidomic studies. One challenge for the shotgun approach is the discrimination of lipid isomers and isobars. Gas-phase charge inversion via ion/ion reactions has been used as an effective method to identify multiple isomeric/isobaric components in a single MS peak by exploiting the distinctive functionality of different lipid classes. In doing so, fatty acyl chain information can be obtained without recourse to condensed-phase separations or derivatization. This method alone, however, cannot provide carbon–carbon double bond (C=C) location information from fatty acyl chains. Herein, we provide an enhanced method pairing photochemical derivatization of C=C via the Paternò–Büchi reaction with charge inversion ion/ion tandem mass spectrometry. This method was able to provide gas-phase separation of phosphatidylcholines and phosphatidylethanolamines, the fatty acyl compositions, and the C=C location within each fatty acyl chain. We have successfully applied this method to bovine liver lipid extracts and identified 40 molecular species of glycerophospholipids with detailed structural information including head group, fatty acyl composition, and C=C location.

Introduction

Amongst all the classes of lipids in mammalian cells, glycerophospholipids (GPs) are the most abundant, constituting approximately 60 mol% of lipid mass within the cell membrane [1, 2]. GPs are the key component in cell membrane structure [3]; they function as signaling molecules [1, 2] and

✉ Scott A. McLuckey
  mcluckey@purdue.edu

✉ Yu Xia
  xiayu@tsinghua.edu.cn

[1] Department of Chemistry, Purdue University, 560 Oval Drive, West Lafayette, IN 47907-2084, USA

[2] Department of Chemistry, Tsinghua University, Beijing 100084, China

secondary messengers in cell metabolism [1–3]. GP profiles have been used as phenotypical signals [3–5] for imaging of diseased tissues [6] and systems biology studies [7–9]. GPs are assembled from three building blocks, a glycerol backbone, two fatty acyl or alkyl chains linked at the *sn1* and *sn2* positions of the glycerol, and a phosphate-containing head group [10–13]. The identity of the head group defines the GP subclass, for example, phosphatidylethanolamine (PE) and phosphatidylcholine (PC) head groups consist of ethanolamine and choline esterified to the phosphate, respectively.

Lipid analysis via mass spectrometry (MS) can be performed using two main approaches: liquid chromatography-mass spectrometry (LC/MS) and direct-infusion electrospray mass spectrometry. The use of LC/MS allows for complex lipid components in a sample to undergo chromatographic separation prior to being analyzed by the MS, thus providing increased sensitivity and selectivity [14–17]. Direct-infusion electrospray mass spectrometry, or shotgun lipid analysis, is a fast and sensitive method that analyzes the lipids directly from the crude extract without chromatographic separation [18–24]. Shotgun analysis benefits from the use of high-resolution MS instruments, which helps distinguish isobaric peaks and allows for more accurate identification due to better

⌖ Springer

peak separation. However, high mass resolving power alone cannot provide isomeric separation. Separation in shotgun lipidomic approaches can also be done via in-solution modifications. Functional group selective modification, such as targeting the vinyl ether bond [4], the GP head groups [25, 26] or a one-step methylation of the phosphate [27], has been demonstrated to improve identification and quantitation for isomeric/isobaric GPs and boosting the detection of low abundance GPs.

Gas-phase ion/ion reactions have been used to separate isomeric and isobaric species post-ionization, thereby obviating the need for in-solution modification. Spraying PCs and PEs in the positive ion mode and subjecting the ions to gasphase ion/ion interaction with a dicarboxylate reagent effectively charge invert the cationic lipids and separate PC and PE isomers based on distinct reaction chemistry between their head groups and the reagent [28, 29]. The negatively charged ions resulting from charge inversion ion/ion reactions provide abundant fatty acyl fragment ions upon collision-induced dissociation (CID), leading to confident identification of fatty acyl composition including the number of carbons and degree of unsaturation [24, 30]. However, the carbon–carbon double bond (C=C) location cannot be determined from such a process.

Notable gas-phase activation methods of determining C=C location of lipids include charge-remote fragmentation induced by high-energy CID [31], ozone-induced dissociation (OzID) [32–34], 193-nm ultraviolet photodissociation (UVPD) [35], radical directed dissociation (RDD) [36, 37], helium metastable atom-activated dissociation (He-MAD) [38, 39], and electron impact excitation of ions from organics (EIEIO) [40, 41]. All these methods either utilize high-energy collisions or require significant instrument alterations. The Xia group introduced using UV-initiated reactions without instrument modification for localization of C=Cs, including ozonolysis [42, 43] and the in-solution Paternò–Büchi (PB) reaction [44–47]. The PB reaction has been employed with subsequent ESI-MS/MS via low-energy CID on multiple classes of lipids [48]. In such a method, acetone serves both as the PB reagent and as a co-solvent for ESI-MS of lipids. Upon 254-nm UV irradiation of the solution, acetone selectively adds onto a C=C, forming a four-membered oxetane ring structure. Low-energy CID of the PB reaction products ruptures the oxetane ring yielding fragment ions that are specific to the C=C location. The PB-MS/MS method is versatile as it can be performed on various MS instruments that have CID and ESI capabilities. Confident structural identification of unsaturated GPs at C=C location level builds upon the capability of determining fatty acyl/alkyl composition. For situations where lipids experience competitive ion suppression, such as detecting lower abundance PC in negative ion mode, or when lipid isobaric and isomeric isomers coexist, fatty acyl chain assignment from MS^2 CID in negative ion mode is often complicated by chemical interferences [46]. Combining the in-solution PB reaction and the gas-phase charge inversion reaction is promising for high-level characterization of GP structures for shotgun lipidomics. In this study, synthetic standards of unsaturated PC and PE were used for method development. The performance of pairing the PB reaction with ion/ion charge inversion for complex mixture analysis was evaluated with a polar lipid extract of bovine liver, which led to confident identification of 40 PC and PE molecular species with detailed structural information including head group, fatty acyl composition, and C=C location.

Materials and methods

Nomenclature

We follow the lipid annotation recommended by LIPID MAPS [49]. In short, PC 16:0_18:2(Δ9,12) identifies the phosphocholine (PC) head group, two fatty acyl chains with the carbon number (the value before the colon, i.e., 16 and 18), the degree of unsaturation (the value after the colon, i.e., 0 and 2), and the location of C=C counting from the carboxylic carbon towards the fatty chain end (i.e., Δ9 and Δ12 in C18:2). The underscore (_) suggests that the *sn* positions of fatty acyl chains are not specified, while a forward slash (/) identifies the fatty acyls occupy the *sn*1 and *sn*2 locations, respectively, as the order indicated in the annotation. Only when the conformation of a C=C is known, a letter E or Z is used to indicate the trans- or cis-conformation, respectively.

Materials

1-Palmitoyl-2-oleoyl-glycero-3-phosphocholine (PC 16:0/18:1(9Z)), *1-palmitoyl-2-oleoyl-sn-glycero-3-phosphoethanolamine* (PE 16:0/18:1(9Z)), and polar lipid extract of bovine liver (in chloroform) were purchased from Avanti Polar Lipid, Inc. (Alabaster, AL). 1,4-Phenylenedipropionic acid (PDPA) and ammonium acetate were purchased from Sigma-Aldrich (St. Louis, MO). Formic acid was purchased from Fisher Chemical. Organic solvents were LC-grade, and ultrapure water was obtained from a purification system at 0.03 μS cm.

The PB reactions in an offline flow microreactor

A flow microreactor was constructed using UV transparent fused silica capillary as the flow cell (fluoropolymer-coated, 100 μm i.d., 363 μm o.d.; Polymicro Technologies/Molex; Phoenix, AZ). The fused silica capillary and a low-pressure mercury lamp with emission centered around 254-nm wavelength (BHK, Inc., Ontario, CA) were placed in parallel with a 1-cm distance, providing an effective UV exposure length of

132

4 cm. For safety considerations, the reactor was enclosed in an aluminum-lined cardboard box to prevent stray UV light. When conducting the PB reaction, the UV lamp was turned on and the lipid solution was pumped through the reactor via a syringe pump at a flowrate of 4–6 μL/min, enabling 4–5-s reaction times. All lipids were dissolved in 69/29/1/1 (*v/v/v/v*) of acetone/water/formic acid/isopropyl alcohol solution for the PB reaction. Ammonium acetate (10 mM) was added to the solvent system for conducting experiments when direct-injection negative ion mode was used. About 5–10 μL of the reaction solution was collected in a pre-pulled nano-ESI tip and immediately subjected to subsequent MS analysis.

Mass spectrometry

For prior analysis of the lipids in the bovine liver polar lipid extract, samples were analyzed using a QTRAP 4000 hybrid triple quadrupole/linear ion trap mass spectrometer (Sciex, Toronto, ON, Canada) equipped with a homebuilt nano-ESI source. The lipid extract was diluted to 100 μM in a 69/29/1/1 (*v/v/v/v*) of acetone/water/formic acid/isopropyl alcohol solvent system. Mass spectrometer parameters were as follows: spray voltage, 1450–1600 V; curtain gas, 3 psi; declustering potential, 80 V; collision gas, high. Precursor ion scan (PIS) and neutral loss (NL) scan (NLS) were employed to identify the head group of the GPs.

Gas-phase charge inversion ion/ion reactions Structural analyses were performed using a TripleTOF 5600 triple quadruple/time-of-flight mass spectrometer (Sciex, Concord, ON, Canada) that was previously modified to perform mutual storage of cation and anions for ion/ion reactions [50]. The dual nano-ESI emitter setup allowed sequential formation of the PB-modified lipid cations and PDPA dianions ([PDPA - 2H]$^{2-}$), which were each mass selected in Q1 and transferred into the q2 linear ion trap for ion/ion reactions. The ions in q2 were mutually stored for 30 ms and the products of interest were isolated via a notched broadband waveform. CID was performed using a single-frequency resonance excitation at *q* value of 0.18. Third generation ion of interest was fragmented by placing it at a *q* value of 0.14 and implementing a third resonance excitation event.

Results and discussion

Conducting the PB reactions in an offline microreactor A graphic representation of the offline flow microreactor for conducting the PB reaction is shown in Fig. 1a and the reaction scheme is shown in Fig. 1b. We have previously shown that using a flow microreactor to initiate the PB reaction allows for high photon efficiency leading to higher yield and the ability to control side reactions [45]. This setup is especially beneficial for the dual-emitter apparatus for alternatively injecting cations and anions for ion/ion reactions. The PB reaction conditions for unsaturated PC and PE were optimized by monitoring the PB product percent yield (the relative ion intensity of the PB products normalized to that of the intact lipid before UV exposure), using PC 16:0/18:1(9Z) and PE 16:0/18:1(9Z) as model compounds, respectively. Figure 1 panels c and d represent typical nano-ESI-MS spectra of the unsaturated PC and PE after the PB reactions. The PB products are clearly detected at *m/z* 818.7 for protonated PC 16:0/18:1(9Z), of the form [^{PB}PC + H]$^+$ in Fig. 1c, and at *m/z* 776.7 for protonated PE 16:0/18:1(9Z), of the form [^{PB}PE + H]$^+$ in Fig. 1d, with limited evidence for side reactions resulting from Norrish type I cleavage of acetone [45]. These PB products have a characteristic 58-Da increase in mass relative to the intact lipids, consistent with one acetone addition to the C=C in lipids. By monitoring the reaction kinetics, we found the PB reaction of PC 16:0/18:1(9Z) plateaued at approximately 6 s with 35% yield (inset of Fig. 1c). For PE 16:0/18:1(9Z), the PB reaction yield was maximized around 3 s at 30% (kinetic curve shown in the inset of Fig. 1d), while longer reaction times slightly decreased the yield due to increased contributions from side reactions. Based on these observations, the reaction time used for later studies was generally between 4 and 5 s to ensure adequate PB product yield and minimize the extent of side reactions.

Charge inversion of the PB reaction products Using the optimized PB conditions for unsaturated PC and PE, we further explored pairing the PB reaction with charge inversion ion/ion reactions and subsequent CID experiments for structural characterization to the C=C location level. The typical workflow for unsaturated PC analysis is illustrated in Fig. 2(a–c), using the model compound PC 16:0/18:1(9Z) as an example. First, the PB product of PC 16:0/18:1(9Z) ([^{PB}PC + H]$^+$) was mass-isolated and subjected to ion/ion reaction with [PDPA - 2H]$^{2-}$. The ion/ion reaction products included dominant complex formation of the two reactant ions, [^{PB}PC + PDPA - H]$^-$ (*m/z* 1038), and a minor peak at *m/z* 802 resulting from demethylation of the ^{PB}PC anion (see Electronic Supplementary Material (ESM) Fig. S1). This ion/ion reaction phenomenon is identical to that of the intact PC cation, suggesting that the modification at the C=C from the PB reaction does not interfere with the charge inversion chemistry (ESM Fig. S2). Collisional activation of the complex ion at *m/z* 1038 mainly led to the formation of [^{PB}PC - CH$_3$]$^-$ ion (*m/z* 802.7, Fig. 2(a)), formed from NL of methylated PDPA (236 Da). In previous work, the operational efficiency of protonated PC species to demethylated species was calculated as about 50%, although absolute efficiency could not be calculated due to the difference in detector response to positive and negative ions [28]. Further CID of this fragment produced abundant fatty acyl anions (Fig. 2(b)), including [C16:0 - H] (*m/z* 255.3) and the PB-modified C18:1 ([^{PB}C18:1 - H]$^-$, *m/z*
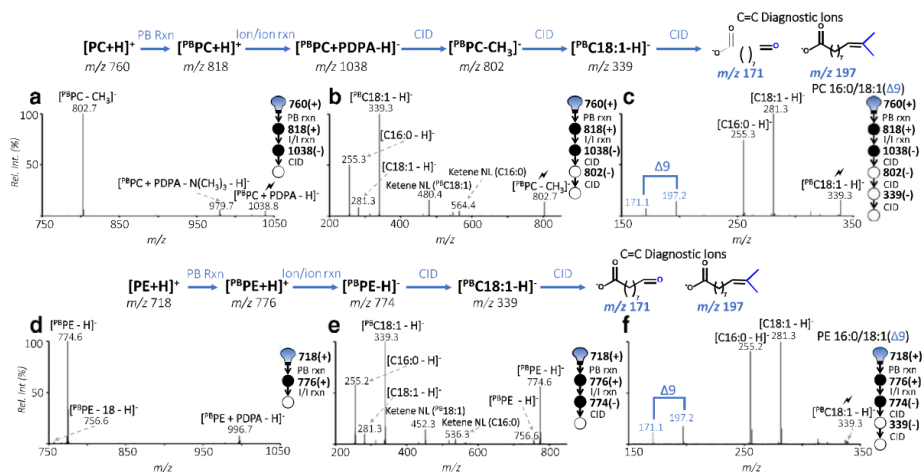
133
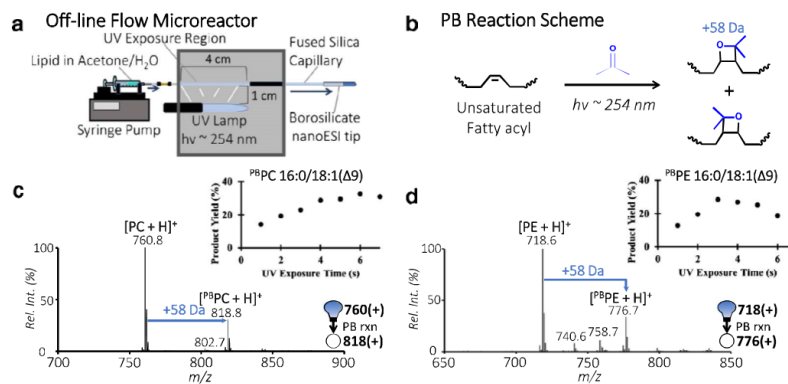
Fig. 1 **a** Schematic of an offline flow microreactor for conducting the PB reaction. **b** The PB reaction scheme, involving acetone addition to a C=C in a fatty acyl chain. The positive ion mode nano-ESI-MS spectra of **c** 5 μM PC 16:0/18:1(9Z) after 5-s UV exposure and **d** 5 μM PE 16:0/ 18:1(9Z) after 4-s UV exposure. Insets in **c** and **d** represent the PB reaction kinetic curve of PC and PE standards, respectively, with respect to UV exposure time. Positively charged ions are represented by "+"

339.2), and fragments (m/z 480.4 and m/z 536.3) due to ketene NL of ^{PB}C18:1 and C16:0, respectively. A small intact C18:1 anion peak at m/z 281.3 was also observed, likely formed from loss of acetone from $[^{PB}$C18:1 - H]$^-$ due to sequential fragmentation. The relatively higher abundances of ketene NL ions and carboxylate anions from the *sn2* chain relative to

those formed from *sn1* chain corroborate that the *sn1* and *sn2* chains are C16:0 and C18:1, respectively, verifying the *sn* positions for the synthetic molecules. In previous studies using charge inversion of PC, the fatty acyl chain determination was the final piece of information provided. In this study, CID of the PB product of the C18:1 ($[^{PB}$C18:1 - H]$^-$, m/z

Fig. 2 Sequence of events post-ion/ion reaction between GP standard cations and PDPA dianion. (a) Ion trap CID of $[^{PB}$PC + PDPA - H]$^-$. (b) Ion trap CID of $[^{PB}$PC - CH$_3]^-$. (c) Subsequent ion trap CID of $[^{PB}$C18:1 - H]$^-$. (d) Result of ion/ion reaction between [PDPA - 2H]$^{2-}$ and $[^{PB}$PE + H]$^+$. (e) Ion trap CID of $[^{PB}$PE - H]$^-$. (f) Subsequent ion trap CID of

$[^{PB}$C18:1 - H]$^-$. Schematics in (a–c) and (d–f) are layouts of the process for determining the GP structure. CID of a target ion is depicted by a lightning bolt (⚡). Cations and anions are represented by "+" or "-", respectively

339.2) produced C=C diagnostic ions at m/z 171.1 and 197.2 (Fig. 2(c)), allowing confident determination of the site of unsaturation at $\Delta 9$.

Figure 2(d–f) demonstrates the process of structural characterization for unsaturated PE, using PE 16:0/18:1(9Z) as an example. The workflow is slightly different from that of the PC, due to the difference in charge inversion ion/ion chemistry between a primary amine (in PE) and a quaternary amine (in PC). As shown in Fig. 2(d), the dominant charge inversion product of $[^{PB}PE + H]^{+}$ (m/z 776.6) is the corresponding deprotonated ion ($[^{PB}PE - H]^{-}$, m/z 774.6), accompanied only by a very small extent of complex formation (the peak at m/z 996.7). Collisional activation of $[^{PB}PE - H]^{-}$ (Fig. 2(e)) resulted in the formation of abundant PB reaction–modified C18:1 ($[^{PB}C18:1 - H]^{-}$, m/z 339.3) and C16:0 ($[C16:0 - H]^{-}$, m/z 255.2) fatty acyl anions as well as the ketene NL of the $sn2$ chain (m/z 452.3) and $sn1$ chain (m/z 536.3). Subsequent CID of $[^{PB}C18:1 - H]^{-}$ produced characteristic C=C diagnostic ions that are 26 Da apart at m/z 171.1 and 197.2, confirming the C=C location at $\Delta 9$ in C18:1.

The above analysis using PC and PE synthetic standards demonstrates that the PB reaction and gas-phase charge inversion ion/ion reactions can be efficiently paired and applied for confident structural identification of GPs at the C=C location level. Charge inversion of PB products exhibits equivalent information to unmodified GPs with the addition of the C=C localization and was applied to a biological extraction sample.

Shotgun analysis of the polar lipid extract from bovine liver

Polar lipid extract from bovine liver was employed as the benchmark test to evaluate the performance of coupling the PB reaction with ion/ion reaction for shotgun lipid analysis. The positive ion mode nano-ESI mass spectrum of the lipid extract is shown in Fig. 3a. By employing linked scans in positive ion mode, i.e., PE via 141-Da NLS and PC via m/z 184 PIS, these two lipid subclasses were identified (ESM Fig. S3); however, the fatty acyl composition could not be obtained. Herein, we exemplify the power of the detailed structural analysis for unsaturated PC and PE by pairing the PB reaction and charge inversion ion/ion reactions. For clarity, those peaks that we demonstrate in later discussions are labeled in red in Fig. 3a (i.e., m/z 744.6, m/z 768.6, m/z 788.7, and m/z 834.7).

Individual PB-reacted peaks were isolated from the UV-irradiated, diluted lipid extract. The PB reaction product (m/z 846.8) of a relatively abundant lipid peak (m/z 788.7) was isolated using a unit mass isolation window and subjected to ion/ion reaction with the PDPA dianion. The resulting spectrum was dominated by ions at m/z 1066.8 from complex formation ($[^{PB}M + PDPA - H]^{-}$), a very minor peak at m/z 844.7 due to double proton transfer, and a small fragment ion (m/z 830.7) due to NL of methylated PDPA (ESM Fig. S4). Based on the distinct ion/ion charge inversion
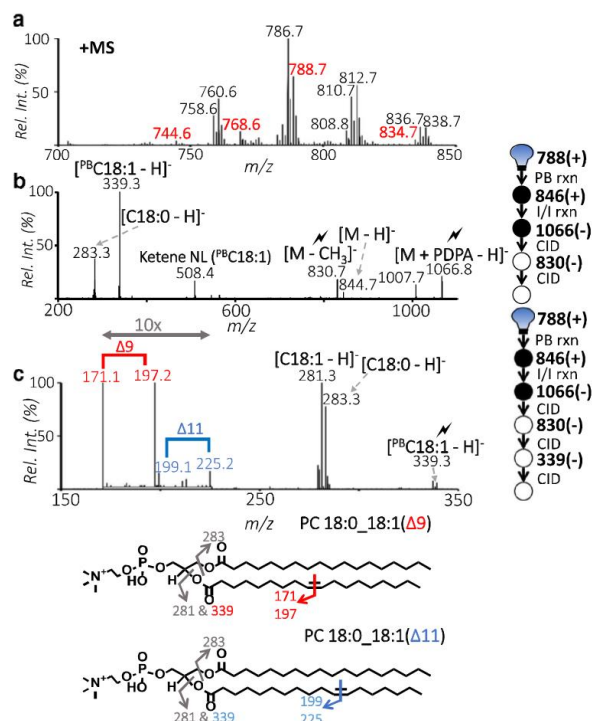
chemistry of PC and PE, i.e., complex formation vs. double proton transfer, it is evident that the peak at m/z 788.7 in Fig. 3a consists of PC 36:1 as a major component and PE 39:1 as a minor component. In order to identify the fatty acyl composition and C=C location in PC 36:1, the ion complex at m/z 1066.8 was subjected to sequential CID experiments as depicted in Fig. 2(a). The CID spectrum of m/z 830.7 ($[^{PB}PC - CH_{3}]^{-}$, Fig. 3b) indicated that PC 36:1 consists primarily of C18:0 and C18:1. The glycerol backbone location of C18:1 is likely at $sn2$ given the high abundance of associated ketene NL; however, the method currently is limited in its ability to determine sn position due to possible coexisting isomers. This is consistent with the fatty acyl composition inferred from charge inversion and CID of the intact ions at m/z 788.7 (ESM Fig. S5). The PB-modified C18:1 ion population was detected at m/z 339.3; further CID of these ions produced two C=C diagnostic ion pairs at m/z 171.1/197.2 and m/z 199.1/225.2, providing definitive evidence for locations of C=Cs at $\Delta 9$ and $\Delta 11$ in C18:1, respectively. Combining all above information, PC 36:1 could be confidently identified as a mixture of PC 18:0_18:1($\Delta 9$) and PC 18:0_18:1($\Delta 11$). The PC 18:0_18:1($\Delta 9$) specie is the major isomer based on the relative abundances of its C=C diagnostic ions relative to those of the $\Delta 11$ isomer (Fig. 3c). Due to the low ion signal of PE 39:1, C=C location determination could not be obtained after ion/ion reaction. The above data highlight that in a single spectrum, it is possible to differentiate GP class isomers, fatty acyl isomers, and C=C isomers (ESM Fig. S6).

Although charge inversion of the PB products was powerful in pinpointing detailed structural information of unsaturated PC and PE, the need of performing multi-step CID made it difficult to analyze lower abundance lipids. Furthermore, CID of the PB-modified polyunsaturated fatty acid anions would not provide as abundant C=C diagnostic ions as performed in the positive ion mode. This limitation can be overcome by conducting ion/ion charge inversion and the PB reaction in two separate experiments, that is, first to charge invert the peak of interest to verify headgroup and fatty acyl identification, then use positive ion mode PB-MS/MS for determination of C=C location. Separately using PB-MS/MS and ion/ion reaction allows for increased sensitivity of C=C diagnostic information and a rapid structural analysis compared to combination of the methods.

Structural analysis of polyunsaturated GPs is demonstrated by probing the ions at m/z 834.7 ($[M + H]^{+}$) in Fig. 3a, because of the structural complexity and minor relative abundance. Based on the PIS for m/z 184 combined with the LipidMaps structural database, the lipid peak was expected to contain PC 40:6. Following the conventional method for fatty acyl identification, the possible PC species (acetate adduct at m/z 892.8, $[M + Ac]^{-}$) was probed in the negative ion mode from nano-ESI of lipid solution added with 10 mM of ammonium acetate. Figure 4a shows the MS^{2} CID spectrum of $[M + Ac]^{-}$, the

135

Fig. 3 a Positive ion mode nano-ESI-MS spectrum of polar lipid extract from bovine liver (100 uM) without PB reaction. **b** Subjecting ions at m/z 788.7 in panel **a** to the PB reaction (m/z 846.8 isolated in positive ion mode), charge inversion ion/ion reaction, and CID of post-ion/ion reaction product ions at m/z 1066.8 and 830.7 (negative ion mode) allows confident identification of this lipid at fatty acyl level. **c** CID spectrum of m/z 339.3 produced in panel **b**. Detection of two pairs of C=C diagnostic ions at m/z 171.1/197.2 and m/z 199.1/225.2 from C18:1 chain identifies the lipids at m/z 788.7 in panel **a** as PC 18:0_18:1(Δ9) and PC18:0_18:1(Δ11)

same nominal m/z as the acetate adduct ion of PC 40:6. The major fragment peaks include ions at m/z 255.3 and 281.3, corresponding to C16:0 and C18:0, respectively, with a few smaller peaks corresponding to other fatty acyl chains. The combination of fatty acyl chains C16:0 and C18:0 would not provide the correct identification of PC 40:6 achieved from positive ion mode, largely due to poor ionization efficiency of the acetate adduct and ion suppression of PC in negative ion mode. Thus, it is evident that in negative ion mode, the ions presented at m/z 892.8 contained isobaric GP species that were not the analyte of interest. Charge inversion ion/ion reaction of m/z 834.7 from positive ion mode produced abundant ions at m/z 1054.8 and 818.8, which are characteristic for the presence of PC 40:6. The appearance of ions at m/z 832.7 suggested the presence of PE 43:6 as a minor component. The CID spectrum of the demethylated PC 40:6 (m/z 818.8) is shown in Fig. 4b. The negative ion mode spectrum contains abundant peaks of C18:0 and C22:6 at m/z 283.3 and 327.3, respectively. This set of data demonstrates the utility of charge inversion ion/ion chemistry in confidently providing fatty acyl

chain information for less abundant PCs, which otherwise would be difficult to obtain using conventional shotgun lipid analysis methods.

In order to assign the locations of unsaturation in C22:6, the PB-MS/MS experiment was performed separately in positive ion mode. Figure 4c shows ion trap CID of m/z 892.8 ($[^{PB}M + H]^+$), which contains six distinct pairs of diagnostic ions (m/z 608.6/634.6, m/z 648.5/674.6, m/z 688.6/714.6, m/z 728.6/754.7, m/z 768.6/794.7, and m/z 808.7/834.7) that align with C=Cs at positions Δ4, Δ7, Δ10, Δ13, Δ16, and Δ19. The diagnostic ions thus allowed for confident identification of PC 18:0_22:6(Δ4, Δ7, Δ10, Δ13, Δ16, Δ19), which contains polyunsaturated omega-3 fatty acyl.

Figure 5a shows MS^2 CID of ions at m/z 766.5, the same nominal mass as deprotonated PE 38:4 in negative ion mode. The fatty acyl chains that correspond to the PE species can be determined as mainly C20:4 and C18:0, classifying the peak as PE 18:0_20:4. Based on Fig. 5a, however, there were still peaks present in high abundance that do not correspond to the lipid class being targeted. For example, a peak that

136
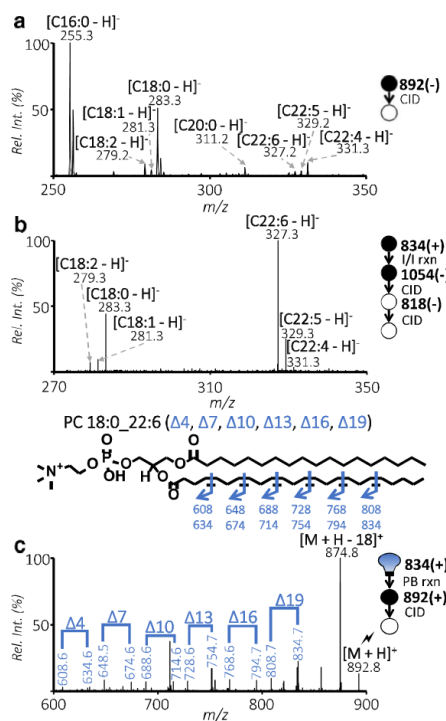
Fig. 4 **a** Direct negative ionization of bovine liver polar lipid extract. Isolation followed by beam-type CID of ions at *m/z* 892.8 (positive *m/z* 834.7 from Fig. 3a complexed with acetate anion, [M + Ac]⁻, 100 μM with 10 mM ammonium acetate). **b** Charge inversion and subsequent ion trap CID spectrum of the peak found at *m/z* 834.7 in the positive ion mode spectrum. **c** Positive ion mode ion trap CID of the PB product of *m/z* 834.7 peak, [^PBM + H]⁺, at *m/z* 892.8

Fig. 5 **a** Direct ionization of bovine liver polar lipid extract in negative ion mode. Isolation and beam-type CID of ions at *m/z* 766.5 (positive *m/z* 768.6 from Fig. 3a). **b** Charge inversion and subsequent ion trap CID spectrum originating from positive ions present at *m/z* 768.6. **c** Positive ion mode beam-type CID of the peak at *m/z* 826.3 (PB product of *m/z* 768.6)

corresponds to C18:2 at *m/z* 279.2 is prominent, but there is no parallel ion for C20:2 (*m/z* 307), the fatty acyl chain that would complement C18:2, suggesting that the C18:2 ion may arise from an isobaric species not related to PE, despite its high abundance. Figure 5b shows the charge inversion of the *m/z* 768.6 [M + H]⁺ ion and subsequent ion trap CID of 766.5 ([M - H]⁻) to determine that the fatty acyl chains present for PE 38:4 to be C18:0 and C20:4 at *m/z* 283.3 and 303.3, respectively, identifying the major species as PE 18:0_20:4, while several other minor components, i.e., PE 18:1_20:3 and PE 16:0_22:4, coexist. Note that the prominent *m/z* 279.2 ion observed in Fig. 5a is largely absent in Fig. 5b, which further suggests that the charge inversion process provides a degree of discrimination against possible isobaric interferences present

in direct negative ion mode ionization. Positive ion mode CID of the *m/z* 768.6 PB product at *m/z* 826.3, shown in Fig. 5c, displays four C=C diagnostic ion pairs (*m/z* 439.2/465.2, *m/z* 479.2/505.2, *m/z* 519.1/545.2, and *m/z* 559.2/585.1), corresponding to the Δ5, Δ8, Δ11, and Δ14 C=C locations on the 20:4 fatty acyl chain (an omega-6 fatty acyl). This set of data identified that PE 18:0_20:4(Δ5, Δ8, Δ11, Δ14) was the major component for the peak *m/z* 786.6 from shotgun analysis in the positive ion mode.

When compared to using direct negative ionization for PC and PE analysis, charge inversion is shown to be efficient at determining fatty acyl chain information that is relevant to the peak of interest. The added ability to pair the fatty acyl chains determined to C=C location information allows novel information where ambiguity is minimized. Polyunsaturated PCs and PEs with greater than two double bonds, along with those

with relative abundances less than 4%, were analyzed using this method for confident double-bond position siting.

It is desirable for a method to be able to distinguish PC and PE isomers with the added ability to determine the C=C location. Investigation of the m/z 744.6 ions in the bovine liver extract via charge inversion is provided in Fig. 6 to illustrate such a capability. Charge inversion followed by CID of the m/z 964.8 ion showed a dominant peak at m/z 742.6, a deprotonated PE 36:2, and a lower abundance peak at m/z 728.6 (demethylated anions of PC 33:2), indicating the coexistence of isomeric PE and PC in the lipid sample (Fig. 6a). Ion trap CID of the m/z 742.6 ion resulted in ions at m/z 279.3, 283.3, and 281.3 representing fatty acyls C18:2, C18:0, and C18:1, respectively, as shown in Fig. 6b. Based on the relative ion intensities of these fatty acyl anions, the PE 36:2 species in the sample was determined to contain PE 18:0_18:2 as a major component with PE 18:1_18:1 as a minor component. The minor PE species was identified as PE 18:1(Δ9)_18:1(Δ9) using beam-type CID of the PB product (m/z 802.7) in positive ion mode (ESM Fig. S7). The PB product (m/z 802.7) of the peak at m/z 744.6 was subjected to charge inversion followed by sequential steps of CID of the ions of m/z 1022.7 and m/z 800.6. Fatty acyl–related products are detected at m/z 337.3, 283.3, 339.3, and 281.3, further confirming that PE 18:0_18:2 and PE 18:1_18:1 are present. The relative abundance of the m/z 337.3 ion was sufficiently high to allow for a subsequent CID for C=C localization. Diagnostic peaks with 26 Da differences are present at m/z 171/197 and m/z 211/237 to determine the double-

bond locations to be at Δ9 and Δ12, identifying the major PE species content to PE 18:0_18:2(Δ9, Δ12) (Fig. 5c).

The isomeric PC 33:2 was analyzed by subjecting the demethylated anions to CID (Fig. 5d). The detection of fatty acyl anions at m/z 281.3, 279.3, 283, 241.3, and 237.2 is C18:1, C18:2, C18:0, C15:0, and C15:2, respectively, meaning isomers PC 15:0_18:2, PC 15:1_18:1, and PC 15:2_18:0 are present. Positive PB product analysis (Fig. 5e) was used to analyze the C=C location. Ion trap CID in positive ion mode resulted in diagnostic ions that are 26 Da apart determining the major components to be PC 15:0_18:2(Δ9, Δ12) and PC 15:1_18:1(Δ9).

It is worth noting that the diagnostic ions for C15:1 with a Δ9 C=C location would be at m/z 676.5 and 702.6, meaning that they overlap with the diagnostic ions of Δ12 C=C in PC 15:0_18:2(Δ9, Δ12). This is a limitation of the direct positive ion mode approach that can be overcome via the charge inversion route, but only when the fatty acyl anion abundances are sufficiently high. The commonly present C18:2(Δ9, Δ12) motif inclined us to ascribe the m/z 676.5 and 702.6 ions as arising from the Δ12 position and do not report the presence of C15:1(Δ9). Further improvement of signal for low abundant monounsaturated fatty acyls will allow for the confident determination of C=C. Nonetheless, by pairing ion/ion charge inversion with the PB reaction, 40 distinct unsaturated PC and PE structures were determined with fatty acyl composition and C=C locations from bovine polar lipid extract as shown in Table 1 (detailed list in ESM Table S1). This level of
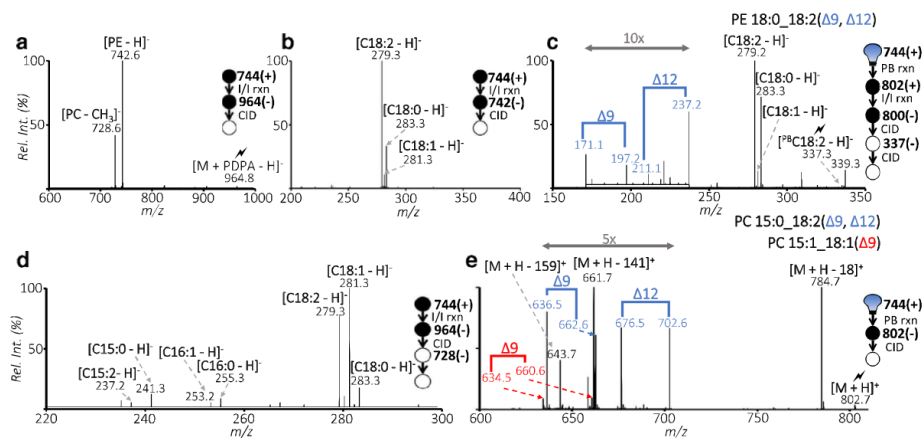
Fig. 6 **a** Charge inversion of cations at m/z 744.6 followed by ion trap CID of ions at m/z 964.8. **b** Sequential CID of ions at m/z 742.8. **c** CID of ions at m/z 337.3 resulting from sequential CID of charge-inverted PB products. **d** Sequential CID of ions at m/z 728.6 in panel a. **e** Positive ion trap CID of PB reaction product at m/z 802.7

Table 1 The identified PCs and PEs in bovine liver polar lipid extract via pairing the PB reaction with ion/ion charge inversion

$[M + H]^+$ (m/z)	Identity of GPs
718.6	PE 16:0_18:1(Δ9)
732.6	PE 17:0_18:1(Δ9)
	PC 14:0_18:1(Δ9)
	PC 14:0_18:1(Δ11)
	PC 16:0_16:1(Δ9)
740.6	PE 18:2(Δ9, Δ12)_18:2(Δ9, Δ12)
744.6	PE 18:0_18:2(Δ9, Δ12)
	PE 18:1(Δ9)_18:1(Δ9)
	PC 15:1_18:1(Δ9)
	PC 15:1_18:1(Δ11)
	PC 15:0_18:2(Δ9, Δ12)
746.6	PE 18:0_18:1(Δ9)
	PE 18:0_18:1(Δ11)
	PC 15:0_18:1(Δ9)
	PC 15:0_18:1(Δ11)
	PC 17:1(Δ9)_16:0
	PC 15:1(Δ9)_18:0
758.6	PC 16:0_18:2(Δ9, Δ12)
760.7	PC 16:0_18:1(Δ9)
	PC 16:0_18:1(Δ11)
766.6	PE 20:5(Δ5, Δ8, Δ11, Δ14, Δ17)_18:0
768.6	PE 18:0_20:4(Δ5, Δ8, Δ11, Δ14)
772.6	PC 17:0_18:2(Δ9, Δ12)
774.7	PC 17:0_18:1(Δ9)
	PC 18:0_17:1(Δ9)
782.6	PC 16:0_20:4(Δ5, Δ8, Δ11, Δ14)
784.6	PC 16:0_20:3(Δ8, Δ11, Δ14)
	PC 18:1(Δ9)_18:2(Δ9, Δ12)
786.7	PC 18:0_18:2(Δ9, Δ12)
	PC 18:1(Δ9)_18:1(Δ9)
788.7	PC 18:0_18:1(Δ9)
	PC 18:0_18:1(Δ11)
808.7	PC 18:1_20:4(Δ5, Δ8, Δ11, Δ14)
	PC 18:0_20:5(Δ5, Δ8, Δ11, Δ14, Δ17)
810.7	PC 18:0_20:4(Δ5, Δ8, Δ11, Δ14)
812.7	PC 18:0_20:3(Δ8, Δ11, Δ14)
834.7	PC 18:0_22:6(Δ4, Δ7, Δ10, Δ13, Δ16, Δ19)
836.7	PC 18:0_22:5(Δ7, Δ10, Δ13, Δ16, Δ19)
	PC 18:1_22:4(Δ7, Δ10, Δ13, Δ16)
838.7	PC 18:0_22:4(Δ7, Δ10, Δ13, Δ16)

identification compares favorably to those reported from UVPD [35] and epoxidation [51].

Conclusion

In this work, we have paired the Paternò–Büchi reaction with charge inversion by ion/ion reaction aiming to achieve high-level structural information for unsaturated PEs and PCs using the shotgun approach. The method allows for confident identification of the double-bond location in a specific fatty acyl chain containing one or two degrees of unsaturation. Double-bond location isomers were distinguished along with the ability to characterize PE and PC isomers. A limitation to conducting charge inversion and PB-MS/MS in one experiment is that C=C diagnostic fragment ions of polyunsaturated fatty acyl chain are difficult to obtain in negative ion mode [48]. This limitation can be overcome by merging accurate fatty acyl chain information from charge inversion in negative ion mode with the information provided by positive ion mode PB-MS/MS for C=C location in two separate experiments.

For relatively abundant PCs and PEs or situations where chemical interference is minimal, charge inversion is not a necessity. However, for PCs and PEs at lower abundances, i.e., 2–10% of the most abundance species, charge inversion significantly reduces chemical interference, leading to both improved sensitivity and specificity for structural identification. As a simple comparison, without charge inversion, we identified 24 GP species (18 PCs and 6 PEs) at C=C location level, while the combined methods allowed for identification of 40 GP species (31 PCs and 9 PEs). Dynamic range of such method is estimated to be 50 times. For GPs of lower than 2% relative abundance, a possible path to improve their identification will be application of this method on GPs that have been modified to improve ionization efficiency, such as ^{13}C-trimethylation enhancement using diazomethane.

Although not demonstrated here, quantitation for lipid C=C location isomers can be achieved in positive ion mode using methods already established from PB-MS/MS, while relative quantitation for fatty acyl composition isomers can be obtained from charge inversion followed by CID. A home-modified Q-TOF instrument has been employed in this study for charge inversion ion/ion reactions and PB-MS/MS; in principle, commercial MS instruments capable of ETD, such as an LTQ-Orbitrap, should support charge inversion as long as the doubly charged reagent anions can be introduced into linear ion trap for ion/ion reactions. Overall, the present work shows that gas-phase charge inversion paired with the PB reaction is a useful method for structural elucidation of unsaturated phospholipids.

Compliance with ethical standards

Conflict of interest The authors declare that they have no conflict of interest.

Publisher's note Springer Nature remains neutral with regard to jurisdictional claims in published maps and institutional affiliations.

References

1. Han X, Gross RW. Shotgun lipidomics: electrospray ionization mass spectrometric analysis and quantitation of cellular lipidomes directly from crude extracts of biological samples. Mass Spectrom Rev. 2005;24(3):367–412.

2. Armstrong D, editor. Lipidomics [Internet]. Totowa, NJ: Humana Press; 2009. (Methods in Molecular Biology; vol. 579). Available from: http://link.springer.com/10.1007/978-1-60761-322-0. Accessed 9 Oct 2017.

3. Han X, Gross RW. Shotgun lipidomics: multidimensional MS analysis of cellular lipidomes. Expert Rev Proteomics. 2005;2(2):253–64.

4. Fhaner CJ, Liu S, Ji H, Simpson RJ, Reid GE. Comprehensive lipidome profiling of isogenic primary and metastatic colon adenocarcinoma cell lines. Anal Chem. 2012;84(21):8917–26.

5. van Meer G, Voelker DR, Feigenson GW. Membrane lipids: where they are and how they behave. Nat Rev Mol Cell Bio. 2008;9(2):112–24.

6. Eberlin LS, Dill AL, Golby AJ, Ligon KL, Wiseman JM, Cooks RG, et al. Discrimination of human astrocytoma subtypes by lipid analysis using desorption electrospray ionization imaging mass spectrometry. Angew Chem Int Ed. 2010;49(34):5953–6.

7. Gross RW, Han X. Lipidomics at the interface of structure and function in systems biology. Chem Biol. 2011;18(3):284–91.

8. Ejsing CS, Sampaio JL, Surendranath V, Duchoslav E, Ekroos K, Klemm RW, et al. Global analysis of the yeast lipidome by quantitative shotgun mass spectrometry. Proc Natl Acad Sci U S A. 2009;106(7):2136–41.

9. Loizides-Mangold U. On the future of mass spectrometry-based lipidomics. FEBS J. 2013;280(12):2817–29.

10. Fahy E, Subramaniam S, Murphy RC, Nishijima M, Raetz CRH, Shimizu T, et al. Update of the LIPID MAPS comprehensive classification system for lipids. J Lipid Res. 2009;50(Supplement):S9–14.

11. Whiley L, Sen A, Heaton J, Proitsi P, García-Gómez D, Leung R, et al. Evidence of altered phosphatidylcholine metabolism in Alzheimer's disease. Neurobiol Aging. 2014;35(2):271–8.

12. Phoenix DA, Harris F, Mura M, Dennison SR. The increasing role of phosphatidylethanolamine as a lipid receptor in the action of host defense peptides. Prog Lipid Res. 2015;59:26–37.

13. Guan Z-Z, Wang Y-N, Xiao K-Q, Hu P-S, Liu J-L. Activity of phosphatidylethanolamine-N-methyltransferase in brain affected by Alzheimers disease. Neurochem Int. 1999;34(1):41–7.

14. Brouwers JF. Liquid chromatographic–mass spectrometric analysis of phospholipids. Chromatography, ionization and quantification. BBA-Mol Cell Bio Lipids. 2011;1811(11):763–75.

15. Wang C, Kong H, Guan Y, Yang J, Gu J, Yang S, et al. Plasma phospholipid metabolic profiling and biomarkers of type 2 diabetes mellitus based on high-performance liquid chromatography/ electrospray mass spectrometry and multivariate statistical analysis. Anal Chem. 2005;77(13):4108–16.

16. Bird SS, Marur VR, Sniatynski MJ, Greenberg HK, Kristal BS. Lipidomics profiling by high-resolution LC–MS and high-energy collisional dissociation fragmentation: focus on characterization of mitochondrial cardiolipins and monolysocardiolipins. Anal Chem. 2011;83(3):940–9.

17. Nygren H, Seppänen-Laakso T, Castillo S, Hyötyläinen T, Orešič M. Liquid chromatography-mass spectrometry (LC-MS)-based lipidomics for studies of body fluids and tissues. In: Metz TO, editor. Metabolic profiling [Internet]. Totowa, NJ: Humana Press; 2011. p. 247–57. Available from: http://link.springer.com/10.1007/978-1-61737-985-7_15. Accessed 15 Nov 2017.

18. Brügger B, Erben G, Sandhoff R, Wieland FT, Lehmann WD. Quantitative analysis of biological membrane lipids at the low picomole level by nano-electrospray ionization tandem mass spectrometry. Proc Natl Acad Sci U S A. 1997;94(6):2339.

19. Han X, Gross RW. Electrospray ionization mass spectroscopic analysis of human erythrocyte plasma membrane phospholipids. Proc Natl Acad Sci U S A. 1994;91(22):10635–9.

20. Han X, Gross RW. Global analyses of cellular lipidomes directly from crude extracts of biological samples by ESI mass spectrometry: a bridge to lipidomics. J Lipid Res. 2003;44(6):1071–9.

21. Han X, Yang K, Gross RW. Multi-dimensional mass spectrometry-based shotgun lipidomics and novel strategies for lipidomic analyses. Mass Spectrom Rev. 2012;31(1):134–78.

22. Lintonen TPI, Baker PRS, Suoniemi M, Ubhi BK, Koistinen KM, Duchoslav E, et al. Differential mobility spectrometry-driven shotgun lipidomics. Anal Chem. 2014;86(19):9662–9.

23. Buré C, Ayciriex S, Testet E, Schmitter J-M. A single run LC-MS/MS method for phospholipidomics. Anal Bioanal Chem. 2013;405(1):203–13.

24. Hsu F-F, Turk J. Electrospray ionization with low-energy collisionally activated dissociation tandem mass spectrometry of glycerophospholipids: mechanisms of fragmentation and structural characterization. J Chromatogr B. 2009;877(26):2673–95.

25. Wasslen KV, Canez CR, Lee H, Manthorpe JM, Smith JC. Trimethylation enhancement using diazomethane (TrEnDi) II: rapid in-solution concomitant quaternization of glycerophospholipid amino groups and methylation of phosphate groups via reaction with diazomethane significantly enhances sensitivity in mass spectrometry analyses via a fixed, permanent positive charge. Anal Chem. 2014;86(19):9523–32.

26. Canez CR, Shields SWJ, Bugno M, Wasslen KV, Weinert HP, Willmore WG, et al. Trimethylation enhancement using ^{13}C-diazomethane (^{13}C-TrEnDi): increased sensitivity and selectivity of phosphatidylethanolamine, phosphatidylcholine, and phosphatidylserine lipids derived from complex biological samples. Anal Chem. 2016;88(14):6996–7004.

27. Wang M, Palavicini JP, Cseresznye A, Han X. Strategy for quantitative analysis of isomeric bis (monoacylglycero) phosphate and phosphatidylglycerol species by shotgun lipidomics after one-step methylation. Anal Chem. 2017;89(16):8490–5.

28. Stutzman JR, Blanksby SJ, McLuckey SA. Gas-phase transformation of phosphatidylcholine cations to structurally informative anions via ion/ion chemistry. Anal Chem. 2013;85(7):3752–7.

29. Rojas-Betancourt S, Stutzman JR, Londry FA, Blanksby SJ, McLuckey SA. Gas-phase chemical separation of phosphatidylcholine and phosphatidylethanolamine cations via charge inversion ion/ion chemistry. Anal Chem. 2015;87(22):11255–62.

30. Pulfer M, Murphy RC. Electrospray mass spectrometry of phospholipids. Mass Spectrom Rev. 2003;22(5):332–64.

31. Tomer KB, Crow FW, Gross ML. Location of double-bond position in unsaturated fatty acids by negative ion MS/MS. J Am Chem Soc. 1983;105(16):5487–8.

32. Thomas MC, Mitchell TW, Harman DG, Deeley JM, Nealon JR, Blanksby SJ. Ozone-induced dissociation: elucidation of double bond position within mass-selected lipid ions. Anal Chem. 2008;80(1):303–11.

33. Brown SHJ, Mitchell TW, Blanksby SJ. Analysis of unsaturated lipids by ozone-induced dissociation. BBA-Mol Cell Bio Lipids. 2011;1811(11):807–17.

34. Pham HT, Maccarone AT, Thomas MC, Campbell JL, Mitchell TW, Blanksby SJ. Structural characterization of glycerophospholipids by combinations of ozone- and collision-induced dissociation mass spectrometry: the next step towards "top-down" lipidomics. Analyst. 2014;139(1):204–14.

35. Klein DR, Brodbelt JS. Structural characterization of phosphatidylcholines using 193 nm ultraviolet photodissociation mass spectrometry. Anal Chem. 2017;89(3):1516–22.

36. Pham HT, Trevitt AJ, Mitchell TW, Blanksby SJ. Rapid differenti- ation of isomeric lipids by photodissociation mass spectrometry of fatty acid derivatives: photodissociation of derivatized fatty acids. Rapid Commun Mass Spectrom. 2013;27(7):805–15.

37. Pham HT, Julian RR. Radical delivery and fragmentation for struc- tural analysis of glycerophospholipids. Int J Mass Spectrom. 2014;370:58–65.

38. Deimler RE, Sander M, Jackson GP. Radical-induced fragmenta- tion of phospholipid cations using metastable atom-activated disso- ciation mass spectrometry (MAD-MS). Int J Mass Spectrom. 2015;390:178–86.

39. Li P, Hoffmann WD, Jackson GP. Multistage mass spectrometry of phospholipids using collision-induced dissociation (CID) and meta- stable atom-activated dissociation (MAD). Int J Mass Spectrom. 2016;403:1–7.

40. Campbell JL, Baba T. Near-complete structural characterization of phosphatidylcholines using electron impact excitation of ions from organics. Anal Chem. 2015;87(11):5837–45.

41. Baba T, Campbell JL, Le Blanc JCY, Baker PRS. Structural identi- fication of triacylglycerol isomers using electron impact excitation of ions from organics (EIEIO). J Lipid Res. 2016;57(11):2015–27.

42. Stinson CA, Zhang W, Xia Y. UV lamp as a facile ozone source for structural analysis of unsaturated lipids via electrospray ionization- mass spectrometry. J Am Soc Mass Spectr. 2018;29(3):481–9.

43. Harris RA, May JC, Stinson CA, Xia Y, McLean JA. Determining double bond position in lipids using online ozonolysis coupled to liquid chromatography and ion mobility-mass spectrometry. Anal Chem. 2018;90(3):1915–24.

44. Ma X, Xia Y. Pinpointing double bonds in lipids by Paternò-Büchi reactions and mass spectrometry. Angew Chem Int Ed. 2014;53(10):2592–6.

45. Stinson CA, Xia Y. A method of coupling the Paternò–Büchi reac- tion with direct infusion ESI-MS/MS for locating the C=C bond in glycerophospholipids. Analyst. 2016;141(12):3696–704.

46. Ma X, Chong L, Tian R, Shi R, Hu TY, Ouyang Z, et al. Identification and quantitation of lipid C=C location isomers: a shotgun lipidomics approach enabled by photochemical reaction. Proc Natl Acad Sci U S A. 2016;113(10):2573–8.

47. Ren J, Franklin ET, Xia Y. Uncovering structural diversity of un- saturated fatty acyls in cholesteryl esters via photochemical reaction and tandem mass spectrometry. J Am Soc Mass Spectrom. 2017;28(7):1432–41.

48. Murphy RC, Okuno T, Johnson CA, Barkley RM. Determination of double bond positions in polyunsaturated fatty acids using the pho- tochemical Paternò-Büchi reaction with acetone and tandem mass spectrometry. Anal Chem. 2017;89(16):8545–53.

49. Liebisch G, Vizcaíno JA, Köfeler H, Trötzmüller M, Griffiths WJ, Schmitz G, et al. Shorthand notation for lipid structures derived from mass spectrometry. J Lipid Res. 2013;54(6):1523–30.

50. Xia Y, Chrisman PA, Erickson DE, Liu J, Liang X, Londry FA, et al. Implementation of ion/ion reactions in a quadrupole/time-of-flight tandem mass spectrometer. Anal Chem. 2006;78(12):4146–54.

51. Cao W, Ma X, Li Z, Zhou X, Ouyang Z. Locating carbon–carbon double bonds in unsaturated phospholipids by epoxidation reaction and tandem mass spectrometry. Anal Chem. 2018;90(17):10286– 92.